Copyright

by

Shivangi Dave

2018

# COMPARATIVE STUDY OF DECELLURALIZED EXTRACELLULAR MATRIX FROM PORCINE DERIVED TISSUES AS A SUBSTRATE FOR IN-VITRO MOUSE MESENCHYMAL STEM CELL CULTURE

by

Shivangi Dave, B.S.

THESIS

Presented to the Faculty of

The University of Houston-Clear Lake

In Partial Fulfillment

Of the Requirements

For the Degree

MASTER OF SCIENCE

in Biotechnology

THE UNIVERSITY OF HOUSTON-CLEAR LAKE

DECEMBER, 2018

COMPARATIVE STUDY OF DECELLURALIZED EXTRACELLULAR MATRIX FROM PORCINE DERIVED TISSUES AS A SUBSTRATE FOR IN-VITRO MOUSE MESENCHYMAL STEM CELL CULTURE

by

Shivangi Dave

APPROVED BY

_____
Richard Puzdrowski, Ph.D., Chair

_____
Leonard J. Giblin III, Ph.D., Committee Member

_____
Larry Rohde, Ph.D., Committee Member

RECEIVED/APPROVED BY THE COLLEGE OF UNIVERSITY OF HOUSTON-CLEAR LAKE:

_____
Said Bettayeb, Ph.D., Associate Dean

_____
Ju Kim, Ph.D., Dean

ACKNOWLEDGEMENTS

After an intensive period of twelve months, today is the day, writing this note of thanks is the finishing touch to my dissertation. I would like to thank people who have supported and helped me so much through this period. I am extremely grateful for having Dr. Richard Puzdrowski as my thesis advisor. The door to Dr. Puzdrowski's office was always open whenever I ran into a trouble spot or had a question about my research or writing. I want to thank him for his excellent cooperation and for all the opportunities I was given to conduct my research. He steered me in the right direction whenever he thought I needed it.

In addition, I would like to thank my thesis committee members Dr. Leonard J. Giblin III and Dr. Larry Rohde for their valuable guidance and stimulating conversations during the process of finalizing my research. I am thankful to Dr.Rohde for allowing me to use his laboratory for tissue culture. I am thankful to Dr. George Guillen for allowing me to use his laboratory for lyophilization equipment. I would like to thank Dr. Cynthia Howard and Charis Peterson for her diligence in analyzing my data. Many thanks to the independent study students: Glory Hughes, Sandy Saman, Arthur and Renee for their aid in conducting the experiments.

I must express my very profound gratitude to my parents and to my friends Saurabh Sawant and Chandni Jaisinghani for providing me with unfailing support and continuous encouragement throughout my study and through the process of researching and writing this thesis. I would also like to acknowledge University of Houston Clear lake for providing support by the research funds.

ABSTRACT

COMPARATIVE STUDY OF DECELLURALIZED EXTRACELLULAR MATRIX FROM PORCINE DERIVED TISSUES AS A SUBSTRATE FOR IN-VITRO MOUSE MESENCHYMAL STEM CELL CULTURE

Shivangi Dave
University of Houston-Clear Lake, 2018

Thesis Chair: Richard Puzdrowski, PhD

The main goal of this research is to create a 3-D natural scaffold for the Mouse Mesenchymal stem cells (MSCs) to carry out in-vitro growth without losing its physiological and morphological characteristics. MSCs are multipotent adult stem cells that can develop into several cell types belonging to bone, skeletal and fat tissues. These cells require extracellular matrix (ECM) for their growth. ECM is a critical environmental factor for cells to maintain normal function. It provides structural and biochemical support to them. Without ECM substrates, in-vivo and in-vitro stem cell research is of limited use. Furthermore, therapeutic applications require large numbers of MSCs. Because of MSCs's biological importance and diverse role, the ECM has been the focal point of increasing interest in the field of regenerative medicine and stem cell research. Therefore, tissue culture plates have been developed providing ECM components to maintain an artificial environment for the cells to grow. However, this approach has limited success since it

provides a flat 2-D growth surface and hence the standard culturing techniques have proven insufficient for this purpose. In addition, the tissue culture plates are expensive. This research is to prepare a complete ECM comprised of all the components required to provide a natural environment for the growth of healthy cells with intact tissues. The context discussed indicates that minimally altered decellularized porcine tissues-derived ECM can provide effective substrates for MSCs. In the present study it was found that bone marrow (BM), adipose and dermis smeared cultivation plates support in-vitro cultivation of MSCs while maintaining homogenous, physiological and stable cell population. Characterization and analyses of BM, adipose and dermis was carried out by performing immunohistochemistry and other staining techniques which demonstrate the presence of major ECM proteins and glycosaminoglycans (GAGs) in the substrates. The results of this research will establish a porcine derived ECM substrate with application potential in high fidelity cultivation techniques for stem cells. On the basis of our results, we suggest that decellularized ECM has a significant impact on tissue reconstruction and regenerative medicine.

TABLE OF CONTENTS

List of Tables ..... ix

List of Figures ..... xi

INTRODUCTION ..... 1

Mesenchymal Stem Cells ..... 1
History of Mesenchymal stem cells ..... 1
Characterization of Mesenchymal stem cells: ..... 2
Long-term *in-vitro* culturing of Mesenchymal stem cells ..... 3
Applications of Mesenchymal stem cells ..... 4
Extracellular matrix ..... 6
Composition and Functions of Extracellular Matrix ..... 6
Importance of Extracellular Matrix ..... 8

METHODOLOGY ..... 10

Decellularization of Bone-marrow, Dermis and Adipose tissues ..... 10
Lyophilization of Bone-marrow, Dermis and Adipose tissues ..... 10
Preparation of Tissues for Histological Analysis ..... 11
Decalcification of Bone-marrow pieces ..... 11
Cryo Sectioning of Bone-Marrow, Dermis and Adipose tissues ..... 11
Hemotoxylin and Eosin Staining ..... 12
Alcian Blue Staining ..... 12
Immunohistochemistry ..... 13
Avidin-Biotin Complex (ABC) – Vectastain kit ..... 13
Fluorescent Immunostaining ..... 14
Thawing and Establishing Mesenchymal Stem Cell Cultures ..... 15
Passaging Mice Mesenchymal Stem Cells ..... 15
Freezing of Mouse Mesenchymal Stem cells ..... 16
Experimental Cultivation Round ..... 17
Cell Morphology ..... 18
Cell Count and Viability ..... 18
Immunophenotyping of Mouse Mesenchymal Stem cells ..... 19
Photomicrographic Documentation and Processing ..... 20
Statistical Analyses ..... 20

RESULTS ..... 21

Histological Analyses ..... 21
The decellularization process ..... 21
ECM structure and composition following decellularization ..... 25
MSCs Morphology ..... 46

DISCUSSION ..... 68

Effects of decellularization on ECM proteins ..... 68
ECM derived from BM, dermis and adipose supports *In-vitro* cultivation of MSCs ..... 70

CONCLUSION ..... 75

REFERENCES ..... 76

LIST OF TABLES

Table 1.1: Brightness measurement of ECM protein fibronectin for fluorescence labelled histological sections of porcine tissues. (Range of intensity on image J: min=0; max=255) ..... 43

Table 1.2: Brightness measurement of ECM protein laminin for fluorescence labelled histological sections of porcine tissues. (Range of intensity on image J: min=0; max=255) ..... 43

Table 1.3: Brightness measurement of ECM protein collagen-I for fluorescence labelled histological sections of porcine tissues. (Range of intensity on image J: min=0; max=255) ..... 44

Table 1.4: Brightness measurement of ECM protein collagen-III for fluorescence labelled histological sections of porcine tissues. (Range of intensity on image J: min=0; max=255) ..... 44

Table 1.5: Brightness measurement of ECM protein collagen-IV for fluorescence labelled histological sections of porcine tissues (Range of intensity on image J: min=0; max=255) ..... 45

Table 2: Summary of ECM proteins and their localization on the porcine tissues based on the brightness measured. ..... 45

Table 3.1: Mean cell count, Standard Deviation and Standard Error Mean of TCT (positive control) with respect to cultivation time. ..... 54

Table 3.2: Mean cell count, Standard Deviation and Standard Error Mean of substrate: dermis with respect to cultivation time. ..... 55

Table 3.3: Mean cell count, Standard Deviation and Standard Error Mean of substrate: BM with respect to cultivation time. ..... 55

Table 3.4: Mean cell count, Standard Deviation and Standard Error Mean of substrate: Adipose tissue with respect to cultivation time. ..... 56

Table 3.5: Mean cell count, Standard Deviation and Standard Error Mean of substrate: nTCT (negative control) with respect to cultivation time. ..... 56

Table 4.1: Comparison of Substrates in terms of p-vlaue for Day-2 cultivation time. ..... 59

Table 4.2: Comparison of Substrates in terms of p-vlaue for Day- 4 cultivation time. ..... 59

Table 4.4: Comparison of Substrates in terms of p-vlaue for Day- 8 cultivation time. ..... 60

Table 4.3: Comparison of Substrates in terms of p-vlaue for Day-6 cultivation time. ..... 60

Table 4.5: Comparison of Substrates in terms of p-vlaue for Day-10 cultivation time. ..... 61

Table 5: Population doubling time for Substrates (in Hours) during the exponential phase. ..... 61

Table 6: Expression of MSC Lineage Specific Surface Markers Based on Immunofluorescence Analyses. ..... 67

LIST OF FIGURES

Figure 1:Macroscopic images of (A) fresh adipose tissue blocks prior to processing and (B) the resultant tissue after decellularization. ..... 21

Figure 2.1: H&E staining (cell nuclei, purple spots; cytoplasm, pink) of (A) fresh adipose tissue, (B) decellularized adipose tissue and (C) lyophilized adipose tissue showing adipocytes (ad). Scale bars represents 0.2mm. ..... 22

Figure 2.2: H&E staining (cell nuclei, purple spots; cytoplasm, pink) of (A) fresh dermis, (B) decellularized dermis and (C) lyophilized dermis showing dermis (d), adipocytes (ad) and blood vessel (bv). Scale bars represents 0.2mm. ..... 23

Figure 2.3: H&E staining (cell nuclei, purple spots; cytoplasm, pink) of (A) fresh BM, (B) decellularized BM and (C) lyophilized BM showing marrow (m), endosteum (e), lacunae (l) and bone trabeculae (bt). Scale bars represents 0.2mm. ..... 24

Figure 3: Sections of porcine tissues (A) fresh adipose, (B) decellularized adipose and (C) lyophilized adipose showing adipocytes (ad); (D) fresh dermis, (E) decellularized dermis and (F) lyophilized dermis showing epidermis (ed), dermis (d) and blood vessel (bv); (G) fresh BM, (H) decellularized BM and (I) lyophilized BM showing marrow (m), endosteum (e) and bone trabeculae (bt). Labelled with Alcian blue stain specific for extracellular matrix protein GAGs.. Arrows indicate GAGs throughout the adipose, dermis and BM tissue ECM. Scale bars represents 0.2mm. ..... 26

Figure 3.1: Sections of porcine tissues (A, D) fresh, (B, E) decellularized and (C, F) lyophilized adipose tissue showing adipocytes (ad). Labelled with antibody specific for extracellular matrix protein fibronectin. Images A, B and C stained using ABC-vectastain kit and Images D, E and F stained using fluorescence kit (filter-FITC). Arrows indicate fibronectin labelling throughout the adipose tissue ECM. Scale bars represents 0.2mm. ..... 28

Figure 3.2: Sections of porcine tissues (A, D) fresh, (B, E) decellularized and (C, F) lyophilized dermis showing dermis (d), epidermis (ed), blood vessel (bv) and adipocytes (ad). Labelled with antibody specific for extracellular matrix protein fibronectin. Images A, B and C stained using ABC-vectastain kit and Images D, E and F stained using fluorescence kit (filter-TRITC). Arrows fibronectin labelling throughout the dermis ECM. Scale bars represents 0.2mm. ..... 29

Figure 3.3: Sections of porcine tissues (A, D) fresh, (B, E) decellularized and (C, F) lyophilized BM showing marrow (m), bone trabeculae (bt), adipocytes (ad) and endosteum (e). Labelled with antibody specific for extracellular matrix protein fibronectin. Images A, B and C stained using ABC-vectastain kit and Images D, E and F stained using fluorescence kit (filter-TRITC). Arrows indicates fibronectin labelling throughout the BM ECM and in endosteum. Scale bars represents 0.2mm. ..... 30

Figure 4.1: Sections of porcine tissues (A, D) fresh, (B, E) decellularized and (C, F) lyophilized adipose tissue showing adipocytes (ad). Labelled with antibody specific for extracellular matrix protein laminin. Images A, B and C stained using ABC-vectastain kit and Images D, E and F stained using fluorescence kit (filter-FITC). Arrows indicates laminin labelling throughout the adipose tissue ECM. Scale bars represents 0.2mm. ..... 31

Figure 4.2: Sections of porcine tissues (A, D) fresh, (B, E) decellularized and (C, F) lyophilized dermis showing dermis (d), epidermis (ed), blood vessel (bv) and adipocytes (ad). Labelled with antibody specific for extracellular matrix protein laminin. Images A, B and C stained using ABC-vectastain kit and Images D, E and F stained using fluorescence kit (filter-TRITC). Arrows indicates laminin labelling throughout the dermis ECM. Scale bars represents 0.2mm. ..... 32

Figure 4.3: Sections of porcine tissues (A, D) fresh, (B, E) decellularized and (C, F) lyophilized BM showing marrow (m), bone trabeculae (bt), endosteum (e) and adipocytes (ad). Labelled with antibody specific for extracellular matrix protein laminin. Images A, B and C stained using ABC-vectastain kit and Images D, E and F stained using fluorescence kit (filter-TRITC and FITC). Arrows laminin labelling throughout the BM ECM and in endosteum. Scale bars represents 0.2mm. ..... 33

Figure 5.1: Sections of porcine tissues (A, D) fresh, (B, E) decellularized and (C, F) lyophilized adipose showing adipocytes (ad), and blood vessels (bv). Labelled with antibody specific for extracellular matrix protein collagen-I. Images A, B and C stained using ABC-vectastain kit and Images D, E and F stained using fluorescence kit (filter- TRITC and FITC). Arrows indicate collagen-I labelling throughout the adipose tissue ECM. Scale bars represents 0.2mm. ..... 34

Figure 5.2: Sections of porcine tissues (A, D) fresh, (B, E) decellularized and (C, F) lyophilized dermis showing dermis (d), and epidermis (ed). Labelled with antibody specific for extracellular matrix protein collagen-I. Images A, B and C stained using ABC-vectastain kit and Images D, E and F stained using fluorescence kit (filter-TRITC and FITC). Arrows indicates collagen-I labelling throughout the dermis ECM. Scale bars represents 0.2mm. ..... 35

Figure 5.3: Sections of porcine tissues (A, D) fresh, (B, E) decellularized and (C, F) lyophilized BM showing marrow (m), endosteum (e), bone trabeculae (bt), blood vessel (bv) and adipocytes(ad). Labelled with antibody specific for extracellular matrix protein collagen-I. Images A, B and C stained using ABC-vectastain kit and Images D, E and F stained using fluorescence kit (filter-TRITCC). Arrows indicates collagen-I labelling throughout the BM ECM and in endosteum. Scale bars represents 0.2mm. ..... 36

Figure 6.1: Sections of porcine tissues (A, D) fresh, (B, E) decellularized and (C, F) lyophilized adipose showing adipocytes(ad). Labelled with antibody specific for extracellular matrix protein collagen-III. Images A, B and C stained using ABC-vectastain kit and Images D, E and F stained using fluorescence kit (filter-FITC).

Arrows indicates collagen-III labelling throughout the adipose tissue ECM. Scale bars represents 0.2mm ..... 37

Figure 6.2: Sections of porcine tissues (A, D) fresh, (B, E) decellularized and (C, F) lyophilized adipose showing dermis (d), blood vessel (bv) and adipocytes(ad). Labelled with antibody specific for extracellular matrix protein collagen-III. Images A, B and C stained using ABC-vectastain kit and Images D, E and F stained using fluorescence kit (filter-TRITC). Arrows indicates collagen-III labelling throughout the dermis. Scale bars represents 0.2mm. ..... 38

Figure 6.3: Sections of porcine tissues (A, D) fresh, (B, E) decellularized and (C, F) lyophilized BM showing marrow (m), bone trabeculae (bt), endosteum (e) and adipocytes(ad). Labelled with antibody specific for extracellular matrix protein collagen-III. Images A, B and C stained using ABC-vectastain kit and Images D, E and F stained using fluorescence kit (filter-TRITC). Arrows indicates collagen-III labelling throughout the BM ECM. Scale bars represents 0.2mm. ..... 39

Figure 7.1: Sections of porcine tissues (A, D) fresh, (B, E) decellularized and (C, F) lyophilized adipose showing adipocytes (ad). Labelled with antibody specific for extracellular matrix protein collagen-IV. Images A, B and C stained using ABC-vectastain kit and Images D, E and F stained using fluorescence kit (filter-FITC). Arrows indicates collagen-IV labelling throughout the adipose tissue ECM. Scale bars represents 0.2mm. ..... 40

Figure 7.2: Sections of porcine tissues (A, D) fresh, (B, E) decellularized and (C, F) lyophilized dermis showing dermis (d), epidermis (ed), blood vessels (bv) and adipocytes (ad). Labelled with antibody specific for extracellular matrix protein collagen-IV. Images A, B and C stained using ABC-vectastain kit and Images D, E and F stained using fluorescence kit (filter-TRITC). Arrows indicates collagen-IV labelling throughout the dermis ECM. Scale bars represents 0.2mm..... 41

Figure 7.3: Sections of porcine tissues (A, D) fresh, (B, E) decellularized and (C, F) lyophilized BM showing marrow (m), bone trabeculae (bt), endosteum (e) and adipocytes (ad). Labelled with antibody specific for extracellular matrix protein collagen-IV. Images A, B and C stained using ABC-vectastain kit and Images D, E and F stained using fluorescence kit (filter- TRITC and FITC). Arrows indicates collagen-IV labelling throughout the BM ECM. Scale bars represents 0.2mm. ..... 42

Figure 8.1: Morphological characteristics of MSCs on TCT (A), dermis-smeared (B), BM-smeared (C), adipose-smeared (D) and nTCT (E) plates. Phase-contrast images of MSCs culture were taken at day-2. Magnification: 4X..... 47

Figure 8.2: Morphological characteristics of MSCs on TCT (A), dermis-smeared (B), BM-smeared (C), adipose-smeared (D) and nTCT (E) plates. Phase-contrast images of MSCs culture were taken at day-4. Magnification: 4X..... 48

Figure 8.3: Morphological characteristics of MSCs on TCT (A), dermis-smeared (B), BM-smeared (C), adipose-smeared (D) and nTCT (E) plates. Phase-contrast images of MSCs culture were taken at day-6. Magnification: 4X..... 49

Figure 8.4: Morphological characteristics of MSCs on TCT (A), dermis-smeared (B), BM-smeared (C), adipose-smeared (D) and nTCT (E) plates. Phase-contrast images of MSCs culture were taken at day-8. Magnification: 4X..... 50

Figure 8.5: Morphological characteristics of MSCs on TCT (A), dermis-smeared (B), BM-smeared (C), adipose-smeared (D) and nTCT (E) plates. Phase-contrast images of MSCs culture were taken at day-10. Magnification: 4X..... 51

Figure 9: Histogram representation of MSCs grown on Adipose-smeared, Dermis-smeared, BM-smeared, TCT and nTCT plates. All dishes were inoculated at 3.5 x $10^4$ cells/ ml (t = 0 day.) in D-MEM-F12-5% MSC-qualified FBS media. Cell counts were done every 2 days for 10 days. Bars represent means ± Standard Error Mean of four experimental rounds..... 57

Figure 10: Growth curve showing log phase on day-2, exponential phase from day-4 to day-8, and death phase on day-10. Data points represent means of four experimental rounds..... 57

Figure 11: Viability of MSCs Cultivated on adipose smeared, dermis smeared, BM-smeared, TCT and nTCT plates. All numbers represent the means of four experimental rounds..... 58

Figure 11.1: Expression of CD29, CD44, Sac-I and CD-117 markers. MSCs were stained over night with PE labelled anti-CD29, anti-CD 44, anti-Sca-I and anti-CD117 (1:5000 dilution; green) antibody after growth on dermis-smeared cover slips and cell nuclei were counterstained with DAPI (blue). Filter- TRITC. Magnification: 20X. Scale bars represents 0.2 mm. ..... 63

Figure 11.2: Expression of CD29, CD44, Sac-I and CD-117 markers. MSCs were stained over night with PE labelled anti-CD29, anti-CD 44, anti-Sca-I and anti-CD117 (1:5000 dilution; green) antibody after growth on BM-smeared cover slips and cell nuclei were counterstained with DAPI (blue). Filter-TRITC. Magnification: 20X. Scale bars represents 0.2 mm. ..... 64

Figure 11.3: Expression of CD29, CD44, Sac-I and CD-117 markers. MSCs were stained over night with PE labelled anti-CD29, anti-CD 44, anti-Sca-I and anti-CD117 (1:5000 dilution; green) antibody after growth on Adipose-smeared cover slips and cell nuclei were counterstained with DAPI (blue). Filter-TRITC. Magnification: 20X. Scale bars represents 0.2 mm. ..... 65

Figure 11.4: Expression of CD29, CD44, Sac-I and CD-117 markers. MSCs were stained over night with PE labelled anti-CD29, anti-CD 44, anti-Sca-I and anti-CD117 (1:5000 dilution; green) antibody after growth on poly-L-lysine coated TCT cover slips and cell nuclei were counterstained with DAPI (blue).Filter-TRITC. Magnification: 20X. Scale bars represents 0.2 mm. ..... 66

# INTRODUCTION

## Mesenchymal Stem Cells

### History of Mesenchymal stem cells

In 1960's and 1970's Friedenstein and coworkers (Friedenstein et al., 1970) demonstrated the osteogenic and fibroblastic potential of bone marrow (BM) sub-populations. It was observed that cell colonies appeared as fibroblast-like, elongated cells and adhered to the tissue culture vessel. The concept of "mesenchymal" stem cells was based on the pioneering work of Tavassoli and Crosby in the 1960's. While studying the importance of localization in the bone, they transplanted BM having boneless fragments in heterotopic sites and noticed the formation of bone tissues at that site, revealing that bone marrow has the capacity to form bone-tissues (Tavassoli et al., 1968). In Friedenstein's second breakthrough (Friedenstein, 1990), he found that in-vivo transplantation of a single progeny of BM stromal cell can generate multiple tissues (bone, cartilage, ligament, adipose tissue, dermis and muscle) and can be distinguished from hematopoietic cells. Hence, these cells were called "BM stromal stem cells" by Owen and Friedenstein. (Owen et al., 1988). The term "Mesenchymal stem cells" (MSCs) was first coined by Arnold Caplan in 1991. Since then based on studies related to the characterization of MSCs there has been constant reevaluation of the nomenclature from "BM stromal cells" (Owen et al., 1988) to "multipotent mesenchymal stromal cells." (International Society for Cellular Therapy, 2005).

**Characterization of Mesenchymal stem cells:**

The minimum criteria for cells to qualify as MSCs include that they should have self-renewing properties for regeneration of tissues after injury, they should include an immature population of heterogenous cells and they should be multipotent (Loeffler et al., 1997). MSCs are typically derived from bone-marrow and can adhere to plastic surfaces in-vitro giving rise to fibroblast like colonies. One of the defining characteristics of MSCs is that they appear spindle-shaped (Pittenger,et al., 1999). In addition to bone marrow, MSCs are also found in umbilical cord blood, adipose tissue (Grontos et al., 2001), fetal liver (Campagnoli et al., 2001) and lungs (Anker et al., 2003). These multipotent cells can differentiate into chondrocytes, adipocytes, osteoblasts and vascular smooth muscle cells (Delome et al., 2009 and Kurpinski et al., 2010). Another way to characterize MSCs is by cell surface markers (Cluster of Differentiation markers). CD markers expressed differentiate MSCs from hematopoietic stem cells. The first study related to cell surface markers led to the development SH2 and SH3 antibodies that can identify MSCs (Pittenger et al.,1999). The markers CD105 and CD70 recognize epitopes on SH2 and SH3 antibodies, respectively, and hence are considered positive markers for MSCs (Barry et al., 1999 and Barry et al., 2001). The negative markers like CD3, CD14, CD19, CD45 or CD34 are not expressed on MSCs because they are hematopoetic antigens and hence they distinctly distinguished hematopoetic cells (Pittenger et al., 1999). The MSCs derived from bone-marrow express CD44, CD29, Sca-I and CD90 (Baddoo et al., 2003, Boiret et al., 2005 and Cognet 1999). It was also found that the expresssion of surface antigens may

change during in-vitro cultivation due to changes in duration between passages, tissue of origin, interspecies differentiation and culture conditions. Some anitgens may be expressed on freshly isolated MSCs but may not be expressed in the cultures. One such example occurred while obtaining MSCs from mouse fetal lungs. CD34 was expressed on freshly isolated MSCs but was not expressed in-vitro (Fibbe et al., 2003). In recent studies it was found that MSCs can interact with cells of both the adaptive and innate immune systems. After in-vivo cultivation it was observed that MSCs can migrate to damaged tissues and inhibit the release of pro-inflammatory cytokines and promote the growth of damaged cells (Uccelli et al., 2008). MSCs that are cultivated should possess three properties for them to qualify for cellular therapy: a) immunoregulatory properties. b) potential of differentiation. c) trophic factors that are involved in tissue regeneration (Ma et al., 2014). These characteristics together with exceptional genomic stability and ethical issues, marks the importance of MSCs in tissue repair and regenerative medicine.

**Long-term *in-vitro* culturing of Mesenchymal stem cells**

Various approaches have been developed for expansion and growth of MSCs. Cells that adhere to plastic tissue culture plates grow within 5-7 days and appear symmetrical. Human MSCs grow most rapidly and retain their multipotential ability when cultured at relatively low densities ranging from $1x10^4$ to $0.4x10^6$ cells/$cm^2$ (Sekiya et al., 2001 and Freidestein et al., 1976). It was observed that initial cell seeding density not only affects the growth of MSCs, but it also affects their phenotypic characteristics. The cells in the growing stage at low density appear spindle shaped and when they are fully confluent they become flat with

split ends (Tropel et al., 2004). When cultured in-vitro MSC growth is characterized by three phases: a) An initial lag phase that lasts for 0-2 days. b) An exponential growth phase where cells reaches confluency. c) The stationary phase (Colter et al., 2001). Recent studies have shown that MSCs when grown under optimal conditions can have 20-50 population doublings. This indicates the great proliferative capacity of these cells and freshly isolated MSCs have proved to have higher differentiation capabilities compared to osteocytes, chrondrocytes and adipocytes. However, extensive subculturing of MSCs can lead to impaired cell function, apoptosis and increased malignant transformations, declining their multipotency (Cognet and Minguell , 1999 ; Rosland et al., 2009). Aging of MSCs can also lead to a decrease in telomerase activity (Kassem, 2004). Culturing of MSCs in serum free media has resulted in resistance to malignant transformation allowing continued expansion at higher passages without any chromosomal alteration. (Chen et al, 2014). The considerable therapeutic applications of MSCs has resulted in increased interest in long term culturing and *in-vitro* expansion of these cells.

**Applications of Mesenchymal stem cells**

MSCs have been shown to modulate immune responses to tissue injury and promote tissue repair *in-vivo*. Actions of MSCs include direct differentiation into bone cells, recruiting other cells, and creating a regenerative environment via production of tropic growth factors (Hang et al., 2018). Some studies suggest that MSCs can differentiate into cells of endoderm and ectoderm, like neurons and hepatocytes, apart from their mesodermal lineage (Schwartz et al., 2002; Tropel et al., 2006). This differentiation potential examined

by *in-vitro* cell based assays using differential media, has led to the current interest in the therapeutic applications of MSCs and to the focus on the immunosuppressive and anti-inflammatory properties of these cells. Clinical trials are underway examining these properties in the treatment of diseases like Alzheimer's, liver cirrhosis, spinal cord injury, organ transplantations and knee cartilage diseases (http://www.clinicaltrials. gov; accessed November 2014). Researchers have been studying the contact dependent mechanism of human adipose MSCs for regulation of inflammatory cytokines. One key mechanism of these anti-inflammatory properties is the secretion of soluble factors with paracrine factors. The paracrine effects in MSC-conditioned medium was observed to protect cardiomyocytes by inhibiting the mitochondrial mediated apoptotic pathway (Park et al., 2012). The tropism of MSCs to tumor sites make them an important vector for therapeutic agent delivery to tumors and metastatic niches. They can be genetically modified by virus vectors to encode for tumor suppressor genes and immunomodulating cytokines (Daria et al., 2018). Adipose MSCs play a protective role against liver fibrosis and are immunocompatible and easier to isolate than bone-marrow MSCs (Schubert et al., 2011). On the other hand, bone marrow cells have the capability to differentiate into hepatic cells and recover liver functions (Jang et al., 2014). Therefore, the use of MSCs could lead to various possibilities of correcting inherited disorders and tissue regeneration. The antiproliferative and immunomodulatory functions of MSCs are being currently studied to develop therapeutic strategies for autoimmune diseases, bone marrow transplantations and various other cell based therapies.

## Extracellular matrix

### Composition and Functions of Extracellular Matrix

Cells, biochemical signals and Extracellular Matrix (ECM) are the underlying components of tissues within the body and during a human or organism's lifetime these tissues keep regenerating. ECM is a non-cellular component that is present in all organs and tissues which acts like glue that binds cells together in connective tissue (Rolfe and Grobbelaar, 2012). ECM is not only necessary for physical scaffolding but also provides biomechanical indicators needed for tissues morphogenesis and homeostasis. It is composed of proteins, water and polysaccharides. Each tissue of the body has ECM with varying composition depending on the development of the tissue through various biochemical and biophysical mechanisms between various cellular components. Earlier it was believed that ECM is a stable component that plays a supportive role in maintaining tissue morphology, but studies show that ECM is also an essential part of the cell's environment that is versatile and influences the foundation of cell biology (Hynes, 2009). ECM is a dynamic structure that is remodeled constantly, enzymatically or non-enzymatically, and its molecular components are exposed to post-translational modifications. Through these modifications ECM generates the mechanical properties for each tissue like elasticity, tensile strength and maintaining water retention. ECM is composed of two main classes of proteins namely, fibrous proteins and proteoglycans (Jarvelainen et al., 2009 and Schaefer et al., 2010). Proteoglycans are present in the extracellular interstitial space within the tissue in the form of a hydrated gel (Jarvelainen

et al., 2009). Proteoglycans are made up of glycosaminoglycans (GAGs) and are covalently attached to the core proteins. GAGs are attached to the core protein perpendicularly giving rise to brush-like structures (Iozzo et al., 2009). GAGs are the most abundant heteropolysaccharides present in the body tissues. Proteoglycans act as cell surface receptors for different enzymes. Proteoglycans present in ECM bind to different growth-factors and cytokines to prevent their degradation by proteases. Proteoglycans and GAGs in particular co-ordinate with proteins like integrins and facilitate cell-cell interactions and cell attachment. GAGs play an important role in coagulation, host defense and wound repair. The fibrous proteins of ECM include fibronectin, laminin and collagen (Alberts et al., 2007). Collagen is the most abundant fibrous protein present in the interstitial ECM of connective tissue such as skin and tendons (Kular et al ., 2014). It constitutes up to 30% of the total proteins present in multicellular organisms. Collagen is fibril-like and comprises the main structural element of the ECM that provides tensile strength, cell-adhesion, supports chemotaxis and directs tissue development (Rozario et al., 2010). There are almost 30 types of collagen identified (I, II, III, IV, V, etc.) and the fibril arrangements gives strength to the connective tissues that are required to withstand mechanical shear and pressure. Collagen type I is the most dominant form of ECM protein found in all the tissues, particularly in skin and tendon. Collagen II is found in the cornea and cartilage, whereas Collagen III is most abundant in the walls of the blood vessels (Kular et al ., 2014). The second fibrous protein in ECM is fibronectin. It is not unique to connective tissue and is expressed by various cell types. Fibronectin is arranged like a mesh

of fibrils, similar to collagen and is linked by integrins (surface receptor). Fibronectin is linked by disulphide bond which can be broken down into identical monomer subunits. Fibronectin is involved in directing the organization of the ECM and plays a crucial role in cell attachment. It is also an important factor for cell migration and has been implicated in cardiovascular diseases and tumor metastasis (Tsang et al., 2010). Fibronectin also has a role in embryonic development where it aids in positioning of cells within the ECM. The third fibrous protein in the ECM is laminin. Laminin is a type of glycoprotein with a trimeric structure. It is mainly involved in cell differentiation and cell migration (Eckes et al., 2010). It is the protein first identified in the embryo and is important for differentiation to the extent that a defect in the gene coding for laminin can have fatal results in the embryo or can affect multiple organs. The structure and composition of the ECM is complex and the realization that the organization of ECM is a crucial aspect of cell behavior has led to the development of new technologies in which ECM fiber size, stiffness and remodeling potential can be controlled and monitored.

**Importance of Extracellular Matrix**

Considering the importance of ECM to so many cellular processes tissue culture models of ECM have been created. Major cancer research has relied on coated tissue culture plates with a mixture of ECM preparations in order to obtain 2D monolayer cell cultures (Kuschel et al., 2006). This environment is technically different from that experienced by cells in the body. The main deficiency is the geometric arrangement of the cells (cells have a flat 2D structure instead of 3D orientation). Due to these deficiencies,

cells cultured on culture plates via conventional methods do not have a similar morphology as that in body. To fix the ECM rigidity, polyacrylamide gels crosslinked with reconstituted basement membrane containing ECM components were developed. To address the aspect of 3-D ECM remodeling, scientists have used natural ECM and reconstituted ECM gels to recapitulate tissue specific differentiation. For example, 3-D organotypic culture assays have been developed containing ECM components for xenotransplantation and tissue engineering. But, this also provides an unnatural environment for cell growth and has provided little improvement. To overcome this issue tissue engineers have developed natural scaffolds by isolating the ECM. These purified ECMs have been used in skin grafts, to enhance healing, and to study tumor progression (Badylak et al., 2007). To grow healthy stem cells in-vitro a natural environment is needed which can be provided by decellularized ECM preparations. In addition to the implantation of stem cells, decellularized ECM preparations have also proven effective in the constructive remodeling of injured tendons and ligaments via xenotransplantation. For this porcine decellularized ECM was used to grow healthy human tenocytes which were then recellularized and used to replace injured tendons and ligaments (Swinehart et al., 2016 and Gundula et al., 2012). Recent studies show that when decellularized rat's hearts were seeded with cardiac cells, the heart tissues were repopulated and differentiated to the extent that the hearts began beating on their own (Ott et al., 2008). Hence decellularized ECM will provide the groundwork needed for studying the fundamental characteristics of the stem cells in tissue engineering.

# METHODOLOGY

## Decellularization of Bone-marrow, Dermis and Adipose tissues

Porcine ribs and feet (no antibiotics, no added hormones, no preservatives) were purchased from a local grocery store. For the BM pieces, the muscle and connective tissue was removed from the porcine ribs, which were then cut into 0.5 - 1.0 $cm^3$ pieces with a saw. The periosteum and compact bone were further removed. For adipose tissue, the fatty tissues were separated from the rib muscle and cut into 1.0-2.0 $cm^3$ with a scalpel. For dermis, skin on porcine feet was removed, scraped to remove deeper tissues and cut into 1.0-2.0 $cm^2$ piece with a scalpel. The tissues were frozen at -20°C and thawed at 37°C three times over a one hour period in a mixture of 0.1 M phosphate buffer (PB) and 2% TritonX-100. Thereafter, the tissues were incubated in 70% ethanol for three days at 4°C on a shaker. After three days, the tissues were incubated in a mixture of DNase I and 0.1 M PB (0.2 mg DNase I in 1 ml 0.1 M PB) for two hours at 37°C. The tissues were rinsed thoroughly in 0.1 M PB at room temperature (R.T) for an hour with continuous shaking. Finally, the tissues were rinsed in 70% ethanol for four hours on a shaker. The tissue pieces were transferred into glass vials (approximately four pieces per vial), were stored at -20°C for 24 hours, then transferred into -80°C freezer before proceeding further.

## Lyophilization of Bone-marrow, Dermis and Adipose tissues

After two days of incubation in a -80°C freezer, the BM, dermis and adipose tissues were lyophilized in a Labconco FreeZone 4.5 lyophilizer attached to a Labconco Model

117 vacuum pump. The tissues were lyophilized for five days at 0.09 mBar, -40°C and afterwards stored at -20°C until used.

## Preparation of Tissues for Histological Analysis

Fresh, decellularized and lyophilized tissue samples were prepared for histological analysis using following procedures:

### Decalcification of Bone-marrow pieces

For histological sectioning fresh, decellularized and lyophilized BM pieces were immersed in a 20% EDTA solution at pH 7.2 in two serparate jars. The jars were kept a on magnetic stirrer for five days with continuous shaking until the bone decalcified and softened.

### Cryo Sectioning of Bone-Marrow, Dermis and Adipose tissues

The fresh, decellularized and lyophilized tissues were fixed in 4% paraformaldehyde for 24 hours at 4°C. The BM pieces were placed in a beaker containing gelatin, the beakers were then placed in a IsotempVaccum Oven (Fisher Scientific) for 5 hours at -22 In.Hg. The tissues were subsequently embedded gelain (10% gelatin and 30% sucrose in 100 ml $H_2O$) in 22 mm square disposable histolgy molds (Peel-A-Way). After the gelatin was solidified the sides of the molds were peeled with a razor. The gelatin embedded tissues were fixed in 4% paraformaldehyde overnight. The embeded tissues were placed on the cryostat stage and frozen using dry ice. 40 µm sections of the tissues were cut and collected in 0.1 M PB. The sections were mounted on glass slides and allowed to dry for 24 hours before proceeding with staining.

## Hemotoxylin and Eosin Staining

The fresh, decellularized and lyophilized tissue samples were analysed for presence of nuclei using hemotoxylin and eosin (H&E). Slide mounted, air dried tissue sections were first immersed in 100 % dehydrant for 3 minutes followed by rinsing in tap water and deionized water briefly. The slides were then immersed in hemotoxylin (VWR®) for 1.5 minutes. Eexcess stain was rinsed off with water. The tissues were then immersed in clarifier for 30 seconds, rinsed with water, and then immersed in bluing reagent for a minute, followed by a rinse in water. Before immersing the tissues in eosin they were rinsed briefly in 100 % dehydrant followed by eosin (Richard-Allan Scientific™) for 1.5 minutes. Finally the tissues were left in 100 % dehydrant for 3 minutes and then in clear-rite 3 until coverslipped. The stained tissues were evaluated by light microscopy.

## Alcian Blue Staining

The fresh, decellularized and lyophilized tissues were stained for GAGs using alcian blue. Slide mounted,air dried sections were first rehydrated with $dH_2O$ for 30 minutes and then stained with 1% Alcian Blue 8GX at a pH of 2.5 for 1 hour (Sigma-Aldrich). After incubation, sections were rinsed in $dH_2O$, followed by rinsing in 50% dehydrant, 70% dehydrant, 95% dehydrant for few seconds respectively. Finally the sections were immersed in clear-rite 3 until coverslipped. Alcian Blue staining was evalauted by light microscopy.

## Immunohistochemistry

The fresh, decellularized and lyophilized tissues were sectioned as decribed above, mounted on glass slides and allowed 24 hours to dry and then rehydrated in 0.1 M PB for 30 minutes at room temperature (R.T). The non-specific proteins in the histological sections were blocked for 15 minutes with 0.1M PB supplemented with horse serum and triton-X 100. To analyze the ECM protein composition of the tissues, they were stained overnight (1:2000 dilution) at 4ºC with primary antibodies namely: monoclonal mouse anti-collagen type I, II, IV, rabbit anti-laminin and rabbit anti-fibronectin (Sigma-Aldrich). The next day the sections were rinsed three times at 10 minute intervals with 0.1 M PB containing horse serum and triton-X 100. Binding of the primary antibodies was revealed using secondary antibodies using two different techniques as follows:

**Avidin-Biotin Complex (ABC) – Vectastain kit**

The sections were incubated for 1 hour in biotinylated secondary antibodies namely: anti-rabbit or anti-mouse (Vector Laboratories). Sections were rinsed three times at 10 minutes intervals with 0.1M PB containing horse serum and triton-X 100. The sections were incubated in ABC reagent (2 drops of reagent A+ 2 drops of reagent B per 10ml 0.1M PB containing triton-X 100, Vector Laboratories) for 45 minutes. The sections were then rinsed three times in at 10 minutes intervals with 0.1 M PB containing horse serum and triton-X 100. The sections were again incubated in biotinylated secondary antibody followed by ABC reagent for 30 minutes each. After the second incubation in ABC reagent, sections were rinsed in 0.1 M PB four times at 10 minutes interval. The

sections were incubated in 0.1 M acetate buffer (pH 6) for 5 minutes. A solution of Diaminobenzidine [(DAB) 5mg] and Nickel Ammonium Sulphate ( 0.16 g) was prepared in 10 ml 0.1 M acetate buffer followed by incubation of sections in the Nickel-DAB solution for 5 minutes. Finally, 1% hydrogen peroxide ($H_2O_2$) was added to the Nickel-DAB solution, producing a brownish-black reaction product indicating positive immunolabeling. The reaction was stopped by rinsing sections with 0.1 M acetate buffer overnight. Next day, sections were rinsed thoroughly in 0.1 M PB, mounted in glycerol and analyzed under light microscope.

**Fluorescent Immunostaining**

Sections were processed with primary antibody as described above. For fluorescent immunostaining the sections were incubated overnight at 4°C with VectaFluor™ DyLight® 594 conjugated anti-mouse or anti-rabbit IgG, secondary antibodies (Vector Laboratories, Inc.) Next day, sections were rinsed thoroughly with 0.1 M PB, mounted in glycerol and analyzed for immune positive staining using Nikon Optiphot-2 microscope with fluorescence microscope attachment. Negative staining controls were performed by omitting the primary antibody incubation step.

## Thawing and Establishing Mesenchymal Stem Cell Cultures

Mouse mesenchymal stem cells (C57BL/6) were purchased from Cyagen Biosciences Inc. and brought up in a 37 °C water bath as recommended by the company. After thawing completely, the cryovial was wiped with 70% EtOH and the cell suspension was transferred into a sterile 15 mL conical tube (17 mm x 120 mm, BD Falcon) in a sterile Biosafety level 2 hood. Pre-warmed 9 ml of MSC growth media [GIBCO® Dulbecco's Modified Eagle Medium: Nutrient Mixture F-12 Media (Life Technologies) supplemented with GIBCO® GlutaMAX™-I (Life Technologies), 5% MSC-qualified FBS (Life Technolgies) and PSG (Life Technologies)] was added to the cell suspension. The cell suspension was then centrifuged (1.7 RPM, 1.45 minutes, R.T). The supernatant was aspirated, and the cells resuspended in 5 mL MSC growth media. For establishing a primary cell culture, 5 mL of cell suspension was transferred into a T75 culture flask (BD Bioscience) with 15 mL MSC growth medium (each vial of Cyagen Mouse C57BL/6 MSCs contains roughly 1 x $10^6$ viable cells / mL). The culture was incubated at 37°C, 5% CO2, in a humidified environment reaching 80% confluence was reached. The medium was changed every second day before cells were sub-cultured.

## Passaging Mice Mesenchymal Stem Cells

At 80% confluence cells were passaged. The spent MSC growth medium was aspirated from the culture vessel and a sufficient volume of pre-warmed GIBCO® 0.25% trypsin-EDTA (Life Technologies) was added to fully cover the adhered cell layer (15 mL for T75 flask). The suspension was incubated at 37°C until complete detachment of cells

from the surface of the flask could be observed using an inverted microscope. Once the MSCs were detached, the surface was flushed with the MSC growth medium to ensure all cells had released. The cell suspension was then transferred to a sterile 15 mL conical tube (17 mm x 120 mm, BD Falcon). The cells were pelleted out after centrifugation (1.7 RPM, 1.45 minutes, room temperature) and the supernatant aspirated. The cells were resuspended in 5ml MSC growth medium. The number of viable cells present in the cell suspension needed to inoculate new T75 flask was determined using Muse® Cell Analyzer. The resuspended cells were seeded at a seeding density of 5,000 cells / $cm^2$ which is equivalent to 3.75 x $10^5$ cells for a T75 flask in 15 ml MSC growth medium. Following seeding, the medium in the cultivation vessel was swirled to evenly distribute the cells and the culture was incubated at 37°C, 5% CO2 in a humidified environment.

**Freezing of Mouse Mesenchymal Stem cells**

Mouse MSCs were frozen according to the protocol provided by Invitrogen (Catalog no. S1502-100). Two freezing media, namely A (40% D-MEM/F-12 medium with GlutaMAX™-I, 60% MSC-qualified FBS) and B (20% DMSO, 80% D-MEM/F-12 medium with GlutaMAX™-I) were prepared fresh. Freezing medium B was kept at 4°C until used, while freezing medium A was allowed to warm to room temperature. The MSCs growth medium was aspirated from the culture vessel and the cells were detached from the surface as described previously in the "Passaging of Mesenchymal Stem Cell" section. After the centrifugation step, the MSCs were resuspended in freezing medium A at a concentration of 2 x $10^6$ cells/ mL. The same volume of freezing medium B was added

dropwise to the cell suspension to bring the final cell concentration to 1 x $10^6$ cells / mL. From the cell suspension 1 mL was aliquots were prepared into a 1.5 mL freezing vials (Corning) and stored at -80°C. After 24 hours at -80°C , freezing vials were transferred to a cryopreservant at -196°C for long-term storage.

**Experimental Cultivation Round**

An experimental cultivation round consisted of the following plate types: nTCT [negative control] (100mm x 15mm; Fisherbrand®), TCT [positive control] (100mm x 20mm; BD Falcon), BM-smeared nTCT (experimental plate), Dermis-smeared nTCT (experimental plate) and Adipose-smeared nTCT (experimental plate). In total, five different incubation times were selected ranging from two to ten days in two-day intervals to cover the lag, exponential, and stationary growth phases. For each incubation time, four plates of each type were seeded at 3.5 x $10^4$ cells / mL in 10 mL MSC growth medium, corresponding to time zero. All plates were then incubated at 37°C, 5% CO2 in a humidified environment for the duration of MSC cultivation (two, four, six, eight, and ten days). At the given incubation point cell morphology and cell growth were analyzed as described below. In addition, immunophenotype was analyzed after cultivation for two, six and ten days.

## Cell Morphology

MSC morphology was assessed using a phase-contrast microscope (Olympus CK2, Dexter Instrument Co., Inc. San Antonio Texas, USA) and photographs were taken at 4 fold magnification (INFINITY1-1M, Lumenera Corporation, Canada) at multiple points in the cultivation dish.

## Cell Count and Viability

Mouse MSCs in culture were counted and analyzed for viability using the Muse Count & Viability kit on the Muse® Cell Analyzer (Merck Millipore, Billerica, MA, USA). According to the use user's kit guide, a dilution of 1:20 was used (20 µL cell suspension + 380 µL Cell count and viability reagent). The readings displayed on the Muse® Cell Analyzer are as follows:

Viable Cells / .....(1)

Viability % .....(2)

Total Cells / mL .....(3)

Total viable cells in original sample .....(4)

Total cells in original sample .....(5)

Dilution Factor .....(6)

Original volume .....(7)

Based on the above readings Cells / $cm^2$ was calculated using the formula:

Cells / $cm^2$ = Total viable cells in original sample / Surface area cultivation vessel.

Population doubling time = (T) ln2/ ln [Xe / Xb]

Where, T = time interval between Xe and Xe (Exponential phase)

Xe = Cell number at the end of the incubation time

Xb = Cell number at the beginning of the incubation time

**Immunophenotyping of Mouse Mesenchymal Stem cells**

MSCs were grown on cover slips coated with 0.01% poly-L-lysine [positive control (Sigma-Aldrich, USA)], BM-smeared, Dermis-smeared, or Adipose-smeared coverslips for day two, six and ten. All the smeared and poly-L-lysine coated coverslips were placed in the nTCT dishes seeded with 3.5 x $10^4$ cells / mL in 10 mL MSC growth medium. On the second, sixth and tenth day cells were fixed in 4% paraformaldehyde, washed in CD buffer [1X PBS (pH 7.2), 0.5% bovine serum albumin, 2 mM EDTA] and analyzed using mouse phycoerythrin labeled anti-CD29, anti-CD44, and anti-Sca-1 antibodies as positive markers for an undifferentiated MSC state and anti-CD117 (Miltenyi Biotec) as negative marker. The phenotype list provided by the MSC supplier (Cyagen Biosciences Inc.) was used as a reference for choosing the above named markers. Based on the manual from Cyagen Biosciences Inc. undifferentiated MSCs should express CD29, CD44 and Sca-1 (>70%) but not CD117 (<5%). Coverslips were incubated for 48 hours at 4°C at an antibody dilution of 1:5000. Afterwards cover slips were washed twice in buffer and mounted in glycerol mixed at a 1:1 dilution with 4',6-diamidino-2-phenylindole (DAPI, Sigma-Aldrich). Fluorescence microscopy images of stained MSCs and nuclei were taken at 20-fold magnification using the TRITC (tetramethyl rhodamine isothiocyanate) and DAPI filters on a Nikon Optihot-2 fluorescence microscope (Nikon).

## Photomicrographic Documentation and Processing

Stained MSCs and ECM proteins were observed by fluorescence and light microscopy (Nikon Optiphot-2 fluorescence microscope; Nikon, Tokyo, Japan). Digital images were taken with a Nikon Digital Camera DXM1200 and ACT-1 Nikon software (Nikon, Tokyo, Japan). Immunohistochemistry images were processed for scaling and measuring the intensity of brightness using Image J (National Institute of health).

## Statistical Analyses

Statistical analyses were done to compare the MSC cell growth on the three experimental substrates, the TCT plates and the nTCT plates. Data were expressed as the Mean (Cells / $cm^2$) ± Standard deviation (SD) of four trials. Independent sample *t*-tests were performed comparing the mean values of the experimental substrates using SPSS16.0 software (SPSS Inc., Chicago, IL, USA). Graphs of the data were plotted using Microsoft Excel. Differences with p-values $<0.05$ were considered statistically significant. The factors were the BM smear vs. Adipose smear vs. Dermis smear vs. TCT vs. nTCT and days of incubation (two, four, six, eight and ten days).

# RESULTS

## Histological Analyses

### The decellularization process

A chemical method was established to decellularize the BM, dermis and adipose tissues in a way that their ECM characteristics were maintained. The protocol was developed using tissues purchased from a local grocery store. At the end of the 7-day extraction process a significant volume of loose white matrix was collected (Fig.1). The tissues were then lyophilized for 5-days. Qualitatively, the decellularized and lyophilized tissues had similar dimensions to the tissue block at the beginning of the processing. Standard histological staining with Hematoxylin and Eosin (H&E) served as a first line of inspection to determine the presence of nuclear structures. The tissues were stained with H&E before and after decellularization. Decellularized tissues showed lack of H & E stained nuclei indicating efficient cell removal as compared to fresh unprocessed tissues which showed heavy nuclear staining throughout the tissues (Fig.2.1, 2.2 and 2.3).

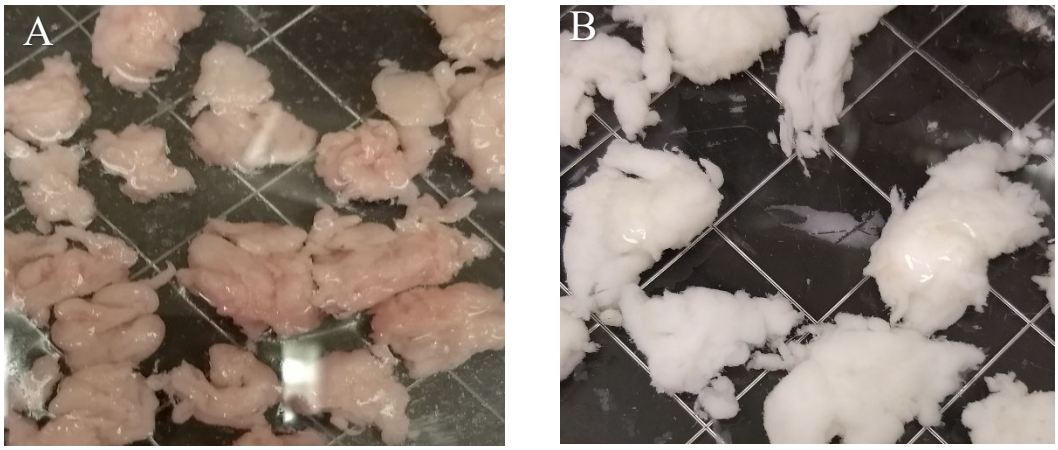


*Figure 1:Macroscopic images of (A) fresh adipose tissue blocks prior to processing and (B) the resultant tissue after decellularization.*

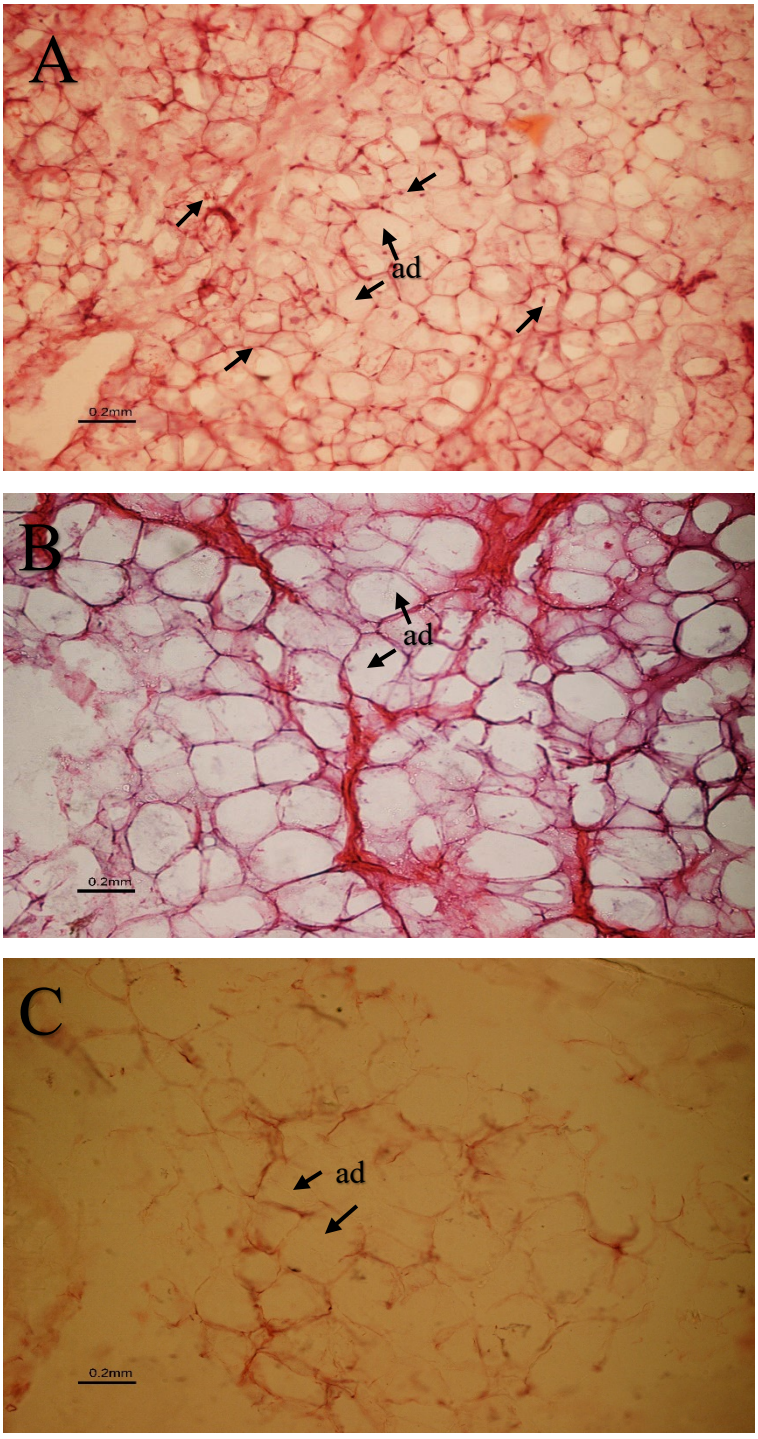


*Figure 2.1: H&E staining (cell nuclei, purple spots; cytoplasm, pink) of (A) fresh adipose tissue, (B) decellularized adipose tissue and (C) lyophilized adipose tissue showing adipocytes (ad). Scale bars represents 0.2mm.*

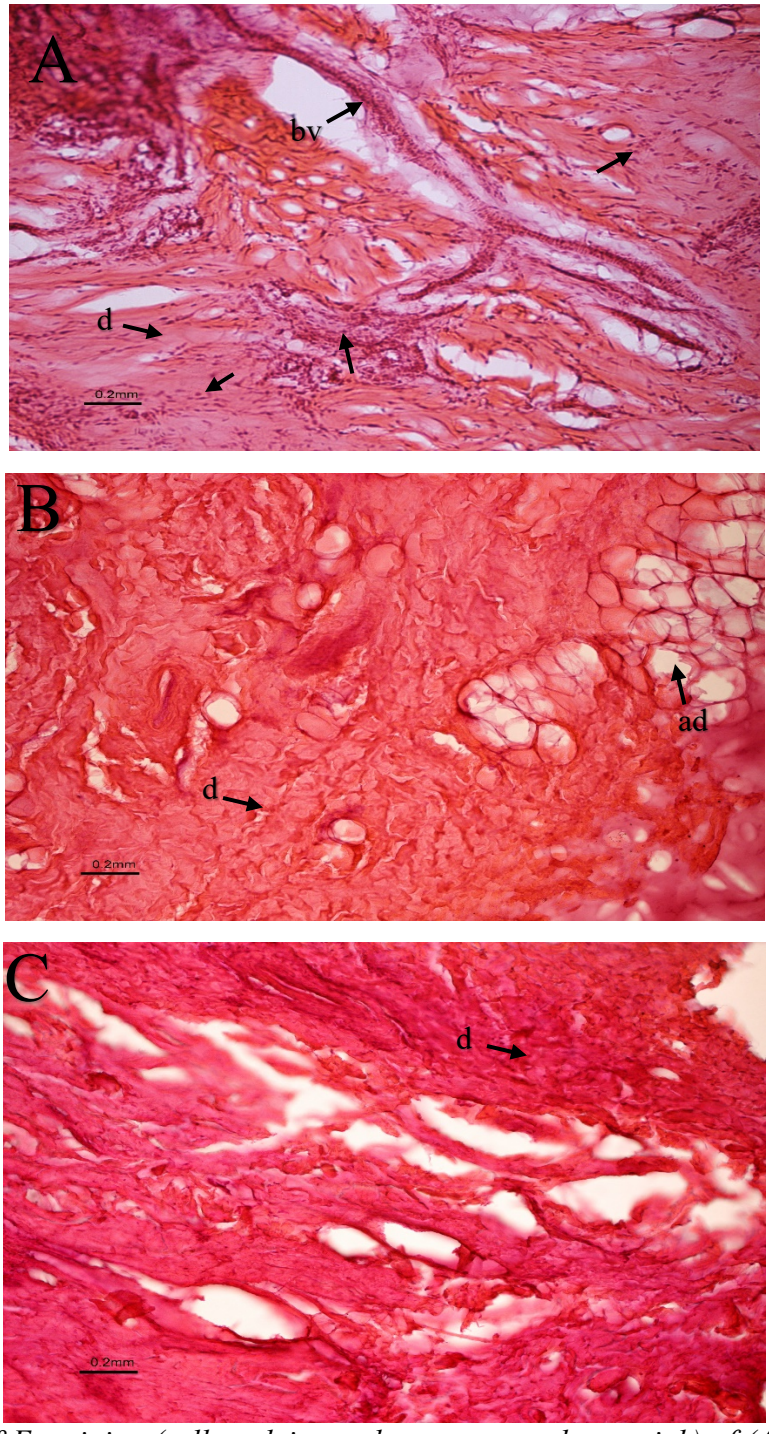


*Figure 2.2: H&E staining (cell nuclei, purple spots; cytoplasm, pink) of (A) fresh dermis, (B) decellularized dermis and (C) lyophilized dermis showing dermis (d), adipocytes (ad) and blood vessel (bv). Scale bars represents 0.2mm.*

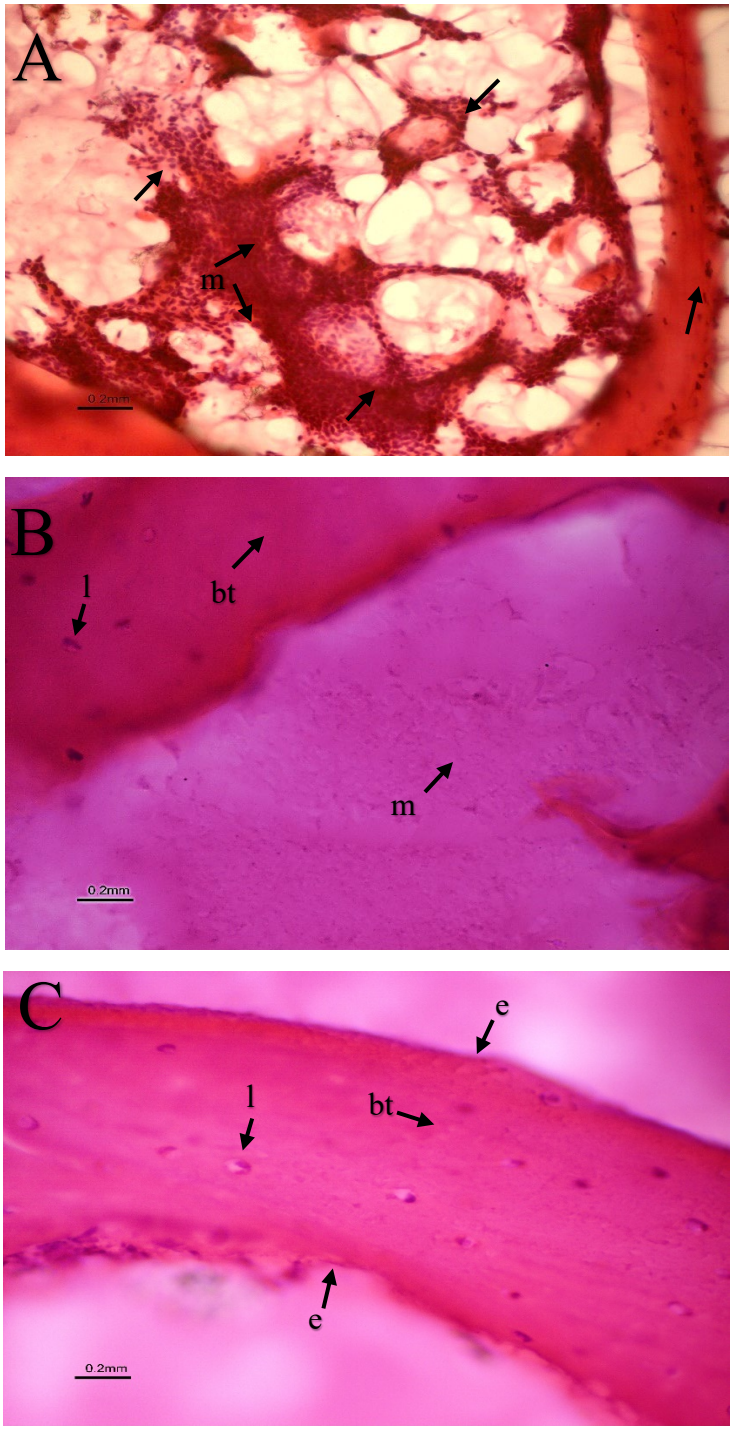


*Figure 2.3: H&E staining (cell nuclei, purple spots; cytoplasm, pink) of (A) fresh BM, (B) decellularized BM and (C) lyophilized BM showing marrow (m), endosteum (e), lacunae (l) and bone trabeculae (bt). Scale bars represents 0.2mm.*

**ECM structure and composition following decellularization**

Using light and fluorescence microscopy, the locations of key ECM proteins including GAGs, fibronectin, laminin and collagen (I, III, IV) in gelatin embedded BM, dermis and adipose sections were mapped.

***GAGs analysis***

Distribution and localization of GAGs in fresh, decellularized and lyophilized BM, adipose and dermis sections was investigated by Alcian Blue staining. The staining pattern as well as the intensity for GAGs was evaluated qualitatively by light microscopy (Fig 3). The highest intensity of GAGs was observed on walls of adipocytes in fresh adipose tissue (Fig 3- A); followed by linings of epidermis and blood vessel in fresh dermis (Fig 3- D); and trabeculae, endosteum and marrow of fresh BM (Fig 3- G). The intensity of GAGs slightly decreased after the tissues were processed and was observed in decellularized and lyophilized adipose tissues ( Fig 3- B and C), dermis (Fig 3- E and F) and BM (Fig 3- H and I). Overall, there was an equal distribution of GAGs throughout the unprocessed and the processed porcine tissues.

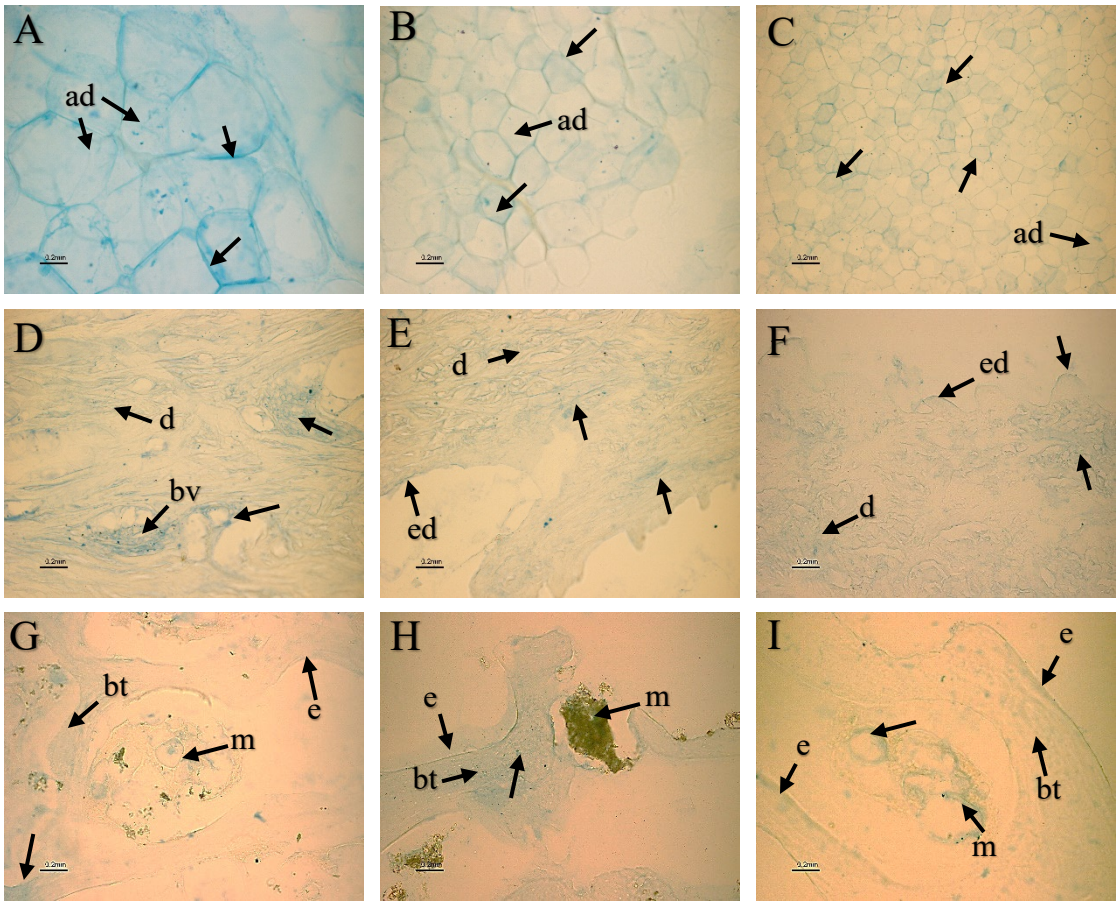


*Figure 3: Sections of porcine tissues (A) fresh adipose, (B) decellularized adipose and (C) lyophilized adipose showing adipocytes (ad); (D) fresh dermis, (E) decellularized dermis and (F) lyophilized dermis showing epidermis (ed), dermis (d) and blood vessel (bv); (G) fresh BM, (H) decellularized BM and (I) lyophilized BM showing marrow (m), endosteum (e) and bone trabeculae (bt). Labelled with Alcian blue stain specific for extracellular matrix protein GAGs.. Arrows indicate GAGs throughout the adipose, dermis and BM tissue ECM. Scale bars represents 0.2mm.*

***Distribution of Fibronectin, Laminin, Collagen I, III and IV***

Immunohistochemistry staining localized the ECM proteins in the fresh, decellularized and lyophilized porcine tissues. Very high levels of fibronectin and laminin were detected in fresh adipose tissue (Fig 3.1- A, D and Fig 4.1- A, D); linings of epidermis and blood vessels of fresh dermis (Fig 3.2- A, D and Fig 4.2- A, D); trabeculae, endosteum

and marrow of fresh BM (Fig 3.3- A, D and Fig 4.3- A, D). Overall, there was an equal distribution of fibronectin and laminin throughout the fresh porcine tissues. Immunolabelling of collagen-I was slightly lower than fibronectin and laminin in terms of brightness as measured using the Image J software but present in high levels in adipose and blood vessel walls of fresh adipose tissue (Fig 5.1- A, D); equally distributed throughout fresh dermis (Fig 5.2- A, D); it was also detected in the marrow, endosteum, trabeculae and the walls of blood vessels in fresh BM, although the amount of immunopositivity varied greatly with some areas having very high levels of expression and others having much lower expression (Fig 5.3- A, D). In contrast collagen-III and collagen-IV was only detected in sporadic regions of fresh adipose (Fig 6.1- A, D and 7.1- A, D), fresh dermis (6.2- A, D and 7.2- A, D) and fresh BM (Fig 6.3- A, D and Fig 7.3- A, D). It was also observed that staining intensity of decellularized adipose (Fig 3.1- B, E; Fig 4.1- B, E; Fig 5.1- B, E; Fig 6.1- B, E; Fig 7.1- B, E), decellularized dermis (Fig 3.2- B, E; Fig 4.2- B, E; Fig 5.2- B, E; Fig 6.2 Fig- B, E; Fig 7.2- B, E) and decellularized BM (Fig 3.3- B, E; Fig 4.3- B, E; Fig 5.3- B, E; Fig 6.3 Fig- B, E; Fig 7.3- B, E) for fibronectin, laminin, collagen-I, collagen-III and collagen-IV, respectively, was reduced as compared to the fresh porcine tissues. Lastly, the staining intensity of lyophilized adipose (Fig 3.1- C, F; Fig 4.1- C, F; Fig 5.1- C, F; Fig 6.1- C, F; Fig 7.1- C, F), decellularized dermis (Fig 3.2- C, F; Fig 4.2- C, F; Fig 5.2- C, F; Fig 6.2 Fig- C, F; Fig 7.2- C, F) and decellularized BM (Fig 3.3- C, F; Fig 4.3- C, F; Fig 5.3- C, F; Fig 6.3 Fig- C, F; Fig 7.3- C, F) for fibronectin, laminin, collagen-I, collagen-III and collagen-IV, respectively, decreased even further and the ECM proteins were unevenly distributed throughout the tissues (Tables 1.1-1.5 and 2).

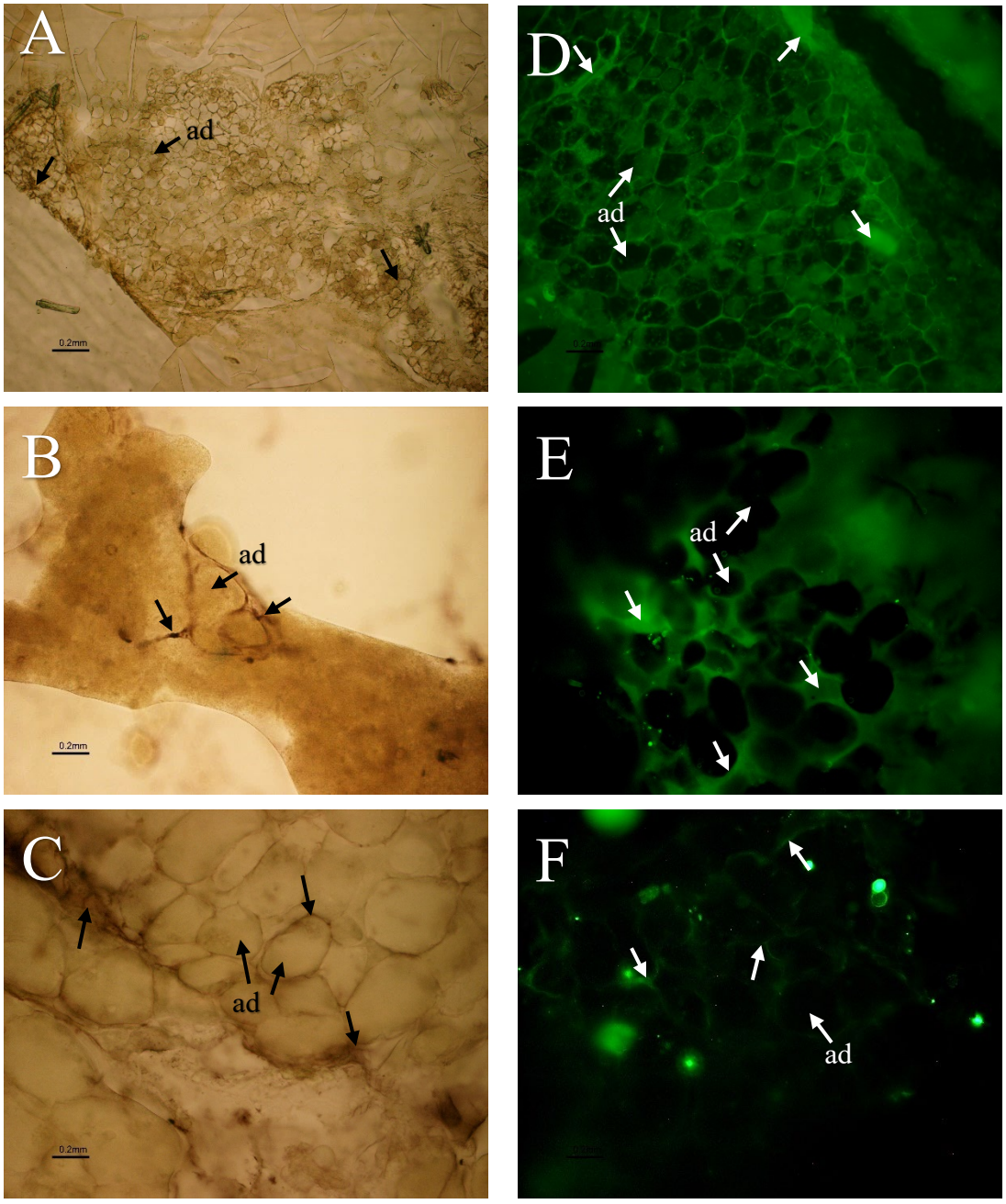


*Figure 3.1: Sections of porcine tissues (A, D) fresh, (B, E) decellularized and (C, F) lyophilized adipose tissue showing adipocytes (ad). Labelled with antibody specific for extracellular matrix protein fibronectin. Images A, B and C stained using ABC-vectastain kit and Images D, E and F stained using fluorescence kit (filter-FITC). Arrows indicate fibronectin labelling throughout the adipose tissue ECM. Scale bars represents 0.2mm.*

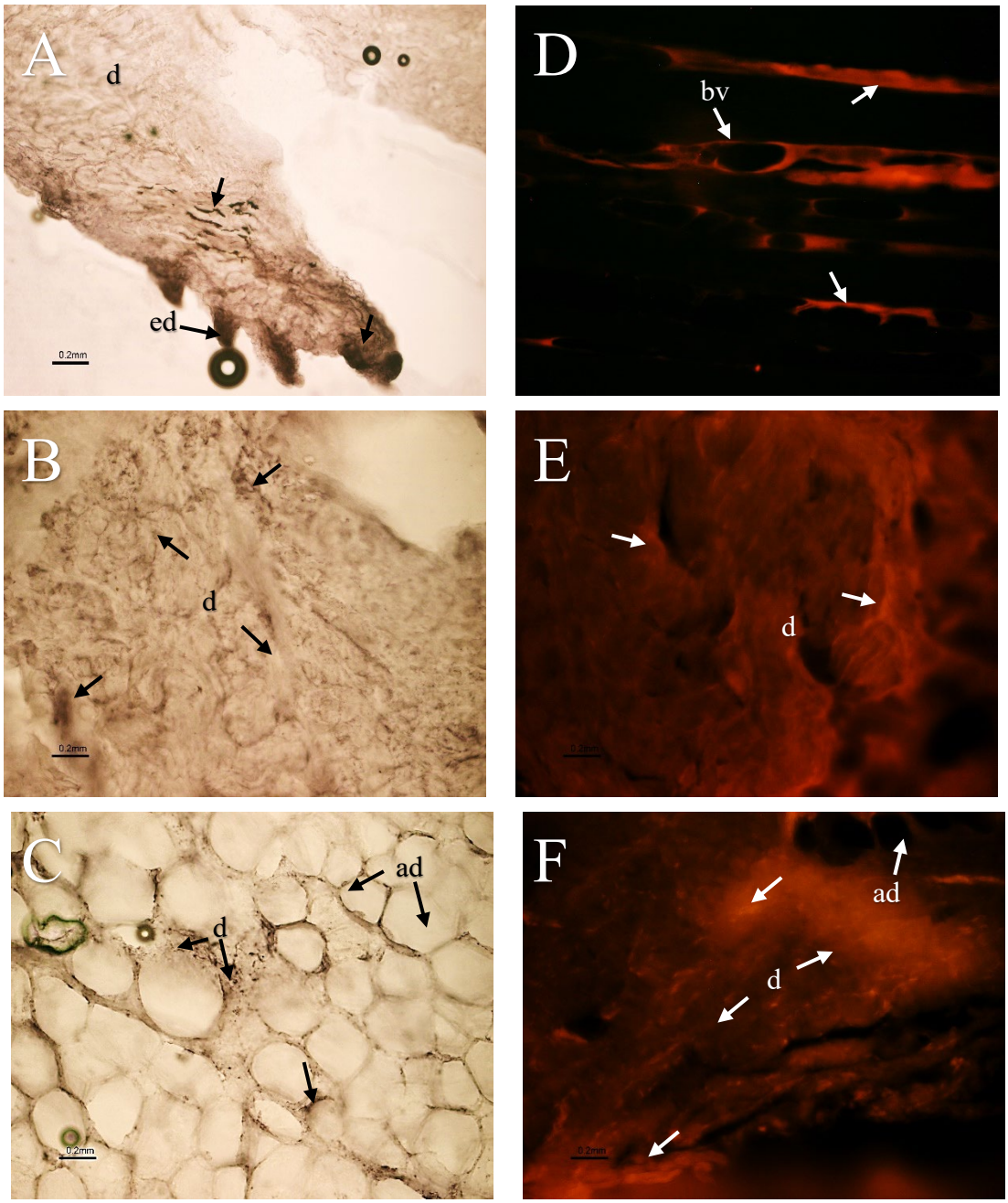


*Figure 3.2: Sections of porcine tissues (A, D) fresh, (B, E) decellularized and (C, F) lyophilized dermis showing dermis (d), epidermis (ed), blood vessel (bv) and adipocytes (ad). Labelled with antibody specific for extracellular matrix protein fibronectin. Images A, B and C stained using ABC-vectastain kit and Images D, E and F stained using fluorescence kit (filter-TRITC). Arrows fibronectin labelling throughout the dermis ECM. Scale bars represents 0.2mm.*

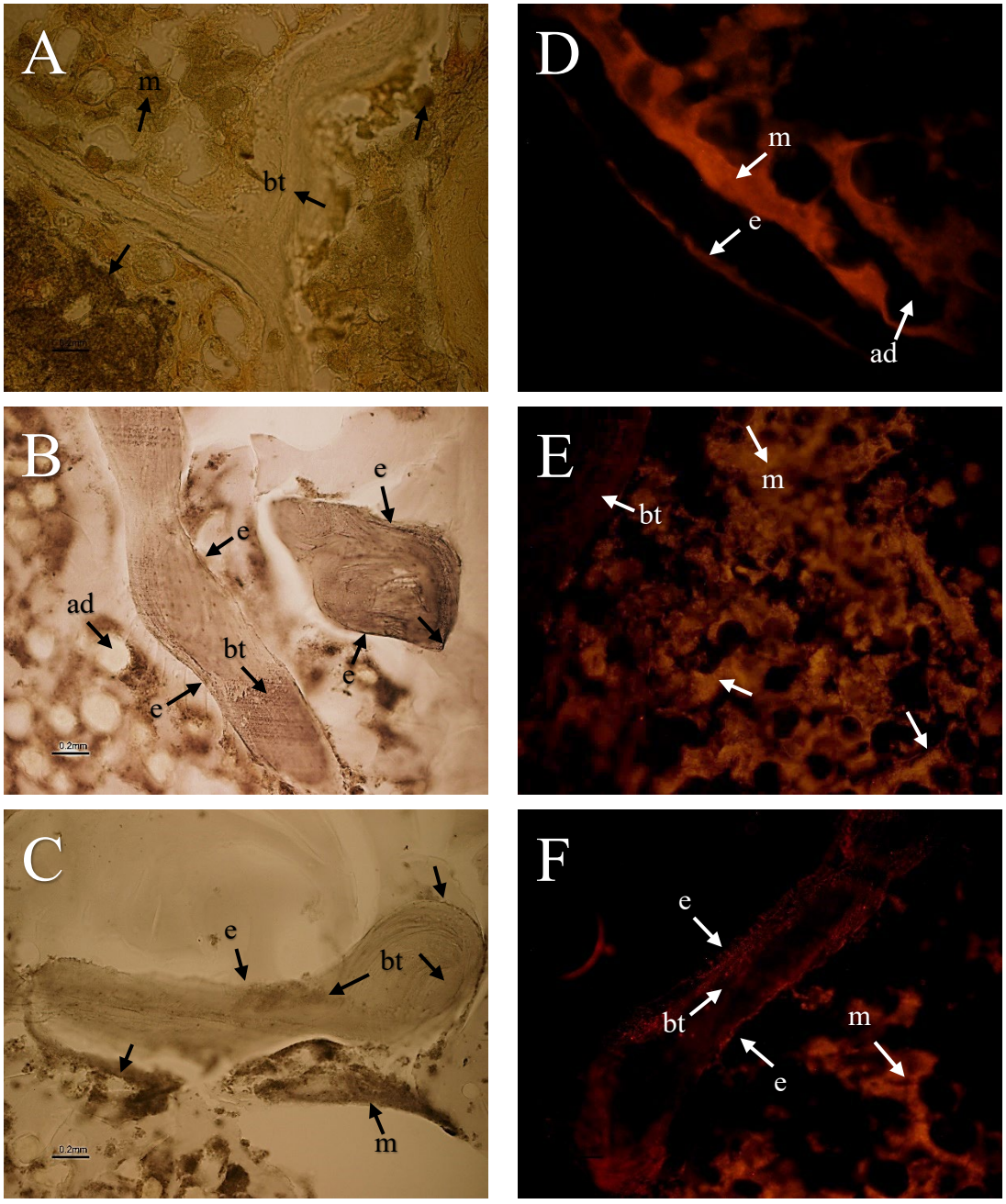


*Figure 3.3: Sections of porcine tissues (A, D) fresh, (B, E) decellularized and (C, F) lyophilized BM showing marrow (m), bone trabeculae (bt), adipocytes (ad) and endosteum (e). Labelled with antibody specific for extracellular matrix protein fibronectin. Images A, B and C stained using ABC-vectastain kit and Images D, E and F stained using fluorescence kit (filter-TRITC). Arrows indicates fibronectin labelling throughout the BM ECM and in endosteum. Scale bars represents 0.2mm.*

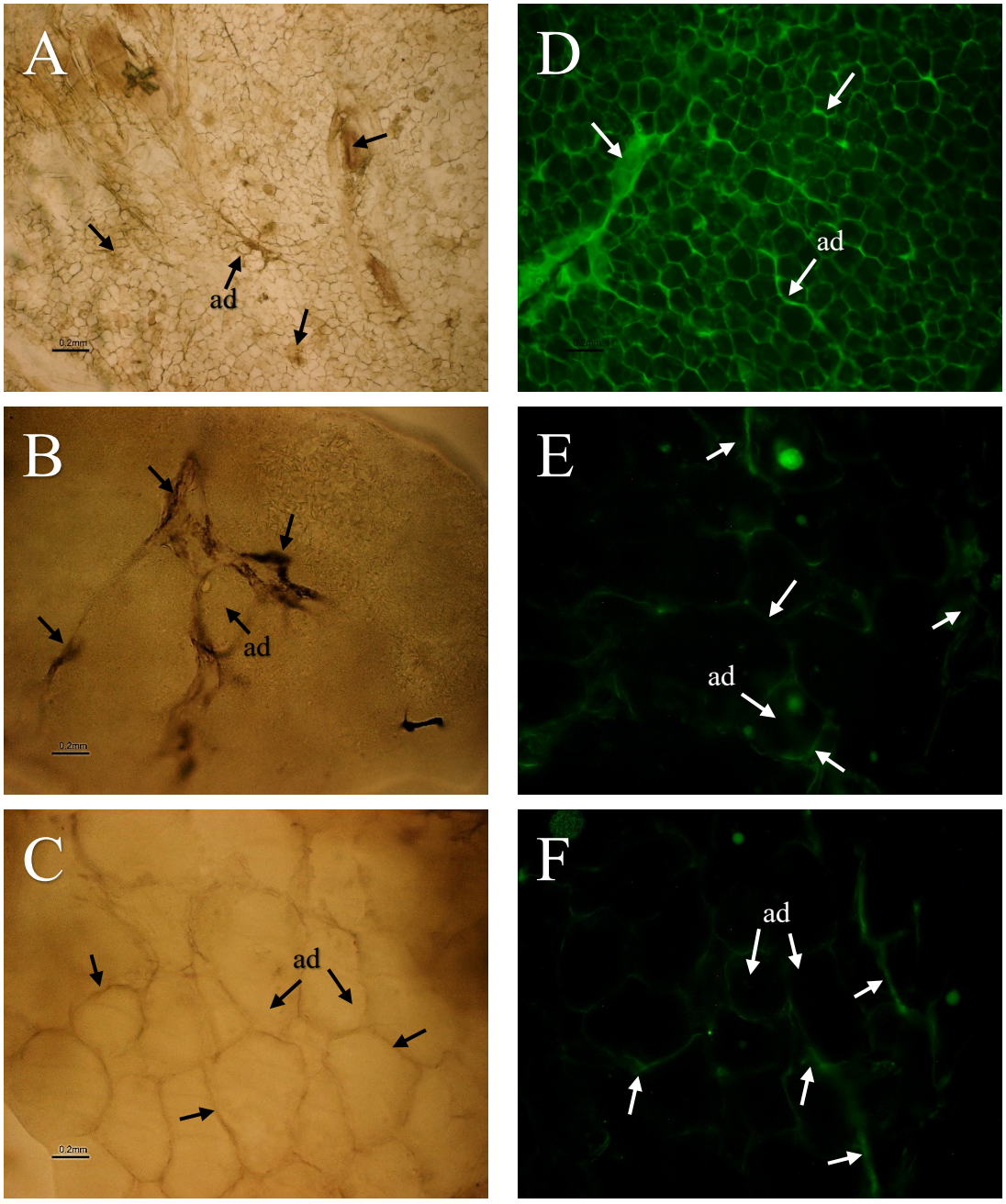


*Figure 4.1: Sections of porcine tissues (A, D) fresh, (B, E) decellularized and (C, F) lyophilized adipose tissue showing adipocytes (ad). Labelled with antibody specific for extracellular matrix protein laminin. Images A, B and C stained using ABC-vectastain kit and Images D, E and F stained using fluorescence kit (filter-FITC). Arrows indicates laminin labelling throughout the adipose tissue ECM. Scale bars represents 0.2mm.*

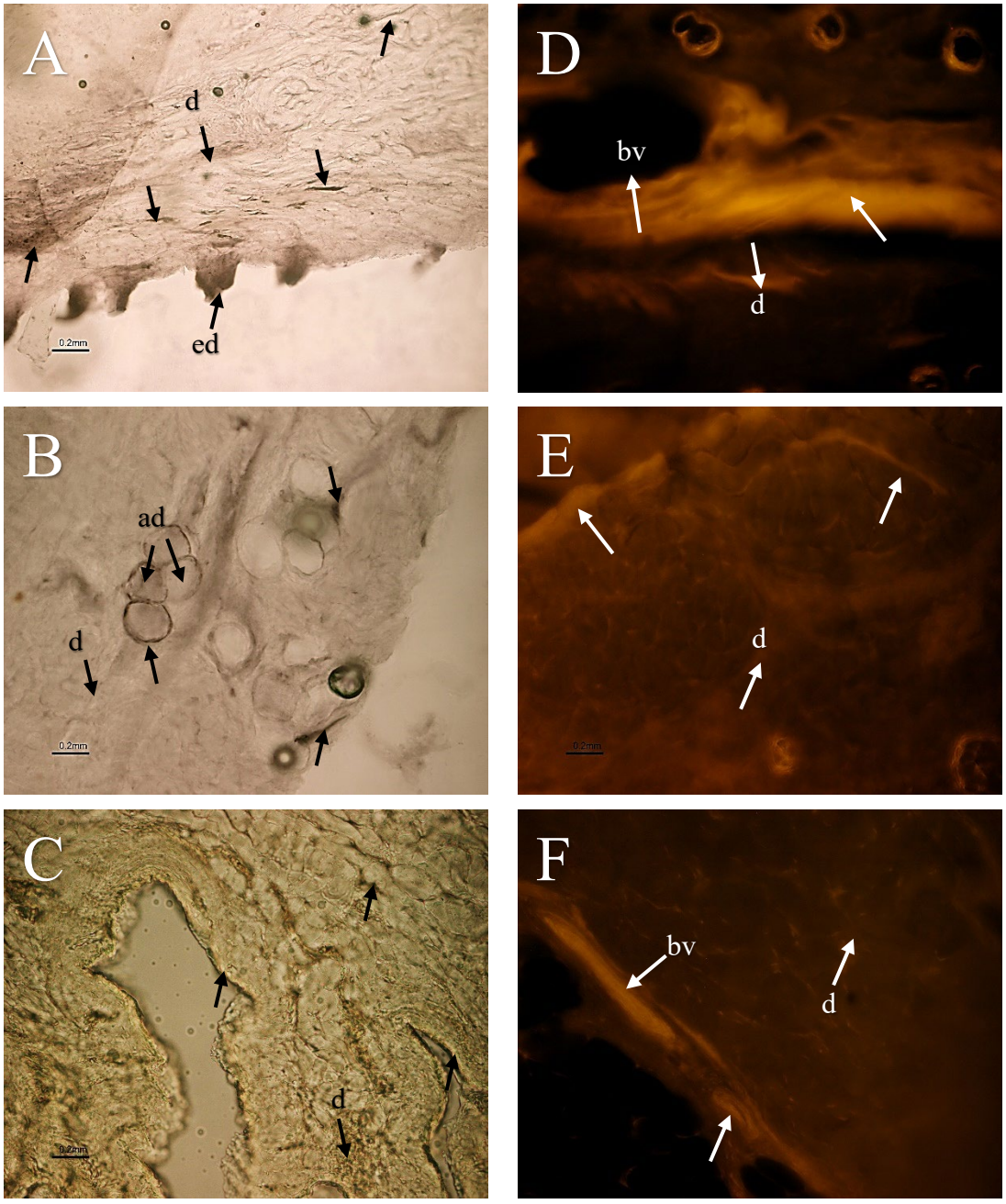


*Figure 4.2: Sections of porcine tissues (A, D) fresh, (B, E) decellularized and (C, F) lyophilized dermis showing dermis (d), epidermis (ed), blood vessel (bv) and adipocytes (ad). Labelled with antibody specific for extracellular matrix protein laminin. Images A, B and C stained using ABC-vectastain kit and Images D, E and F stained using fluorescence kit (filter-TRITC). Arrows indicates laminin labelling throughout the dermis ECM. Scale bars represents 0.2mm.*

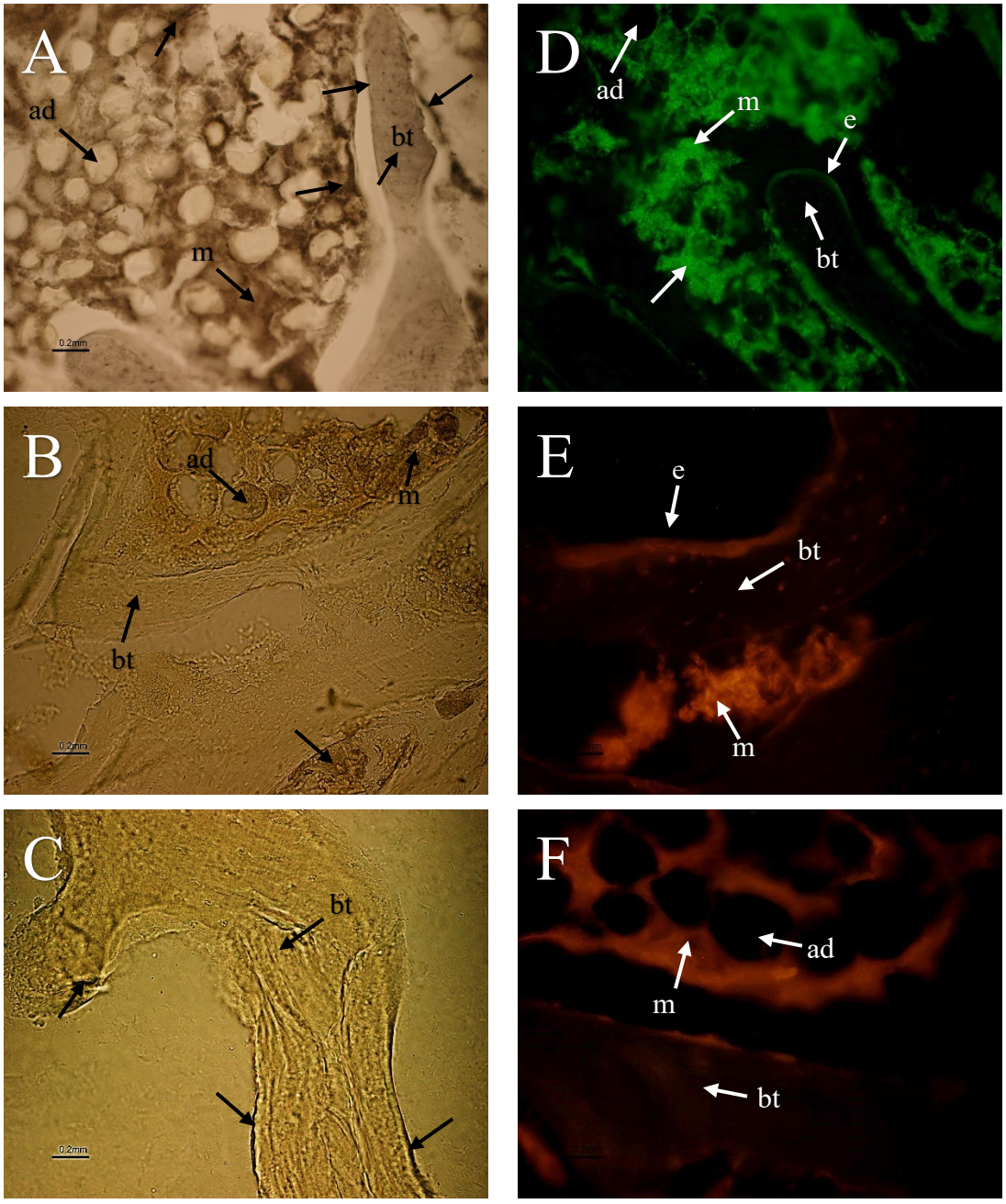


*Figure 4.3: Sections of porcine tissues (A, D) fresh, (B, E) decellularized and (C, F) lyophilized BM showing marrow (m), bone trabeculae (bt), endosteum (e) and adipocytes (ad). Labelled with antibody specific for extracellular matrix protein laminin. Images A, B and C stained using ABC-vectastain kit and Images D, E and F stained using fluorescence kit (filter-TRITC and FITC). Arrows laminin labelling throughout the BM ECM and in endosteum. Scale bars represents 0.2mm.*

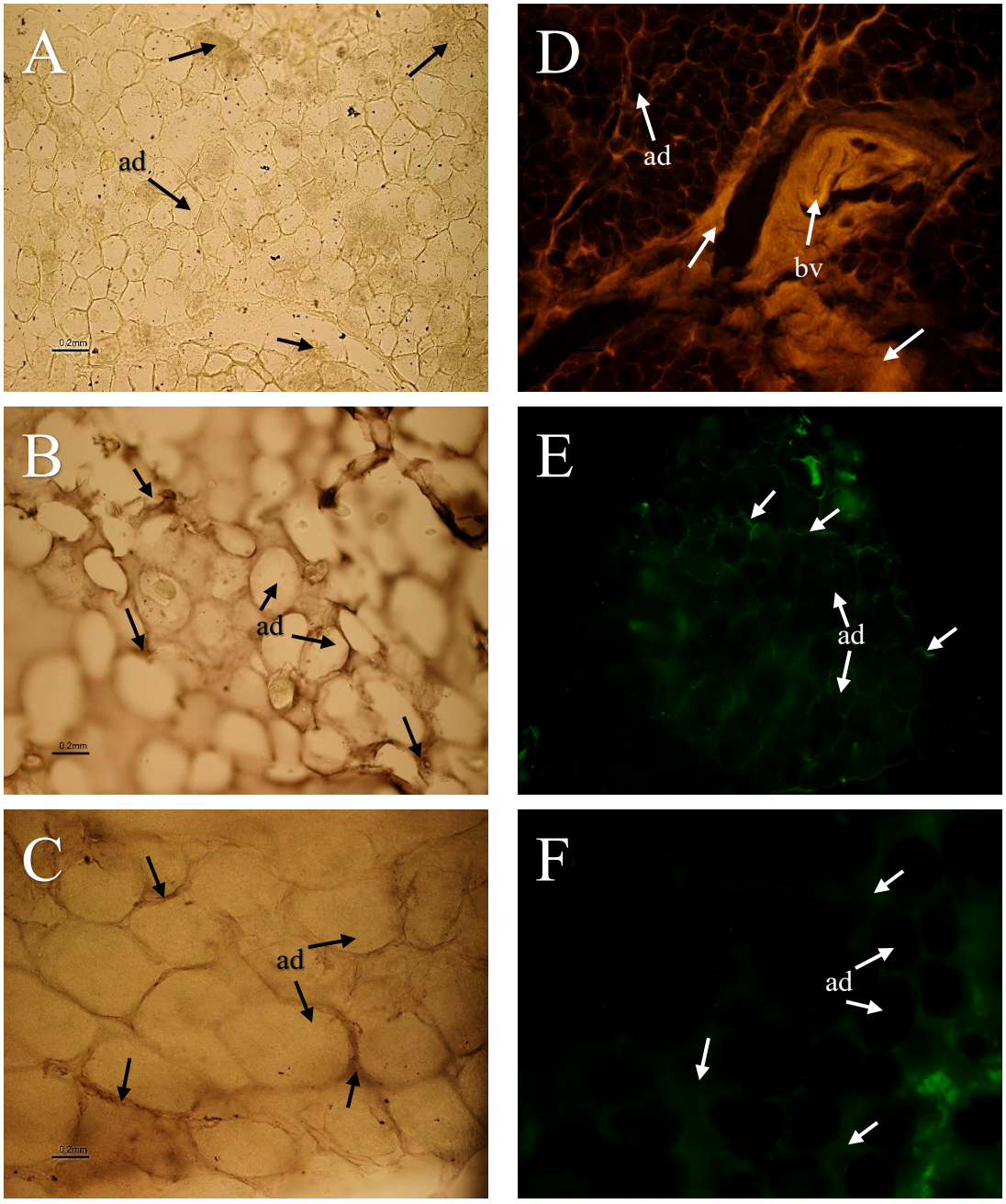


*Figure 5.1: Sections of porcine tissues (A, D) fresh, (B, E) decellularized and (C, F) lyophilized adipose showing adipocytes (ad), and blood vessels (bv). Labelled with antibody specific for extracellular matrix protein collagen-I. Images A, B and C stained using ABC-vectastain kit and Images D, E and F stained using fluorescence kit (filter-TRITC and FITC). Arrows indicate collagen-I labelling throughout the adipose tissue ECM. Scale bars represents 0.2mm.*

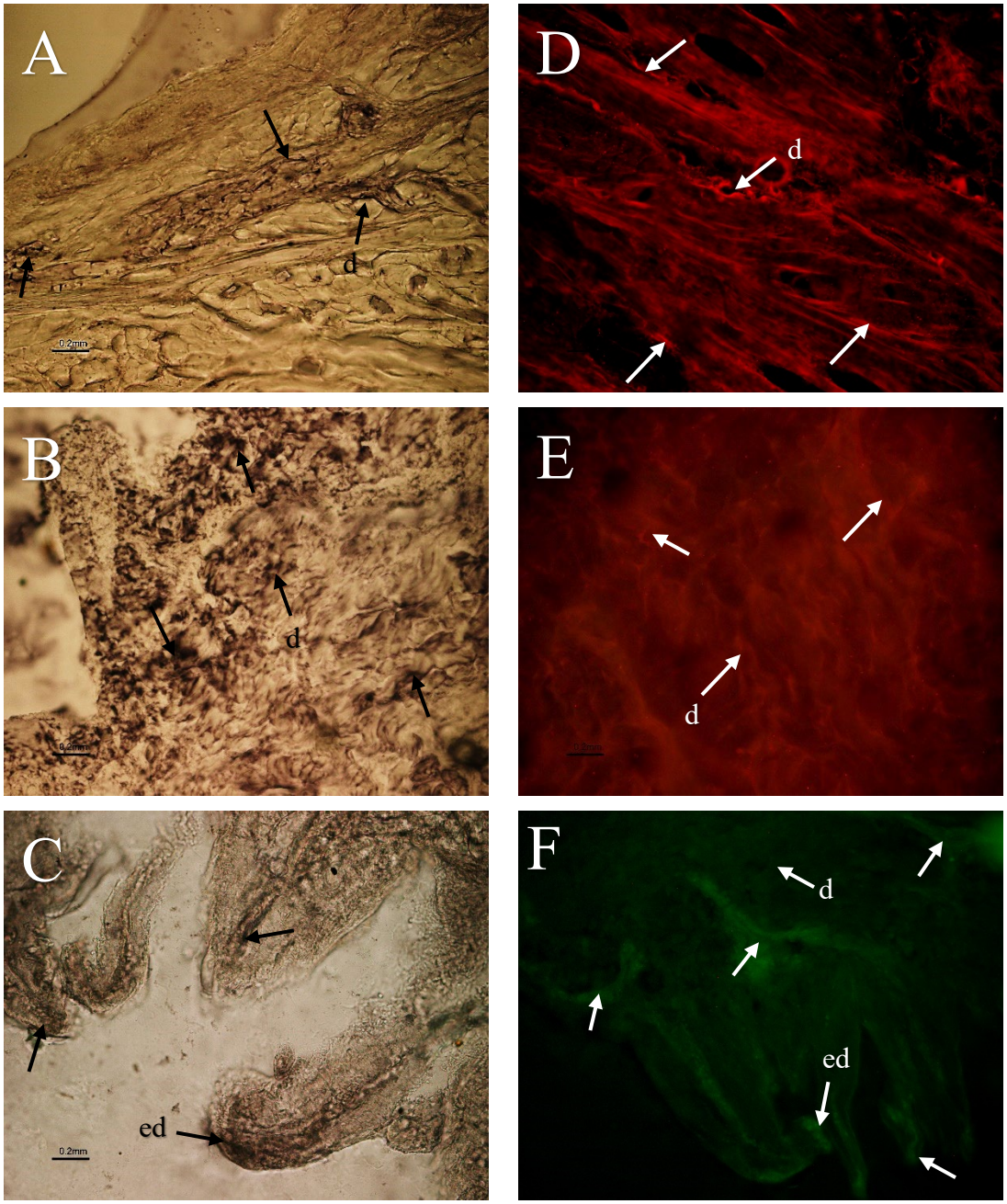


*Figure 5.2: Sections of porcine tissues (A, D) fresh, (B, E) decellularized and (C, F) lyophilized dermis showing dermis (d), and epidermis (ed). Labelled with antibody specific for extracellular matrix protein collagen-I. Images A, B and C stained using ABC-vectastain kit and Images D, E and F stained using fluorescence kit (filter-TRITC and FITC). Arrows indicates collagen-I labelling throughout the dermis ECM. Scale bars represents 0.2mm.*

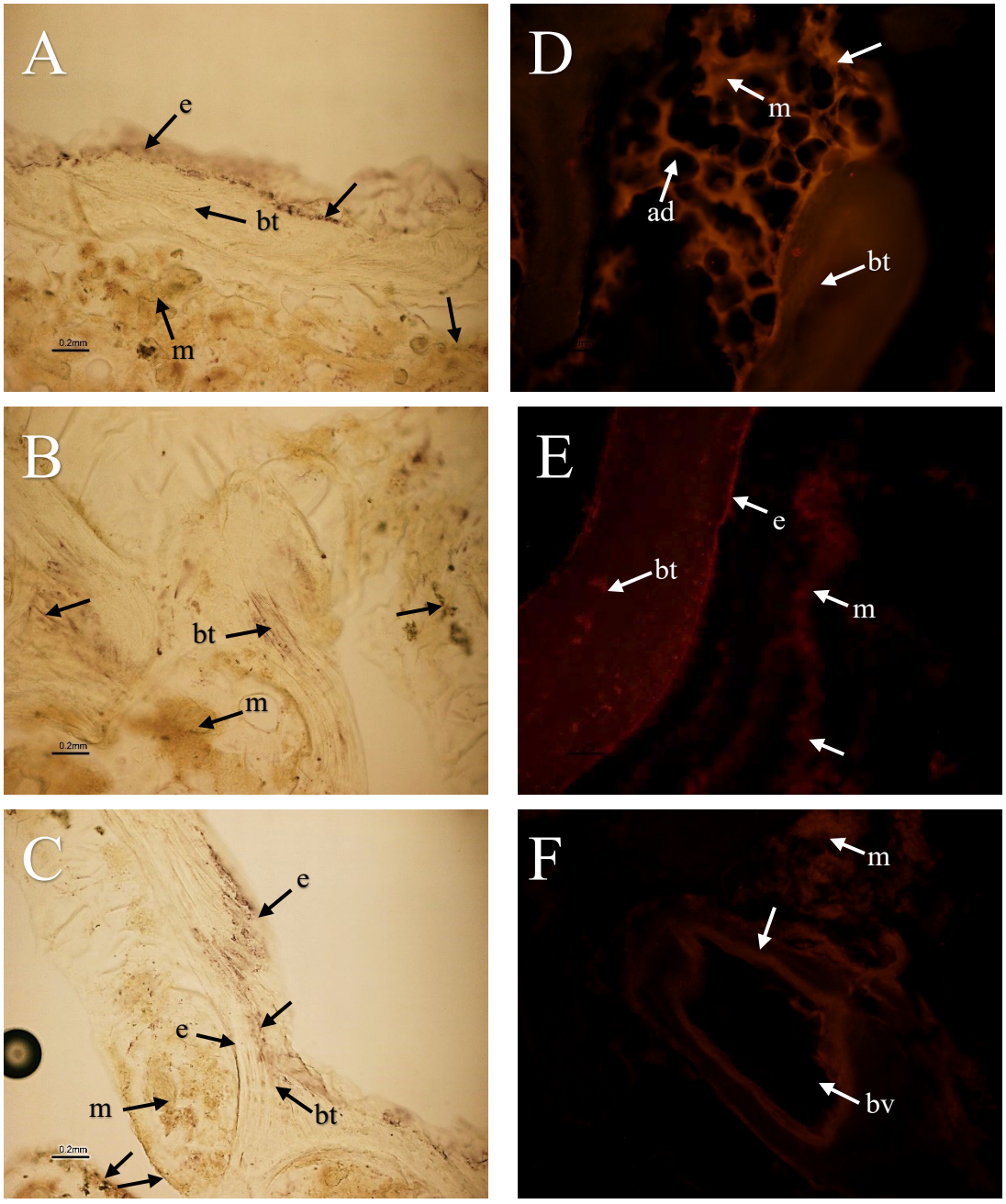


*Figure 5.3: Sections of porcine tissues (A, D) fresh, (B, E) decellularized and (C, F) lyophilized BM showing marrow (m), endosteum (e), bone trabeculae (bt), blood vessel (bv) and adipocytes(ad). Labelled with antibody specific for extracellular matrix protein collagen-I. Images A, B and C stained using ABC-vectastain kit and Images D, E and F stained using fluorescence kit (filter-TRITCC). Arrows indicates collagen-I labelling throughout the BM ECM and in endosteum. Scale bars represents 0.2mm.*

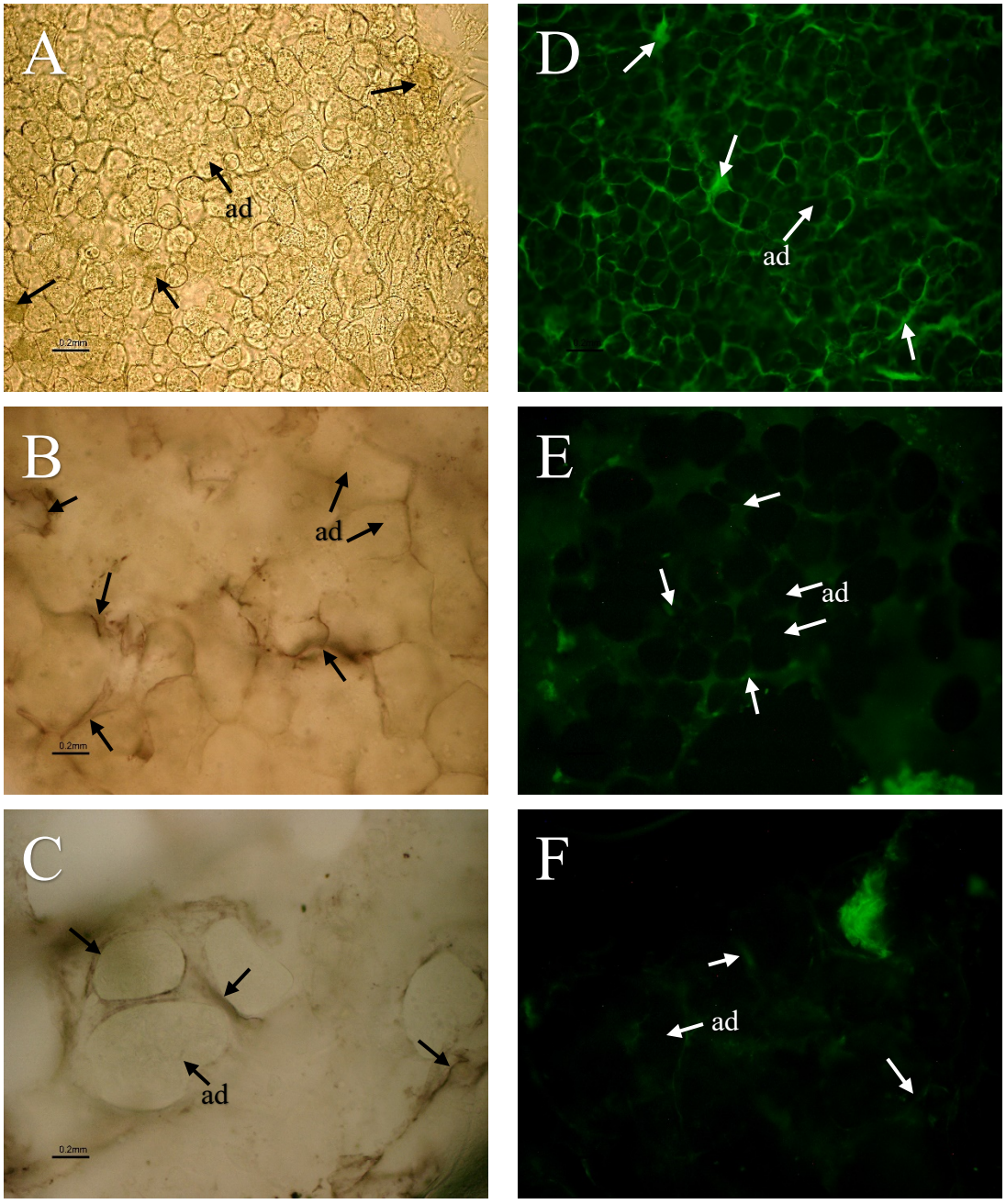


*Figure 6.1: Sections of porcine tissues (A, D) fresh, (B, E) decellularized and (C, F) lyophilized adipose showing adipocytes(ad). Labelled with antibody specific for extracellular matrix protein collagen-III. Images A, B and C stained using ABC-vectastain kit and Images D, E and F stained using fluorescence kit (filter-FITC). Arrows indicates collagen-III labelling throughout the adipose tissue ECM. Scale bars represents 0.2mm*

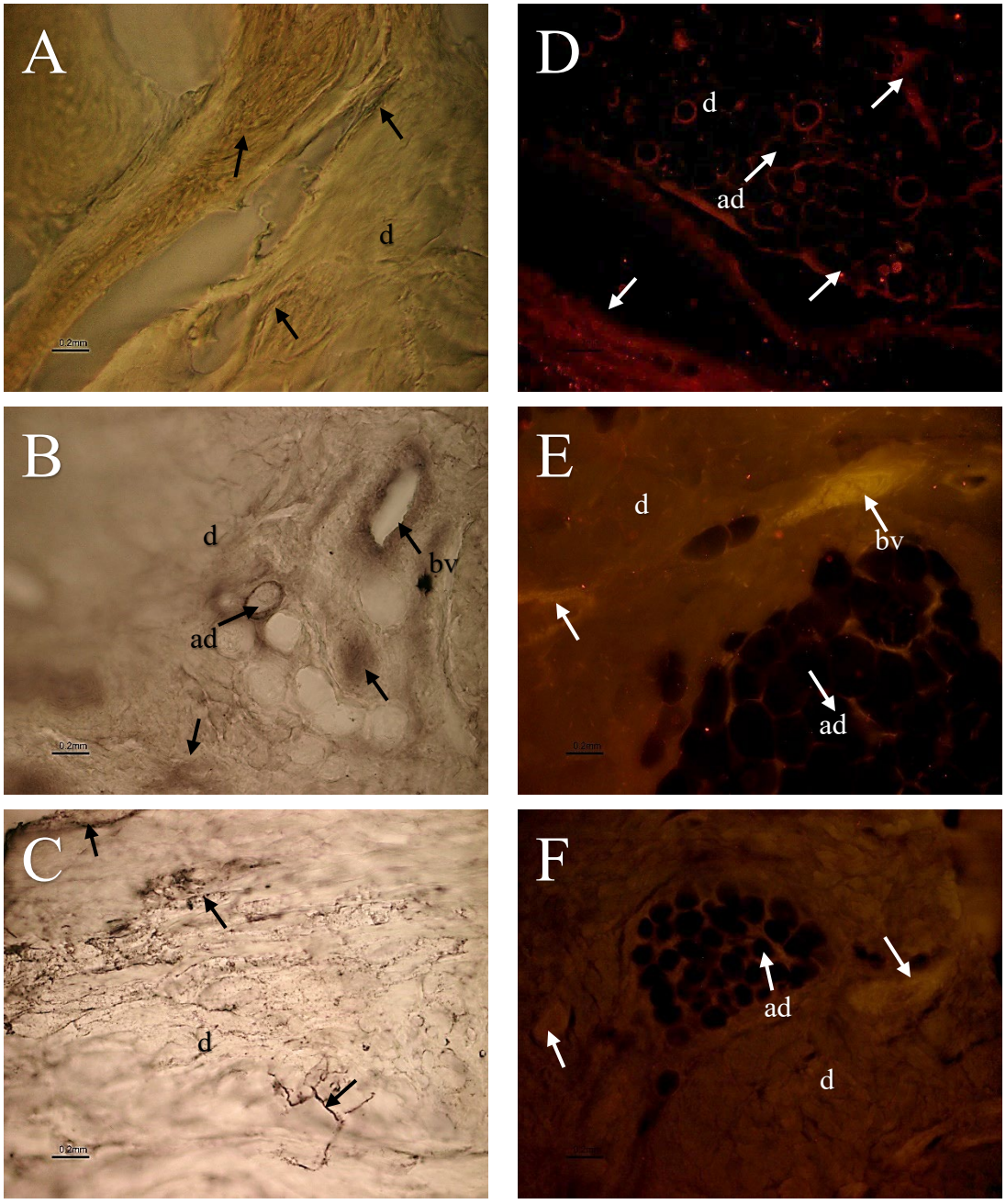


*Figure 6.2: Sections of porcine tissues (A, D) fresh, (B, E) decellularized and (C, F) lyophilized adipose showing dermis (d), blood vessel (bv) and adipocytes(ad). Labelled with antibody specific for extracellular matrix protein collagen-III. Images A, B and C stained using ABC-vectastain kit and Images D, E and F stained using fluorescence kit (filter-TRITC). Arrows indicates collagen-III labelling throughout the dermis. Scale bars represents 0.2mm.*

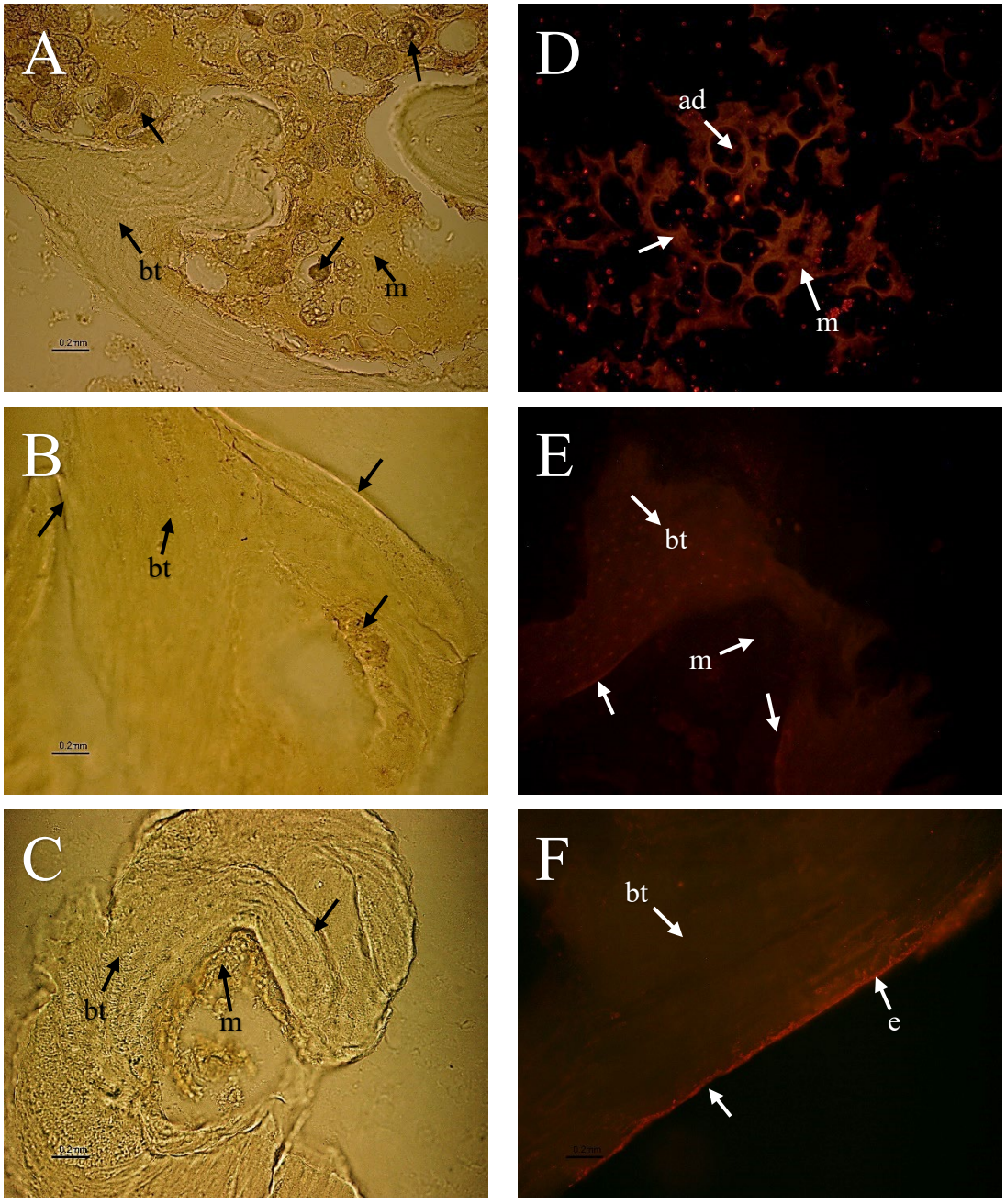


*Figure 6.3: Sections of porcine tissues (A, D) fresh, (B, E) decellularized and (C, F) lyophilized BM showing marrow (m), bone trabeculae (bt), endosteum (e) and adipocytes(ad). Labelled with antibody specific for extracellular matrix protein collagen-III. Images A, B and C stained using ABC-vectastain kit and Images D, E and F stained using fluorescence kit (filter-TRITC). Arrows indicates collagen-III labelling throughout the BM ECM. Scale bars represents 0.2mm.*

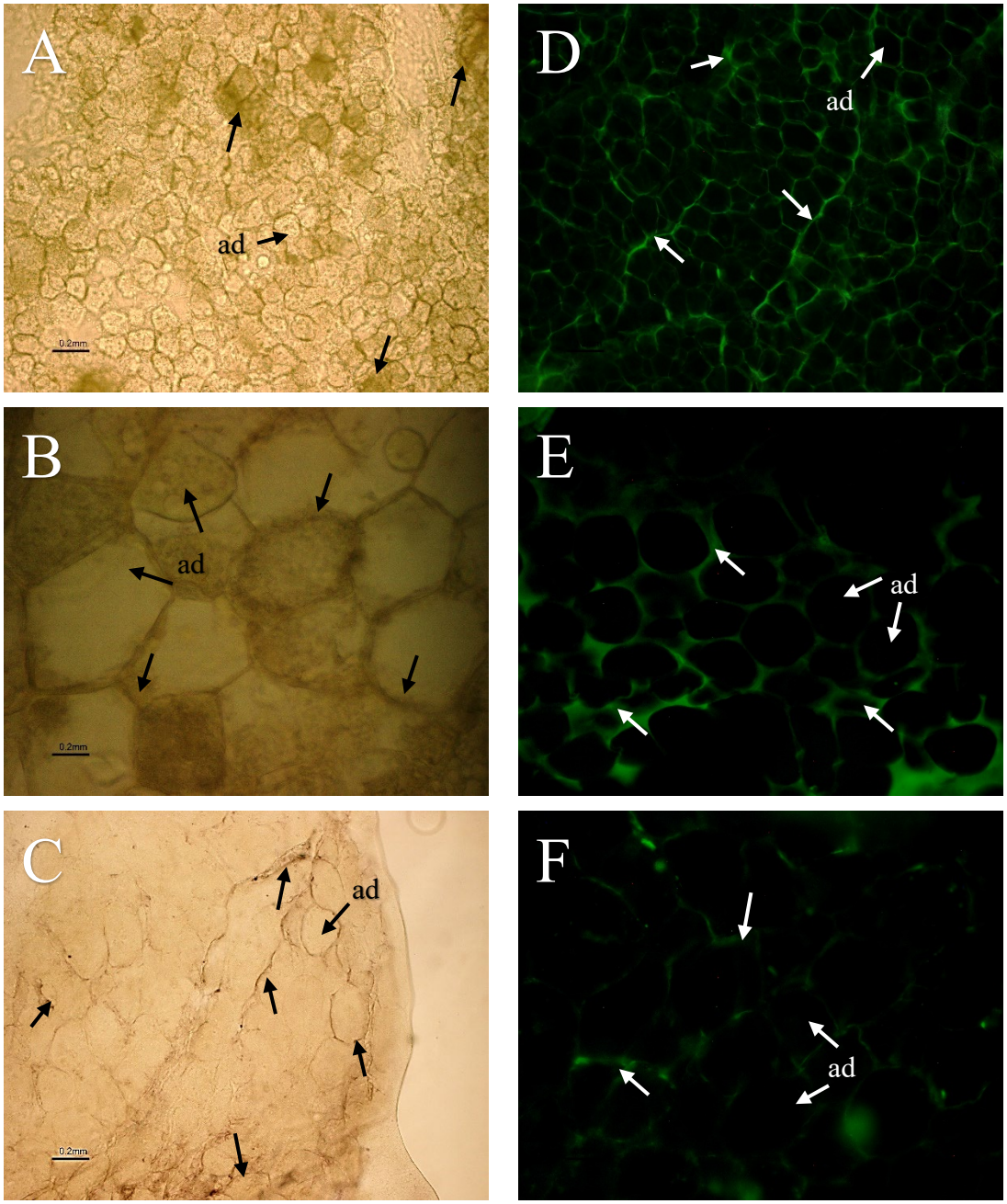


*Figure 7.1: Sections of porcine tissues (A, D) fresh, (B, E) decellularized and (C, F) lyophilized adipose showing adipocytes (ad). Labelled with antibody specific for extracellular matrix protein collagen-IV. Images A, B and C stained using ABC-vectastain kit and Images D, E and F stained using fluorescence kit (filter-FITC). Arrows indicates collagen-IV labelling throughout the adipose tissue ECM. Scale bars represents 0.2mm.*

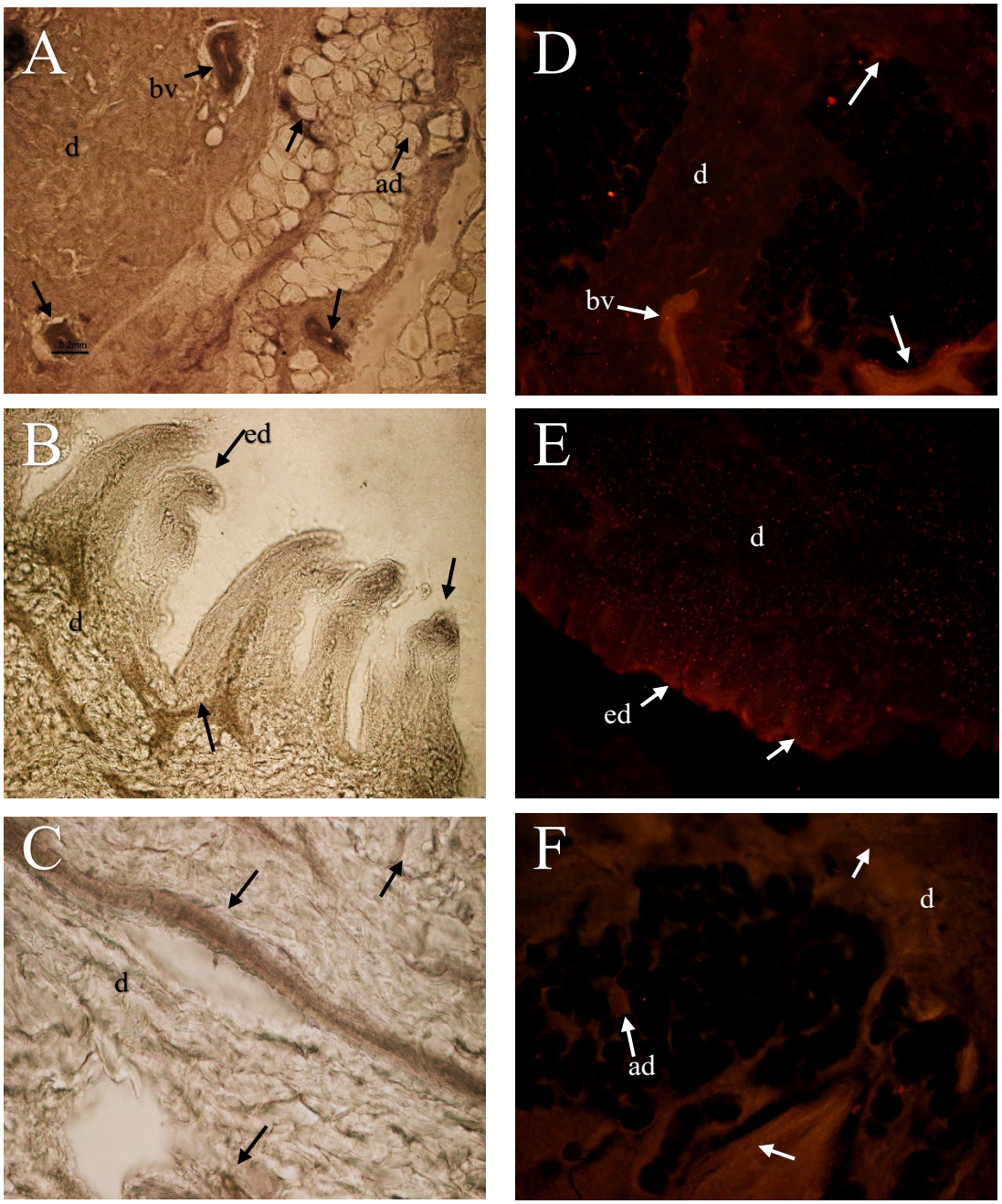


*Figure 7.2: Sections of porcine tissues (A, D) fresh, (B, E) decellularized and (C, F) lyophilized dermis showing dermis (d), epidermis (ed), blood vessels (bv) and adipocytes (ad). Labelled with antibody specific for extracellular matrix protein collagen-IV. Images A, B and C stained using ABC-vectastain kit and Images D, E and F stained using fluorescence kit (filter-TRITC). Arrows indicates collagen-IV labelling throughout the dermis ECM. Scale bars represents 0.2mm*

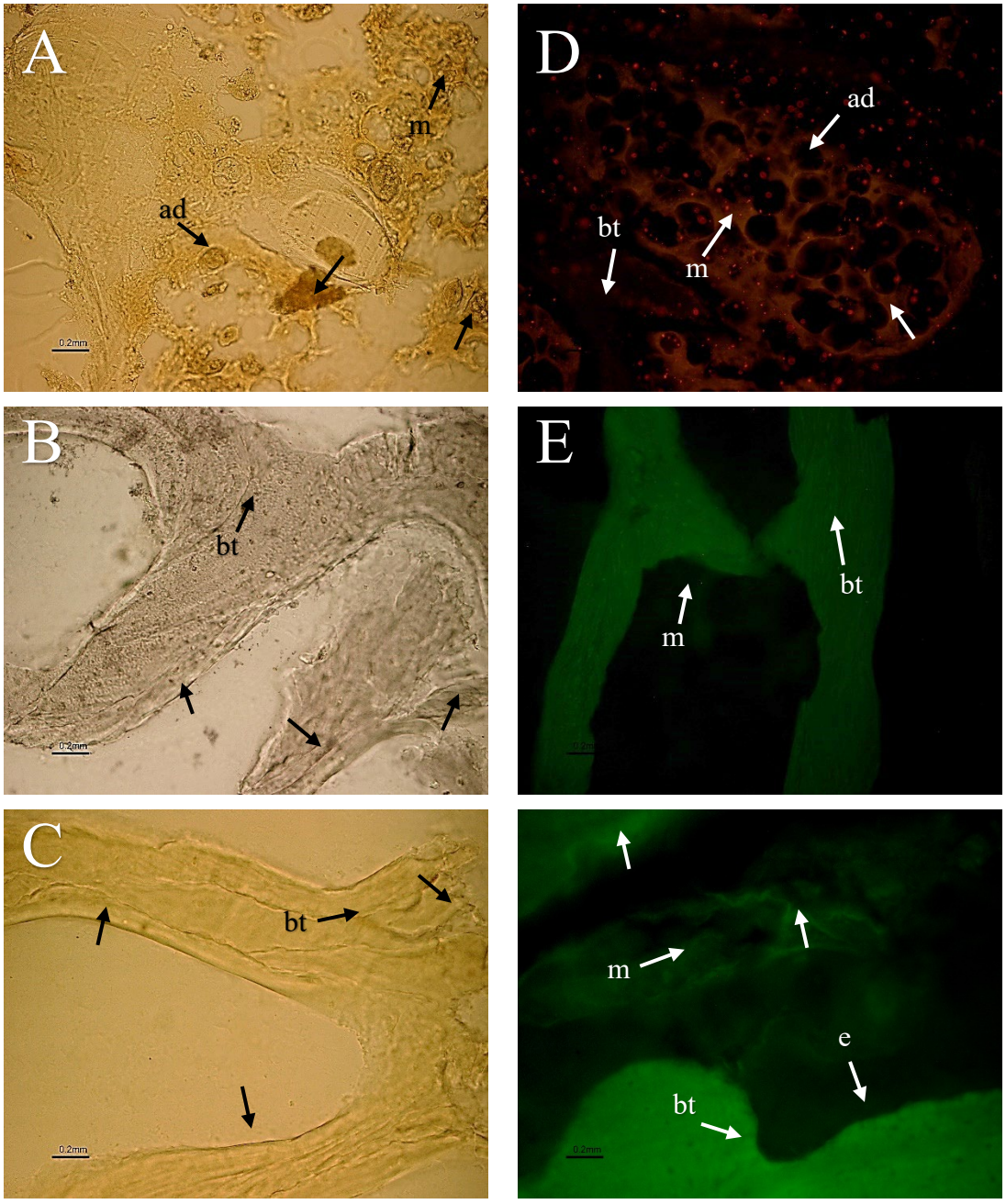


*Figure 7.3: Sections of porcine tissues (A, D) fresh, (B, E) decellularized and (C, F) lyophilized BM showing marrow (m), bone trabeculae (bt), endosteum (e) and adipocytes (ad). Labelled with antibody specific for extracellular matrix protein collagen-IV. Images A, B and C stained using ABC-vectastain kit and Images D, E and F stained using fluorescence kit (filter- TRITC and FITC). Arrows indicates collagen-IV labelling throughout the BM ECM. Scale bars represents 0.2mm.*

*Table 1.1: Brightness measurement of ECM protein fibronectin for fluorescence labelled histological sections of porcine tissues. (Range of intensity on image J: min=0; max=255)*

| Porcine tissues | | Brightness |
|---|---|---|
| Fresh | Adipose | 213 |
| | Dermis | 123 |
| | Bone-Marrow | 138 |
| Decellularized | Adipose | 129 |
| | Dermis | 72 |
| | Bone-Marrow | 90 |
| Lyophilized | Adipose | 107 |
| | Dermis | 61 |
| | Bone-Marrow | 90 |

*Table 1.2: Brightness measurement of ECM protein laminin for fluorescence labelled histological sections of porcine tissues. (Range of intensity on image J: min=0; max=255)*

| Porcine tissues | | Brightness |
|---|---|---|
| Fresh | Adipose | 204 |
| | Dermis | 122 |
| | Bone-Marrow | 126 |
| Decellularized | Adipose | 164 |
| | Dermis | 89 |
| | Bone-Marrow | 78 |
| Lyophilized | Adipose | 124 |
| | Dermis | 78 |
| | Bone-Marrow | 53 |

*Table 1.3: Brightness measurement of ECM protein collagen-I for fluorescence labelled histological sections of porcine tissues. (Range of intensity on image J: min=0; max=255)*

| Porcine tissues | | Brightness |
|---|---|---|
| Fresh | Adipose | 204 |
| | Dermis | 127 |
| | Bone-Marrow | 109 |
| Decellularized | Adipose | 178 |
| | Dermis | 122 |
| | Bone-Marrow | 74 |
| Lyophilized | Adipose | 127 |
| | Dermis | 100 |
| | Bone-Marrow | 48 |

*Table 1.4: Brightness measurement of ECM protein collagen-III for fluorescence labelled histological sections of porcine tissues. (Range of intensity on image J: min=0; max=255)*

| Porcine tissues | | Brightness |
|---|---|---|
| Fresh | Adipose | 117 |
| | Dermis | 101 |
| | Bone-Marrow | 109 |
| Decellularized | Adipose | 106 |
| | Dermis | 72 |
| | Bone-Marrow | 64 |
| Lyophilized | Adipose | 92 |
| | Dermis | 54 |
| | Bone-Marrow | 62 |

*Table 1.5: Brightness measurement of ECM protein collagen-IV for fluorescence labelled histological sections of porcine tissues (Range of intensity on image J: min=0; max=255)*

| Porcine tissues | | Brightness |
|---|---|---|
| Fresh | Adipose | 119 |
| | Dermis | 102 |
| | Bone-Marrow | 70 |
| Decellularized | Adipose | 95 |
| | Dermis | 68 |
| | Bone-Marrow | 60 |
| Lyophilized | Adipose | 88 |
| | Dermis | 52 |
| | Bone-Marrow | 59 |

*Table 2: Summary of ECM proteins and their localization on the porcine tissues based on the brightness measured.*

| ECM proteins | Fresh AD | Dec AD | Lyo AD | Fresh Dermis | Dec Dermis | Lyo Dermis | Fresh BM | Dec BM | Lyo BM |
|---|---|---|---|---|---|---|---|---|---|
| Fibronectin | +++ | ++ | ++ | +++ | ++ | + | +++ | ++ | ++ |
| Laminin | +++ | ++ | ++ | +++ | ++ | + | +++ | ++ | + |
| Collagen-I | ++ | ++ | ++ | ++ | ++ | ++ | ++ | ++ | + |
| Collagen-III | ++ | ++ | ++ | ++ | ++ | + | ++ | + | + |
| Collagen-IV | ++ | ++ | ++ | ++ | ++ | ++ | ++ | + | + |

+++, bright expression; ++, moderate expression; +, faint expression; - absent.
Grading is for positive areas.
Dec- Decellularized, Lyo- lyophilized, AD- Adipose, BM- Bone-marrow

## MSCs Morphology

The cell morphology of MSCs cultivated on TCT, nTCT plates, and nTCT dishes smeared with adipose, dermis and BM for two, four, six, eight, and ten days, respectively, was analyzed. Phase-contrast photomicrographs of MSC cultures were taken after each incubation period. The MSCs described here were characterized by their ability to proliferate in culture with an attached well spread morphology. Independent from the passage number of MSCs (eighth) used to seed the dishes at time zero. MSCs attached to the bottom of the TCT, nTCT, adipose-smeared, dermis-smeared and BM-smeared plates after incubation of 24h. The cell morphologies of MSCs grown on all the cultivation substrates were similar. On days 2-4, the cells showed obvious enlargement and proliferation, forming small colonies with several tens of fusocellular, triangular and polygonal cells (Fig 8.1 and Fig 8.2). MSCs reached 90% confluency on day 6 (Fig 8.3 ). On days 6-8, most adherent cells displayed a spindle shaped characteristic of fibroblast with flat cell bodies having cell processes connected to adjacent cells (Fig 8.3 and Fig 8.4) The cells were rapidly duplicating and the cell morphology mainly spindle-shaped or triangular. Furthermore, with proliferation of MSCs cultivated on TCT, dermis-smeared, BM-smeared and adipose smeared plates, the surface area accessible for cell adhesion decreased and on all the substrates. MSCs were overlapping forming multilayers on day 10. In contrast, MSCs seeded on adipose-smeared plates (Fig 8.1-D, Fig 8.2- D, Fig 8.3-D, Fig 8.4- D and Fig 8.5- D) grew relatively poorly, however, the cell morphology was similar to that of the other substrates. The MSCs seeded on nTCT plates (negative control) attached poorly to the polystyrene surface and by day 6 had mostly lost the MSC morphological characteristics exhibited by the cells grown on the TCT plates and experimental substrates (Fig 8.3- E). By day 10 there was an overall decrease in cell density in nTCT plates with small round cells that tended to form free-floating spherical cell aggregates (8.5- E).

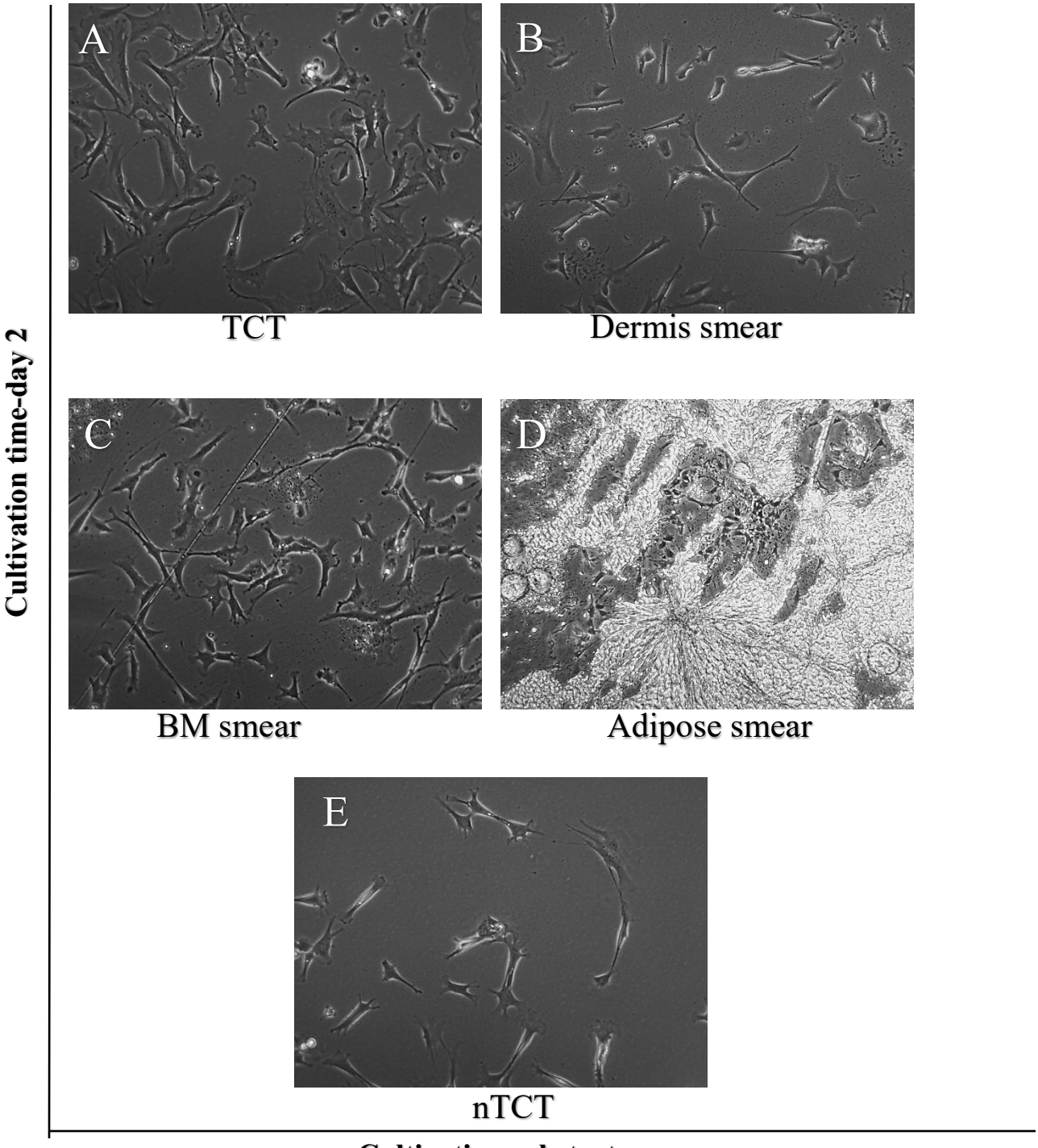


*Figure 8.1: Morphological characteristics of MSCs on TCT (A), dermis-smeared (B), BM-smeared (C), adipose-smeared (D) and nTCT (E) plates. Phase-contrast images of MSCs culture were taken at day-2. Magnification: 4X.*

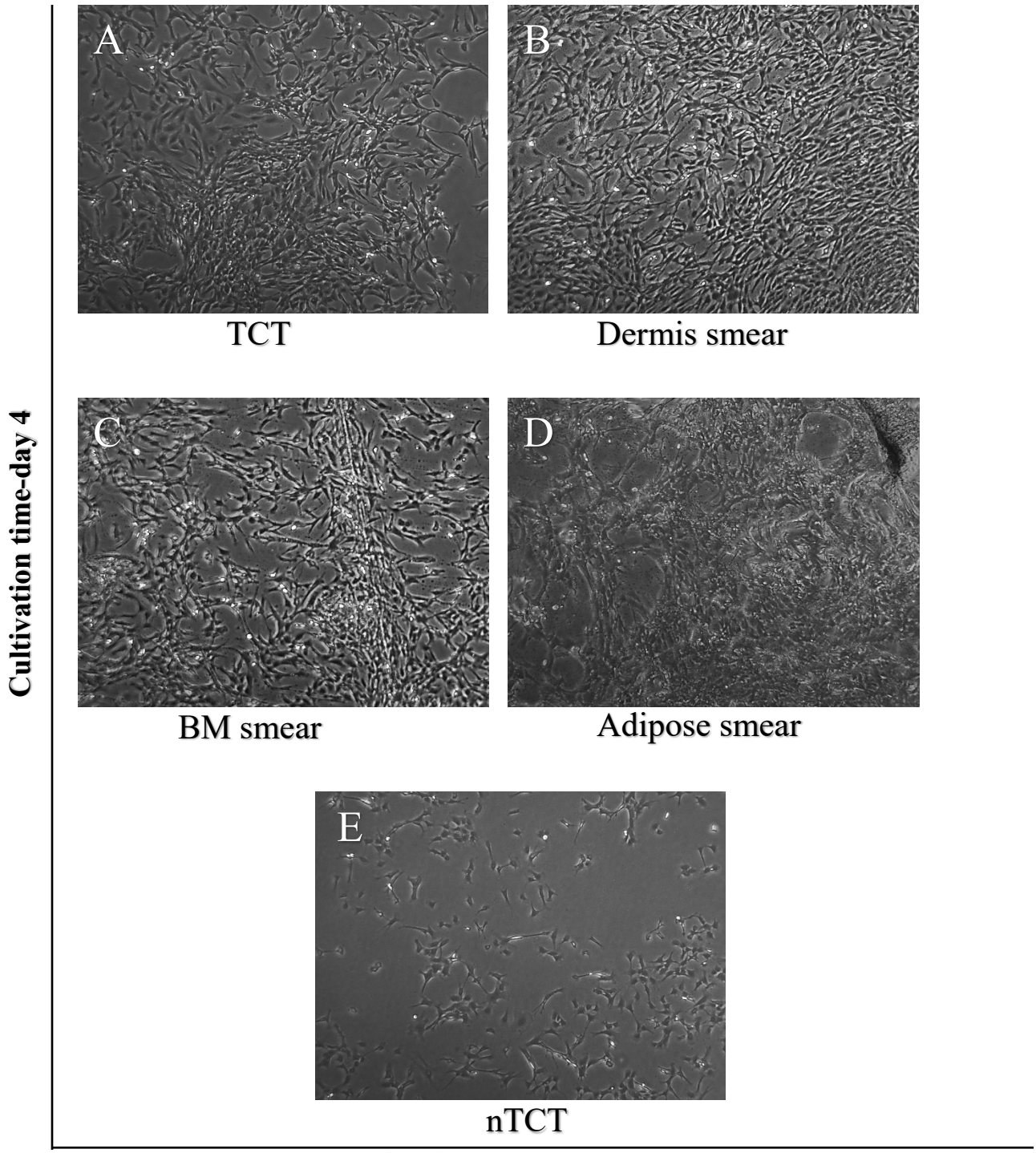


*Figure 8.2: Morphological characteristics of MSCs on TCT (A), dermis-smeared (B), BM-smeared (C), adipose-smeared (D) and nTCT (E) plates. Phase-contrast images of MSCs culture were taken at day-4. Magnification: 4X*

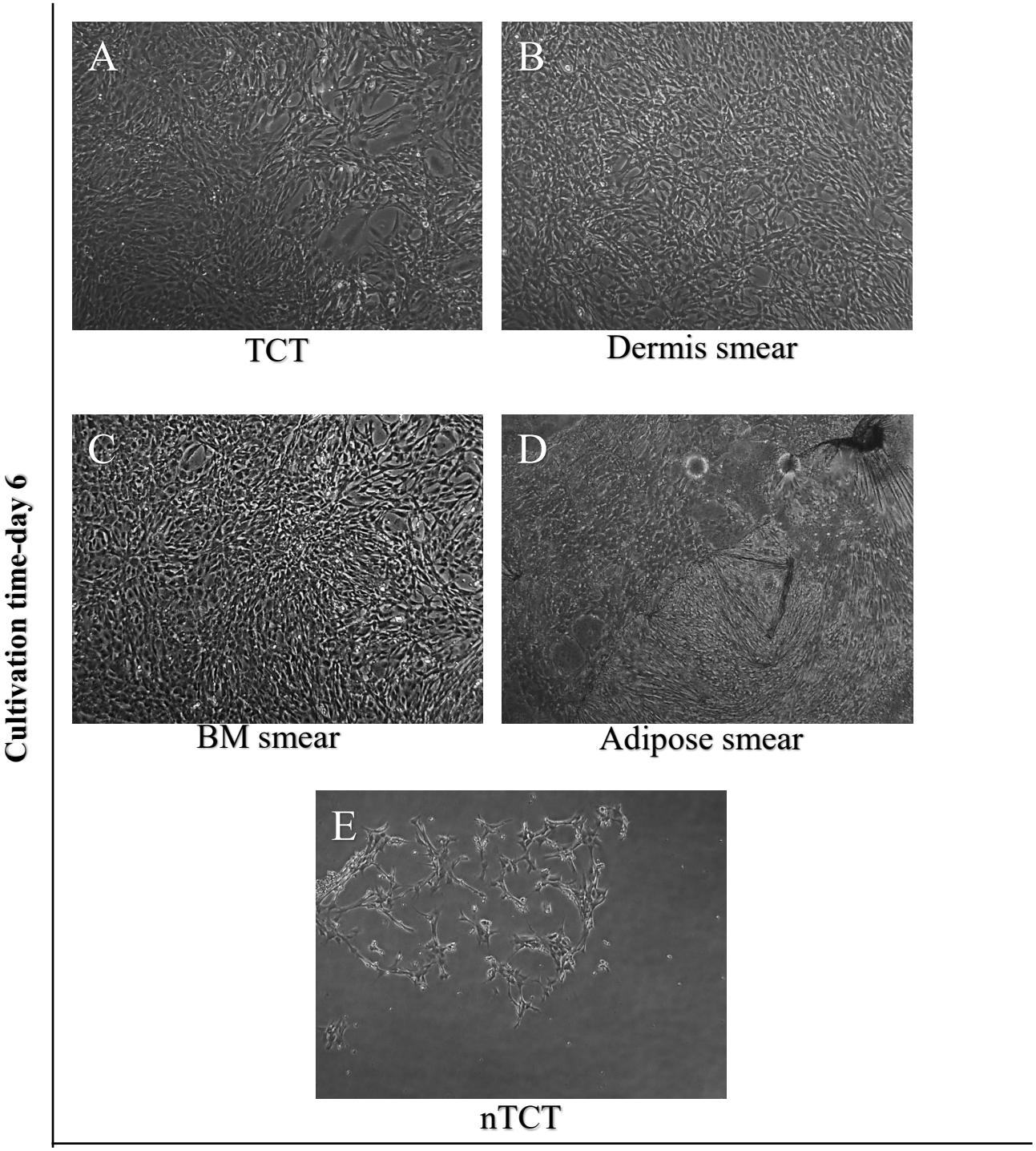


*Figure 8.3: Morphological characteristics of MSCs on TCT (A), dermis-smeared (B), BM-smeared (C), adipose-smeared (D) and nTCT (E) plates. Phase-contrast images of MSCs culture were taken at day-6. Magnification: 4X*

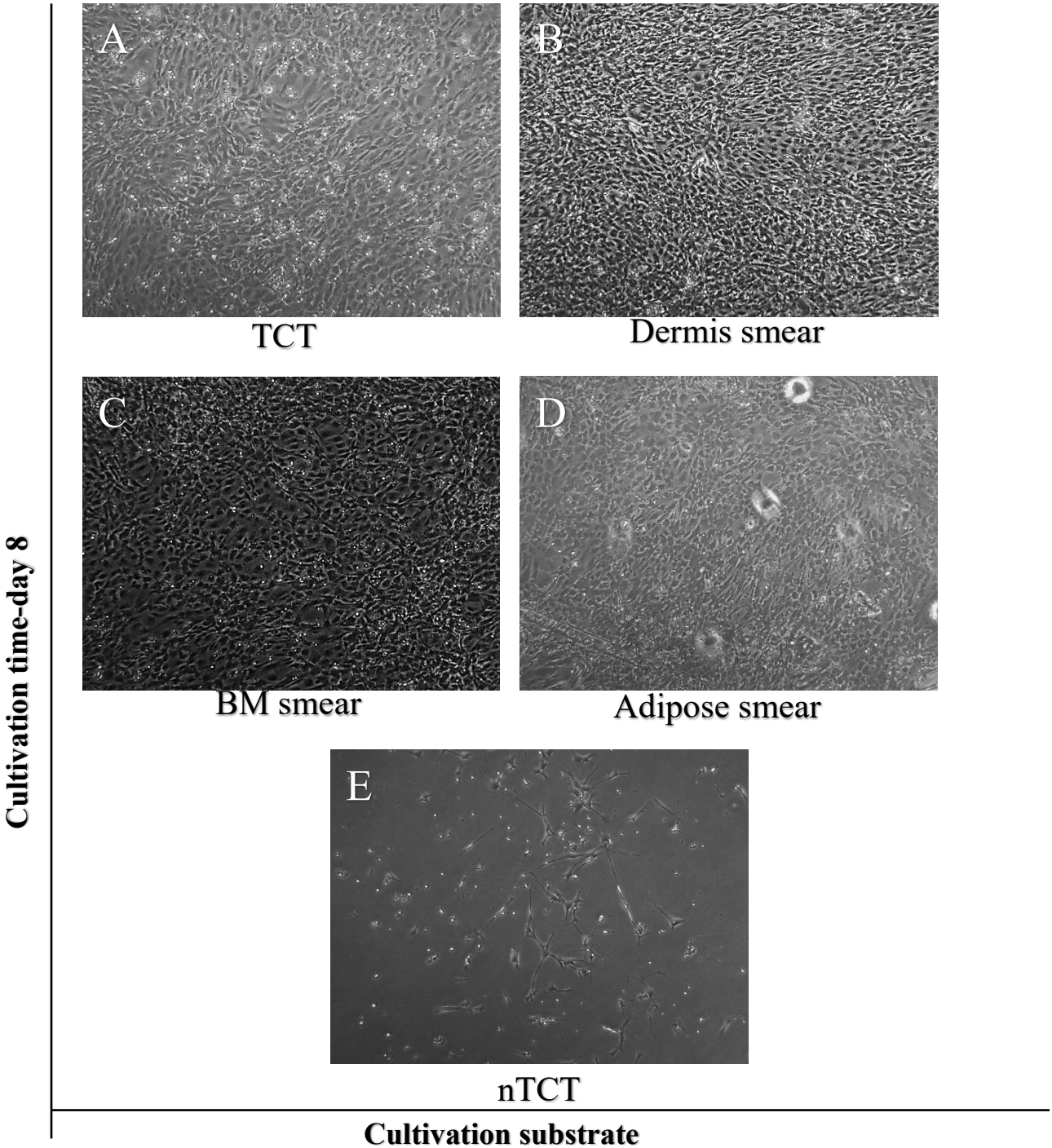


*Figure 8.4: Morphological characteristics of MSCs on TCT (A), dermis-smeared (B), BM-smeared (C), adipose-smeared (D) and nTCT (E) plates. Phase-contrast images of MSCs culture were taken at day-8. Magnification: 4X.*

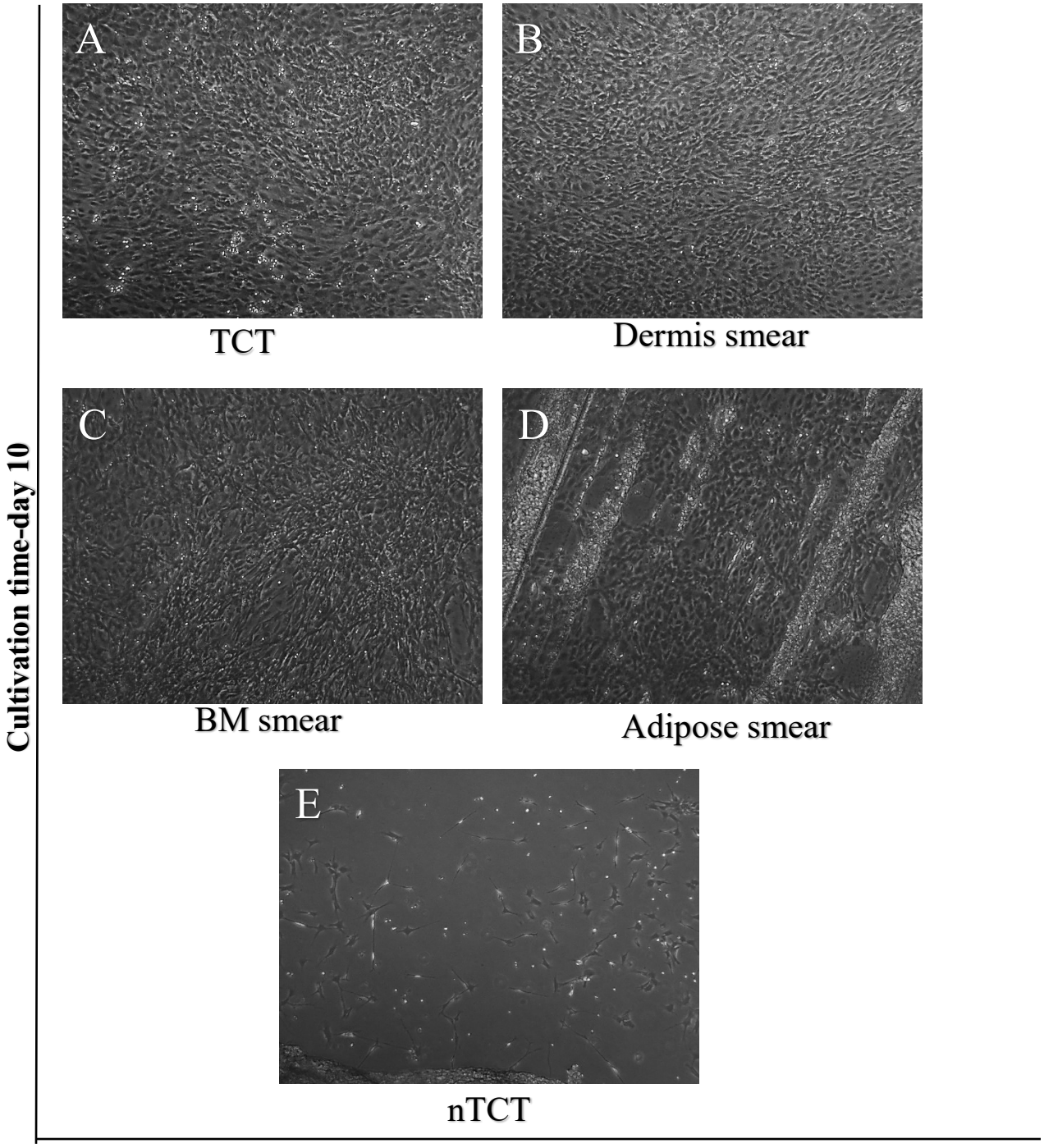


*Figure 8.5: Morphological characteristics of MSCs on TCT (A), dermis-smeared (B), BM-smeared (C), adipose-smeared (D) and nTCT (E) plates. Phase-contrast images of MSCs culture were taken at day-10. Magnification: 4X.*

## Cell growth in culture

Cell growth of MSCs was examined to assess if the BM-derived ECM substrate, Adipose derived ECM substrate and Dermis derived ECM substrate preparations could support long-term culture of MSCs. After seeding nTCT (negative control), TCT (positive control), Dermis-smeared, Adipose-smeared and BM-smeared plates with MSCs, cell counts were performed every second day over a total cultivation time of ten days. The data is presented graphically in Fig 9 and Fig 10. As shown, BM-smeared, Dermis-smeared and Adipose smeared surfaces supported cell growth of MSCs. Unlike cells seeded on nTCT and Adipose-smeared plates, MSCs grown on BM-smeared, Dermis-smeared and TCT plates were able to enter exponential growth after two days. BM-smeared, Dermis -smeared and TCT plates entered stationary phase on day eight, followed by the death phase on day ten. The growth profile of the MSCs cultured on BM-smeared dishes is more similar to the positive control culture plate. Independent t-tests were performed to compare cell growth on the various substrates, [null hypothesis ($H_o$)=BM smeared= Dermis smeared= Adipose smeared= TCT= nTCT, if p-value is greater than 0.05 then there is no significant difference between the mean number of cells grown on the substrates; accepting the null hypothesis, however if p-value is less than 0.05 then $H_o$ is rejected i.e. there is significant difference between the mean number of cells grown on the substrates]. The results indicated no significant difference between two growth substrates (TCT= BM), hence accepting the $H_o$ hypothesis based on their p-values on day 6 (exponential phase) (Table 4.3). The mean cell count and SD of MSCs cultivated on BM-smeared plates on day 6 was 61009 ±

32665.8 cells/ $cm^2$, slightly higher than TCT plates on day 6 which was 59539 ± 15005.9 cells/ $cm^2$. The growth profile of the MSCs cultured on the Dermis-smeared plates was less than TCT and BM-smeared plates. However, t-test indicated no significant difference between the growth substrates (TCT= BM = Dermis), hence accepting the $H_o$ hypothesis based on their p-values during the exponential phase (Table 4.3). The mean cell count and SD of MSCs cultivated on Dermis-smeared plates is 29419 ± 3606.67 cells/ $cm^2$ which is lower than that of the TCT and BM-smeared plates. The growth profile of the MSCs culture on Adipose-smeared plates is less than BM-smeared, Dermis-smeared and positive control. The t-test indicated a significance difference between these growth substrates and the adipose smeared substrates, rejecting the $H_o$ hypothesis based on their p-values during the exponential phase (Table 4.3). The mean cell count and SD of MSCs cultivated on Adipose-smeared plates is 4183.6 ± 1633.39 cells/ $cm^2$ , which is significantly lower than both of the smeared substrates and the positive control. The growth profile, mean cell count and SD (1362.1 ± 601.9 ) of MSCs grown on nTCT (negative control) is lowest of all cultivation plates. The t-tests performed a significance difference between the other growth substrates and the nTCT plates, rejecting the $H_o$ hypothesis based on their p-values during the exponential phase (Table 4.3).

The population doubling time (PDT) measures the amount of time (hours) it takes for the MSC population to double. Cell cultures from all the cultivation substrates did not undergo a prolonged lag phase. Instead, cells entered exponential growth phase directly after a short adaptation time of approximately 24 hours. Consistent with this observation, the PDT of

the TCT plates was shorter (27.94 hours), followed by BM smeared plates (29.04 hours) and dermis (40.07 hours). Inspite of low mean ± SD for adipose smeared plates it had the highest PDT of 71.52 hours (Table 5). On all the substrates the percentage of cell viability decreased gradually during the cultivation period with the greatest decreases in cell viability occurring between days 8 and 10 (Fig 11).

*Table 3.1: Mean cell count, Standard Deviation and Standard Error Mean of TCT (positive control) with respect to cultivation time.*

| Days | Substrate: TCT Mean cell count (Cells/$cm^2$) | Standard Deviation (SD) | Standard Error Mean |
|---|---|---|---|
| 0 | 446 | 0 | 0 |
| 2 | 5466.8 | 2126.42 | 1063.21 |
| 4 | 32699 | 19777.9 | 9888.95 |
| 6 | 59539 | 15005.9 | 9888.95 |
| 8 | 36328 | 8848 | 4424 |
| 10 | 10838 | 1397.01 | 698.5 |

*Table 3.2: Mean cell count, Standard Deviation and Standard Error Mean of substrate: dermis with respect to cultivation time.*

| Days | Substrate: Dermis Mean cell count (Cells/$cm^2$) | Standard Deviation (SD) | Standard Error Mean |
|---|---|---|---|
| 0 | 446 | 0 | 0 |
| 2 | 5566.2 | 1074.3 | 537.15 |
| 4 | 19167 | 2524.3 | 1262.15 |
| 6 | 29419 | 3606.67 | 1803.33 |
| 8 | 27955 | 1639.22 | 819.61 |
| 10 | 10848 | 7637.52 | 3818.76 |

*Table 3.3: Mean cell count, Standard Deviation and Standard Error Mean of substrate: BM with respect to cultivation time.*

| Days | Substrate: BM Mean cell count (Cells/$cm^2$) | Standard Deviation (SD) | Standard Error Mean |
|---|---|---|---|
| 0 | 446 | 0 | 0 |
| 2 | 6129 | 3896.16 | 1948.08 |
| 4 | 32001 | 16967.4 | 8483.7 |
| 6 | 61009 | 32665.8 | 16332.9 |
| 8 | 36615 | 8990.11 | 4495.05 |
| 10 | 4146.5 | 2727.5 | 1161.55 |

*Table 3.4: Mean cell count, Standard Deviation and Standard Error Mean of substrate: Adipose tissue with respect to cultivation time.*

| Days | Substrate: Adipose tissue Mean cell count (Cells/$cm^2$) | Standard Deviation (SD) | Standard Error Mean |
|---|---|---|---|
| 0 | 446 | 0 | 0 |
| 2 | 1639 | 1070.61 | 535.30 |
| 4 | 3737.9 | 2501.82 | 1250.91 |
| 6 | 4183.6 | 1633.39 | 816.69 |
| 8 | 4613.5 | 2804.76 | 1402.38 |
| 10 | 4164.5 | 2727.5 | 1363.75 |

*Table 3.5: Mean cell count, Standard Deviation and Standard Error Mean of substrate: nTCT (negative control) with respect to cultivation time.*

| Days | Substrate: nTCT Mean cell count (Cells/$cm^2$) | Standard Deviation (SD) | Standard Error Mean |
|---|---|---|---|
| 0 | 446 | 0 | 0 |
| 2 | 6329 | 4151.64 | 2075.82 |
| 4 | 2859.1 | 608.15 | 304.07 |
| 6 | 1362.1 | 601.9 | 300.95 |
| 8 | 1005.2 | 455.97 | 227.93 |
| 10 | 442.56 | 209.16 | 104.58 |

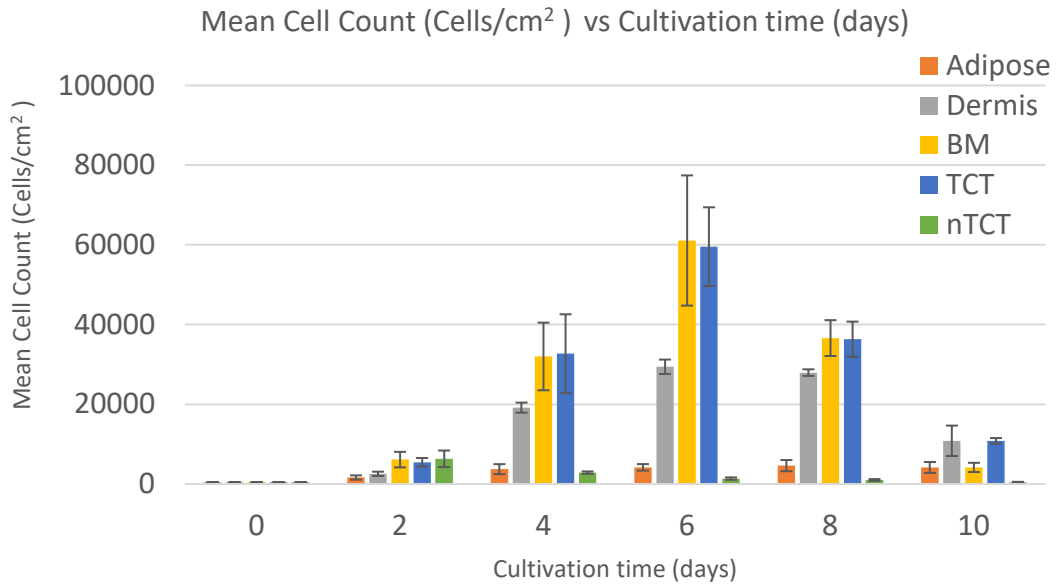


*Figure 9: Histogram representation of MSCs grown on Adipose-smeared, Dermis-smeared, BM-smeared, TCT and nTCT plates. All dishes were inoculated at 3.5 x $10^4$ cells/ml (t = 0 day.) in D-MEM-F12-5% MSC-qualified FBS media. Cell counts were done every 2 days for 10 days. Bars represent means ± Standard Error Mean of four experimental rounds.*

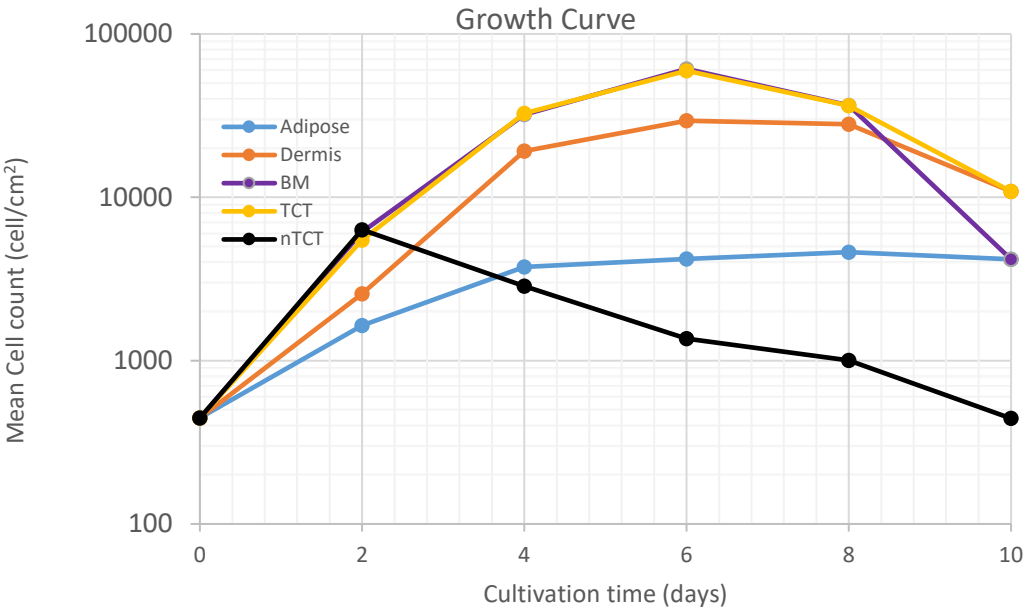


*Figure 10: Growth curve showing log phase on day-2, exponential phase from day-4 to day-8, and death phase on day-10. Data points represent means of four experimental rounds.*

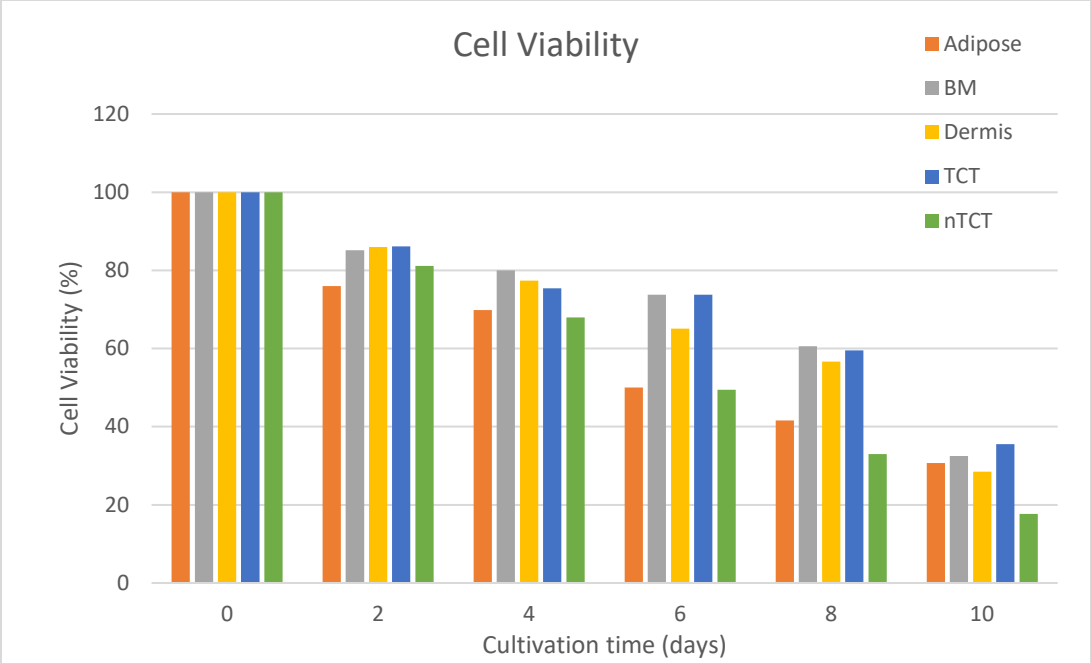


*Figure 11: Viability of MSCs Cultivated on adipose smeared, dermis smeared, BM-smeared, TCT and nTCT plates. All numbers represent the means of four experimental rounds.*

*Table 4.1: Comparison of Substrates in terms of p-vlaue for Day-2 cultivation time.*

| Substrate | P-value |
|---|---|
| TCT vs Dermis | 0.065 |
| TCT vs BM | 0.778 |
| TCT vs AD | 0.028 |
| TCT vs nTCT | 0.728 |
| BM vs Dermis | 0.164 |
| BM vs AD | 0.101 |
| BM vs nTCT | 0.778 |
| Dermis vs AD | 0.267 |
| Dermis vs nTCT | 0.065 |
| AD vs nTCT | 0.029 |

*Highlighted P-values <0.05 show significance

*Table 4.2: Comparison of Substrates in terms of p-vlaue for Day- 4 cultivation time.*

| Substrate | P-value |
|---|---|
| TCT vs Dermis | 0.265 |
| TCT vs BM | 0.959 |
| TCT vs AD | 0.027 |
| TCT vs nTCT | 0.024 |
| BM vs Dermis | 0.228 |
| BM vs AD | 0.043 |
| BM vs nTCT | 0.041 |
| Dermis vs AD | 0.000 |
| Dermis vs nTCT | 0.001 |
| AD vs nTCT | 0.539 |

*Highlighted P-values <0.05 show significance

*Table 4.3: Comparison of Substrates in terms of p-vlaue for Day-6 cultivation time.*

| Substrate | P-value |
|---|---|
| TCT vs Dermis | 0.764 |
| TCT vs BM | 0.198 |
| TCT vs AD | 0.063 |
| TCT vs nTCT | 0.004 |
| BM vs Dermis | 0.147 |
| BM vs AD | 0.040 |
| BM vs nTCT | 0.035 |
| Dermis vs AD | 0.000 |
| Dermis vs nTCT | 0.000 |
| AD vs nTCT | 0.034 |

*Highlighted P-values <0.05 show significance

*Table 4.4: Comparison of Substrates in terms of p-vlaue for Day- 8 cultivation time.*

| Substrate | P-value |
|---|---|
| TCT vs Dermis | 0.154 |
| TCT vs BM | 0.965 |
| TCT vs AD | 0.004 |
| TCT vs nTCT | 0.004 |
| BM vs Dermis | 0.149 |
| BM vs AD | 0.004 |
| BM vs nTCT | 0.004 |
| Dermis vs AD | 0.000 |
| Dermis vs nTCT | 0.000 |
| AD vs nTCT | 0.044 |

* Highlighted P-values <0.05 show significance

*Table 4.5: Comparison of Substrates in terms of p-vlaue for Day-10 cultivation time.*

| Substrate | P-value |
|---|---|
| TCT vs Dermis | 0.998 |
| TCT vs BM | 0.048 |
| TCT vs AD | 0.009 |
| TCT vs nTCT | 0.001 |
| BM vs Dermis | 0.429 |
| BM vs AD | 0.133 |
| BM vs nTCT | 0.009 |
| Dermis vs AD | 0.179 |
| Dermis vs nTCT | 0.011 |
| AD vs nTCT | 0.072 |

*Highlighted P-values <0.05 show significance

*Table 5: Population doubling time for Substrates (in Hours) during the exponential phase.*

| Substrate | Population doubling time (Hours) |
|---|---|
| TCT | 27.94 |
| BM | 29.04 |
| Dermis | 40.07 |
| Adipose | 71.52 |

## Immunophenotyping of MSCs

The morphological homogeneity and undifferentiated state of the MSCs at the eighth passage was examined by immunophenotyping analysis based on the expression of CD proteins. MSCs cultivated for two, six and ten days on poly-L-lysine, BM- smeared, Adipose-smeared and Dermis-smeared coverslips were stained against positive and negative surface markers lineage specific for MSCs. Markers were selected based on the flow-cytometry cell-surface protein profile characterized by the supplier of the cells. The antigenic phenotype was carefully checked using positive cell surface markers (CD44, CD29 and Sca-I) and a negative cell surface marker (CD117). The results of the immunofluorescences analyses are summarized in Table 6 and representative images illustrating the expression profile of MSCs at passage eight are shown in Fig 11.1, 11.2, 11.3 and 11.4. Immunophenotypic evaluation demonstrated that MSCs grown on BM smeared, Dermis smeared, Adipose smeared and poly-L-lysine coated coverslips were uniformly positive for CD44 (>90%), CD29 (>90%), Sca-I (>70%). In all cases cells lacked expression of CD117 (<5%), a typical marker for hematopoietic stem cells. MSCs from the eight passage, grown on all the cultivation substrates showed a virtually identical phenotype.

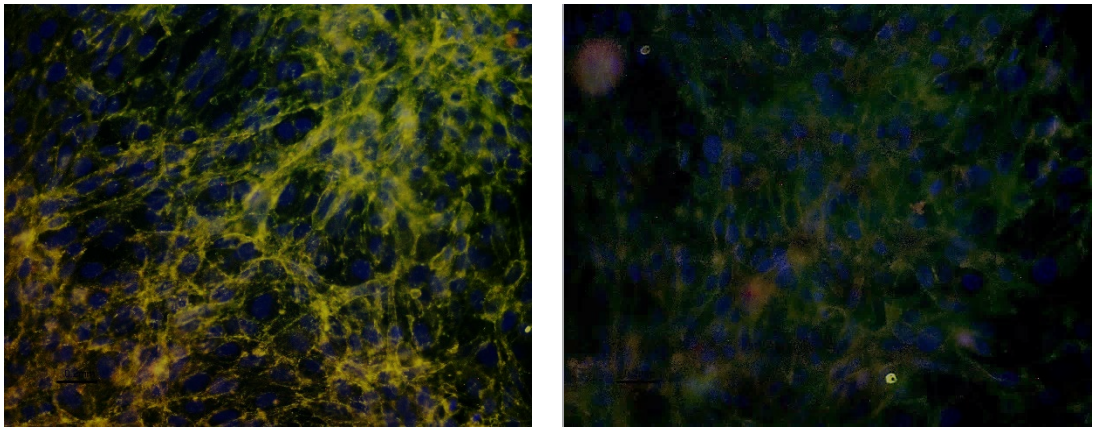

CD 29 CD 44

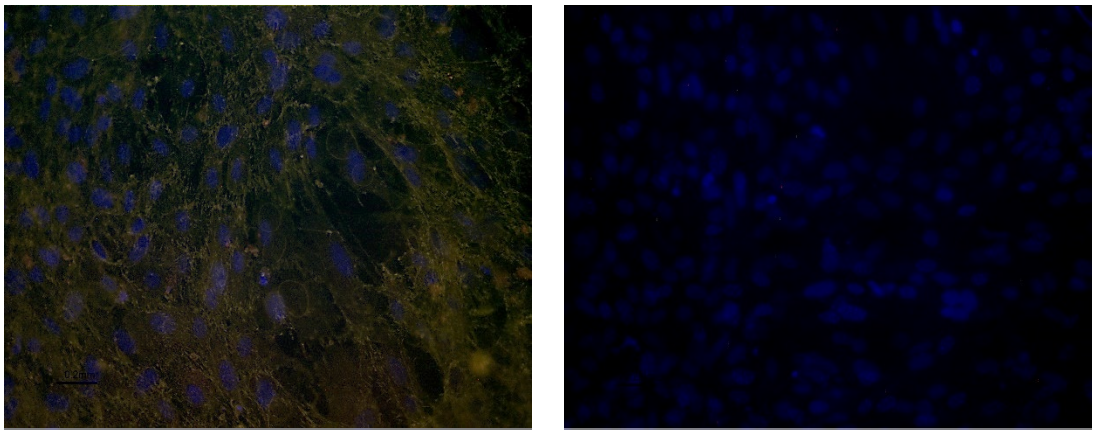

Sca-I CD 117

---

## Cultivation substrate: Dermis

*Figure 11.1: Expression of CD29, CD44, Sac-I and CD-117 markers. MSCs were stained over night with PE labelled anti-CD29, anti-CD 44, anti-Sca-I and anti-CD117 (1:5000 dilution; green) antibody after growth on dermis-smeared cover slips and cell nuclei were counterstained with DAPI (blue). Filter- TRITC. Magnification: 20X. Scale bars represents 0.2 mm.*

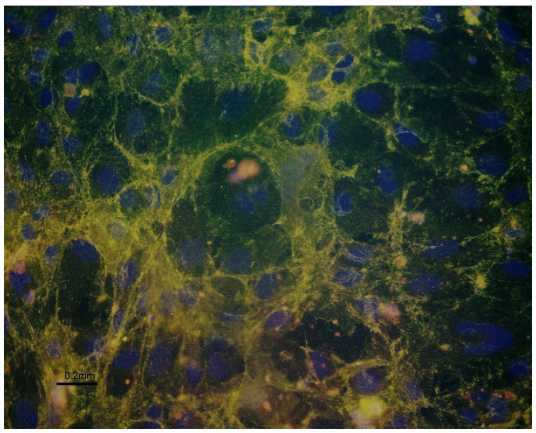

CD 29

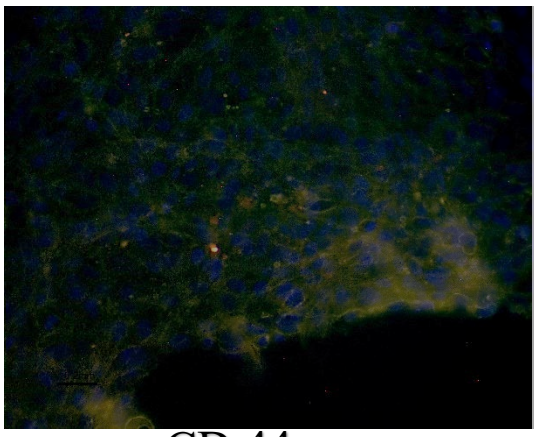

CD 44

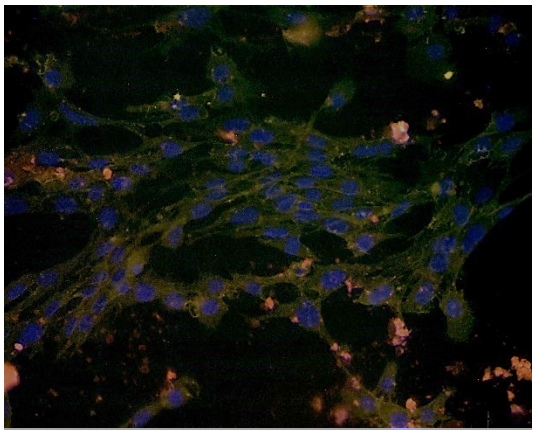

Sca-I

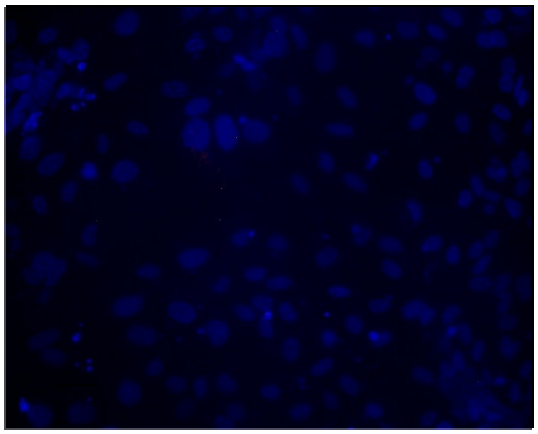

CD 117

---

## Cultivation substrate: Bone-Marrow

*Figure 11.2: Expression of CD29, CD44, Sac-I and CD-117 markers. MSCs were stained over night with PE labelled anti-CD29, anti-CD 44, anti-Sca-I and anti-CD117 (1:5000 dilution; green) antibody after growth on BM-smeared cover slips and cell nuclei were counterstained with DAPI (blue). Filter-TRITC. Magnification: 20X. Scale bars represents 0.2 mm.*

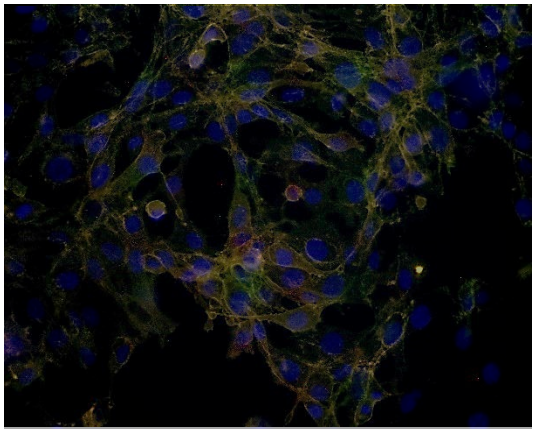

CD 29

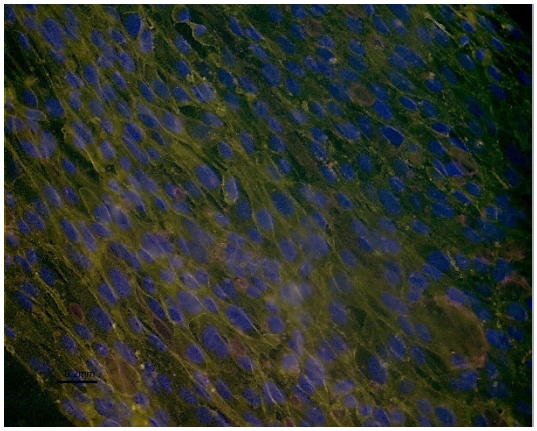

CD 44

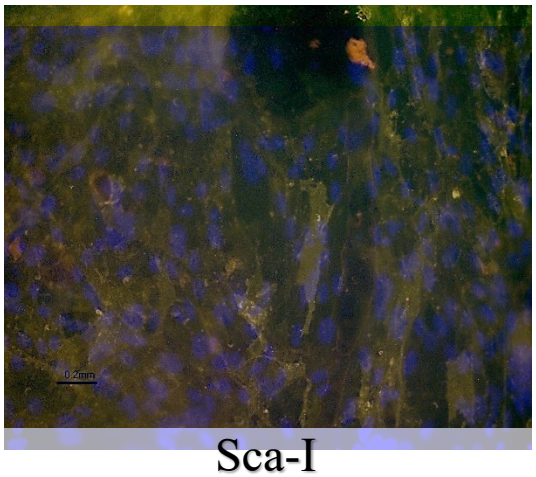

Sca-I

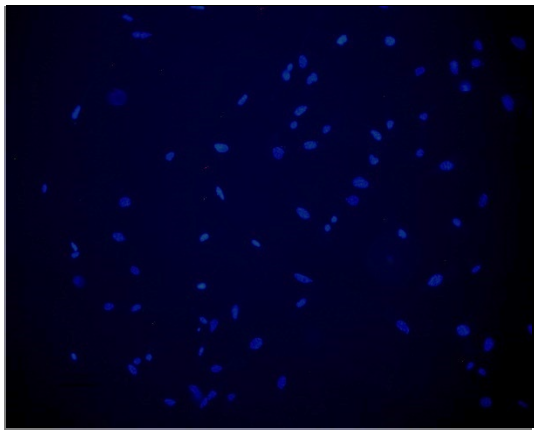

CD 117

---

## Cultivation substrate: Adipose tissue

*Figure 11.3: Expression of CD29, CD44, Sac-I and CD-117 markers. MSCs were stained over night with PE labelled anti-CD29, anti-CD 44, anti-Sca-I and anti-CD117 (1:5000 dilution; green) antibody after growth on Adipose-smeared cover slips and cell nuclei were counterstained with DAPI (blue). Filter-TRITC. Magnification: 20X. Scale bars represents 0.2 mm.*

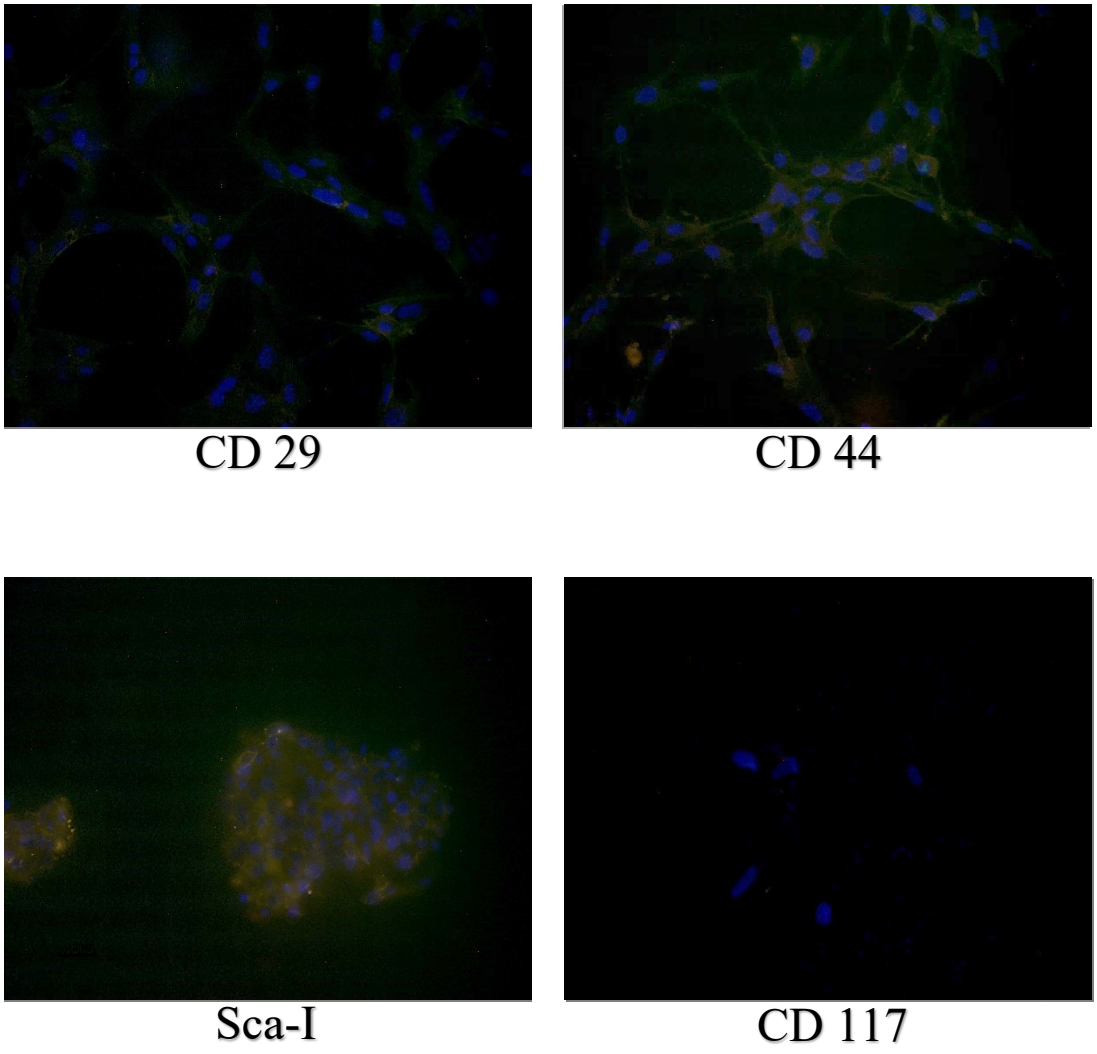


Cultivation substrate: TCT (positive control)

*Figure 11.4: Expression of CD29, CD44, Sac-I and CD-117 markers. MSCs were stained over night with PE labelled anti-CD29, anti-CD 44, anti-Sca-I and anti-CD117 (1:5000 dilution; green) antibody after growth on poly-L-lysine coated TCT cover slips and cell nuclei were counterstained with DAPI (blue).Filter-TRITC. Magnification: 20X. Scale bars represents 0.2 mm.*

*Table 6: Expression of MSC Lineage Specific Surface Markers Based on Immunofluorescence Analyses.*

| Cultivation Substrates | Cell surface markers | | | |
|---|---|---|---|---|
| | Positive markers | | | Negative Marker |
| | CD44 | CD29 | Sca-I | CD117 |
| BM smeared | H | H | V | A |
| Adipose smeared | H | H | V | A |
| Dermis smeared | H | H | V | A |
| Poly-L-lysine coated TCT | H | H | V | A |

*Expression ranges: H: high (>90%), V: variable (>70%), A: absent (<5%).

# DISCUSSION

## Effects of decellularization on ECM proteins

Decellularized ECM not only acts as a supporting material but also as a cellular behavior regulator, including cell survival, proliferation, morphogenesis, and differentiation (Badylak, 2007). Decellularized ECM is a useful tissue engineering matrix, because it imitates the compositions, microstructure, and biomechanical properties of the native ECM (Song et al., 2011 and Mosser et al., 2006). Porcine tissues including small intestines, dermis, adipose tissue, tendons and bone-marrow have been used to overcome the manufacturing limitations of human sources. A number of decellularization protocols have been established to maximize the decellularization results while minimizing the unfavorable effects on the composition, biological activity and ECM properties of the tissues (Crapo et al., 2011). Many groups have reported different methods for decellularization of porcine tissues and the effectiveness of removal of cellular components, ECM content and distribution. Results show that each of the decellularization methods investigated (enzymatic, mechanical or chemical) resulted in scaffold characteristics that were distinct in structural and biochemical properties. This shows how important it is to tailor the decellularization protocol based on the tissue of interest (Brown et al., 2011). In the present study, ECM was isolated from porcine dermis, BM and adipose tissue by a combination of chemical, enzymatic and mechanical methods of decellularization. The tissues were exposed to extremely temperatures (freezing and thawing) and effectively decellularized after a relatively short exposure to ethanol, triton-

X 100, DNase-I and lyophilization. Chemical and enzymatic agents are needed to remove the cellular components that adhere to the ECM proteins (Stone et al., 1998). In this study, the optimized decellularization was highly effective in removing the DNA and cellular components as demonstrated by H&E staining of processed tissues (Fig 2.1- B, C; Fig 2.2- B, C; Fig 2.3- B, C). Moreover, the fibrous structures of the decellularized ECM were similar to that observed in intact native ECM (Fig 2.1-A, Fig 2.2- A, Fig 2.3- A). Porcine tissues have been previously reported as containing many ECM components, including Fibronectin, Laminin, Elastin, Collagen-I, III, IV, and VII ( Brown et al., 2011 and Choi et al., 2011). The retention of ECM composition was a central goal during decellularization. Histological analysis clearly showed that abundant ECM components, such as GAGs, Fibronectin, Laminin, Collagen-I, III, and IV preserved in the decellularized porcine ECM. However, the amount of these ECM components decreased when the tissues where decellularized and further decreased when the tissues were lyophilized. This was determined by measuring the brightness of the histological sections that had undergone staining for the ECM proteins. Reducing the decellularization agents and processing time should help in maintaining the ECM components even after processing the tissues. Even though ethanol is known to effectively remove cells from dense tissues and inactivate pyrogens, protein precipitation–including collagen–have been demonstrated (Crapo et al., 2011). Future studies are necessary to evaluate the potential effects of decellularization on BM-derived ECM, dermis-derived ECM and adipose-derived ECM. Furthermore, characterization of ECM proteins, using high-performance liquid chromatography or mass

spectrometry, could assess the degree of ECM alteration during decellularization in more detail. The preserved ECM derived from porcine tissues can be important for cell adhesion and differentiation and thus would be favorable for tissue repair and remodeling (Nelson and Tien, 2005).

**ECM derived from BM, dermis and adipose supports *In-vitro* cultivation of MSCs**

Some studies suggests that tissue-specific ECM may be most beneficial and effective in maintaining highly specific cell phenotypes (Brown et al., 2011). The decellularized tissue-specific ECM will be beneficial for stem cell research and the production of cells for stem cell therapies. Hence, development of cultivation substrates for MSCs that resemble the natural cellular environment has emerged as an important research area for self-expansion of cells in large-scale cultures. For example, one of the studies has shown that dysfunctional bone-marrow cells are killed and replaced with healthy stem cells, but to grow these healthy stem cells *in-vitro* environment required a decellularized ECM preparation (Heuther and McCance, 2008). However, not much work has been done on protecting the multipotency of MSCs during long-term expansion on traditional tissue culture plates, therefore testing of alternative cultivation substrates is needed. The key deficiencies of cells grown on plastic or glass substrate are the geometric arrangement of the cells (2 dimensional plane rather than the 3 dimensional orientation within tissue) and the lack of a physiologically relevant cell attachment substrate (e.g. minimally altered ECM). Due to these deficiencies, cells cultured via traditional methods do not have the same morphology and physiology as the same cell type in the body.

Furthermore, in order to sustain the cells, high doses of growth hormone and other substances must be added to the cultures, which further damage the normal physiology of the cells. Even with maximal artificial chemical stimulation of cell growth through the application of cell growth factors, cells typically only survive in traditional cultures for 1 or 2 weeks. Therefore, these traditional cultures have limited utility. Work has been done on cell-derived ECM and multiple protein coatings which has been shown to support proliferation and differentiation potential of MSCs during *in-vitro* cultivation (Lu et al., 2011). Closer approximation of cell phenotype and heterogeneity of the *in-vivo* microenvironment can be provided by tissue-specific ECM (Kusuma et al., 2012). Supported by the concept introduced by Richard Schofield in 1978, decellularized tissue-specific ECMs may be able to prolong the expansion of functional MSCs without loss of their proliferation capacity and undifferentiated phenotype. Based on this concept and previous studies which demonstrated decellularized porcine BM ECM supported the *in-vitro* cultivation of MSCs (Mueller, 2015). Moreover, previous work in this laboratory illustrated the efficiency of the BM-derived, substrate for *in vitro* cultivation of HEK 293 cells (Jay et al., 2013). However, additional research was required to show that ECM derived from porcine tissues can be an effective substrate. Therefore, in the present study the sustainability of decellularized porcine BM, dermis and adipose derived ECM for *in vitro* cultivation of mouse MSCs was investigated. Driven by the hypothesis that BM-smeared, dermis-smeared and adipose smeared surfaces would have a beneficial effect within 2D cultivation of MSCs by imitating native ECM *in vitro*, its impact on essential cellular parameters, like cell growth and cell phenotype, was analyzed.

To diminish the potential for adverse immune reactions and enhance feasibility for large-scale application, the decellularized BM-derived substrate was transferred onto cultivation dishes via smearing. Even though the 3D orientation of the tissue is lost , direct smearing is observed to effectively transfer proteins of the tissue on to the plates (Hebert-Magee, 2014 and Mueller, 2015). In contrast to other techniques like protein coated hydrogel or cell derived ECM, smearing non-tissue culture plates (nTCT) with porcine derived ECM is relatively simple, cost effective and time saving. Therefore, mouse MSCs were cultivated on nTCT plates smeared with dermis, adipose and BM ECM. As a control, MSCs were grown on standard tissue culture plates (TCT) and nTCT plates for ten days along with smeared plates. In addition to analyzing cell growth, cell morphology and expression of MSC-lineage specific surface markers were assessed during the cultivation time. Overall, MSCs cultivated on BM-smeared, dermis-smeared and Adipose-smeared plates were able to grow on these substrates similar to the TCT plates. The cell growth and phenotype of the smeared substrates and TCT plates showed comparable results. Cells cultured on BM-smeared, dermis-smeared, adipose-smeared and TCT plates exhibited similar morphologic characteristics (triangular and spindle-shaped cellular appearance) prior to reaching confluency. Post- confluency the cell morphology changed and MSCs formed multilayers and granules in the cytoplasm (Ha-Jing et al., 2007). Moreover, the results of the present study demonstrate that like TCT plates, BM smeared, adipose smeared and dermis smeared plates do not undergo differentiation over the assessed duration of cultivation. Apart from maintaining the uniform morphological and phenotypic characteristics, porcine derived

substrates supported proliferation of MSCs. After repeating the cultivation rounds four times, mean cell counts and SD were calculated, and t-tests were performed to compare the growth on the various substrates. The results of these statistical analyses demonstrated that the dermis-smeared , BM-smeared and TCT plates showed no significant differences in their ability to support MSC growth expressed in terms of Cells / $cm^2$. However, when the growth curves of the substrates were compared it showed that BM-smeared and TCT plates during the exponential phase had overlapping curves, and dermis smeared plates had a curve slightly below them. It was also observed that adipose-smeared plate were significantly different when compared to BM-smeared, dermis-smeared and TCT plates in terms of supporting MSC cell growth. Except the nTCT the mean cell count and the growth curve was the lowest for adipose smeared plates, indicating that this substrate is able to support MSC growth in culture but not as effectively as BM-derived substrate, dermis-derived substrate and TCT plates. This could possibly be due to the high lipid content of adipose interfering with the growth of the MSCs. Porcine adipose tissue cannot not be easily decellularized, because it is very dense. In addition, lipids trapped within the adipose tissue may congeal, resulting in adverse effects in decellularization and lyophilization. Adipose tissue needs a complete disruption of lipids and so decellularization protocol involving lipid extraction is required. Studies have shown that homogenization of adipose tissue at an appropriate temperature can remove the lipids and improve the efficiency of decellularization (Choi et al., 2009).

Immunofluorescence microscopy for MSC-lineage specific surface markers also showed no significant phenotypic difference between the cells grown on BM-derived, dermis-derived, adipose-derived and TCT plates. All the cell populations were positive for CD29, CD44, Sca-I and negative for CD117. These results were consistent with previous studies on undifferentiated MSCs (Bayda et al., 2014; Zheng et al., 2014; Mueller 2015).

# CONCLUSION

The results of the present study demonstrate the potential of decellularized dermis-derived ECM, BM-derived ECM and adipose-derived ECM smear substrate to support cell growth of mouse MSCs during 2D cultivation *in vitro* expansion while maintaining their undifferentiated phenotype. Since analyses were performed for a limited time-frame, a future study would be to assess the long-term effectiveness of porcine-derived substrate by continuing the cell passage until reaching senescence or spontaneous differentiation of MSCs. A morphological study could be carried out to examine the differentiation of the MSCs into osteocytes, adipocytes or chondrocytes on the prepared substrates. This can be valuable to establish a prolonged, native-like regulated *ex vivo* expansion environment. Exploring different decellularization methods that achieve decellularize while maintaining ECM protein. Further, a decellularization method to reduce excess lipid content in adipose tissue may help in studying the growth pattern on adipose-derived ECM.

On basis of the present study, its suggested that decellularized ECM has a significant impact on cell fate. Porcine derived substrates can be a promising cultivation surface for *in vitro* expansion of mouse MSCs and provide a framework for future studies and regenerative medicine.

REFERENCES

Friedenstein AJ, Chailakhjan RK and Lalykina KS. (1970). The development of fibroblast colonies in monolayer cultures of guinea-pig bone marrow and spleen cells. *Cell Tissue Kinet*, 1970; 3:393–403.

Friedenstein AJ. (1990). Osteogenic stem cells in bone marrow. *Bone and mineral research*, 243–272.

Tavassoli M and Crosby WH. (1968). Transplantation of marrow to extramedullary sites. *Science*, 161:54–56.

Owen M and Friedenstein AJ. (1988). Stromal Stem cells: Marrow derived Osteogenic Precursors. *Ciba Found Symp*, 136:42-60.

Caplan AI. (1990). Mesenchymal Stem cells. *Journal of Orthopedic Research,* 9:641-650.

Horwitz E, Blanc K, Dominici M, et al. (2005). Clarification of the nomenclature for MSC: The International Society of Cellular therapy position statement. *Cytotherapy*, 7:393–395.

Loeffler M and Potten C. (1997). Stem cells and cellular pedigrees-a conceptual introduction. *Stem Cells*, 1–28.

Pittenger M, Mackay A, Beck S, Jaiswal R, Douglas R, Mosca J, Moorman M, Simonetti D, Craig, Marshak D. (1999). Multilineage Potential of Adult Human Mesenchymal Stem cells. *Science,* 284:143-147. DOI: 10.1126/science.284.5411.143.

Delorme B, Ringe J, Pontikoglou C, Gaillard J, Langonne A, Sensebe L, Noel D, Jorgensen C, Haupl T, Charbord P. (2009) Specific Lineage-Priming of Bone

Marrow Mesenchymal Stem Cells Provides the Molecular Framework for Their Plasticity. *Stem Cells*, 27:1142–1151.

Kurpinski K, Lam H, Chu J, Wang A, Kim A, Tsay E, Agrawal S, Schaffer DV, Li S. (2010). Transforming growth factor-beta and notch signaling mediate stem cell differentiation into smooth muscle cells. *Stem Cells*, 28:734–742.

Barry F, Boynton RE, Haynesworth S, Murphy JM, Zaia J. (1999). The monoclonal antibody SH-2, raised against human mesenchymal stem cells, recognizes an epitope on endoglin (CD105) *Biochem Biophys Res Commun*, 265:134–139.

Barry F, Boynton R, Murphy M, Zaia J. (2001). The SH-3 and SH-4 Antibodies Recognize Distinct Epitopes on CD73 from Human Mesenchymal Stem Cells. *Biochem Biophys Res Commun*. 289:519–524.

Baddoo M, Hill K, Wilkinson R, Gaupp D, Hughes C, Kopen GC, Phinney DG. (2003). Characterization of mesenchymal stem cells isolated from murine bone marrow by negative selection. *J Cell Biochem* 89: 1235-1249.

Boiret N, Rapatel C, Veyrat-Masson R, Guillouard L, Guérin J-J, Pigeon P, Descamps S, Boisgard S, Berger MG. (2005). Characterization of nonexpanded mesenchymal progenitor cells from normal adult human bone marrow. *Exp Hematol* 33: 219-225.

Cognet PA, Minguell JJ. (1999). Phenotypical and functional properties of human bone marrow mesenchymal progenitor cells. *J Cell Physiol* 181: 67-73.

Gronthos S, Franklin DM, Leddy HA, Robey PG, Storms RW, Gimble JM. (2001). Surface protein characterization of human adipose tissue-derived stromal cells. *J Cell Physiol* 189: 54-63.

Campagnoli C, Roberts IA, Kumar S, Bennet PR, Bellantuono I, Fisk NM. (2001). Identification of mesenchymal stem/progenitor cells in human first-trimester fetal blood, liver and bone marrow. *Blood*, 98: 2396-2402

Anker PS, Noort WA, Scherjon SA, Kleijburg-van der Keur C, Kruisselbrink AB, van Bezooijen RL, Beekhuizen W, Willemze R, Kanhai HH, Fibbe WE. (2003). Mesenchymal stem cells in human second-trimester bone marrow, liver, lung, and spleen exhibit a similar immunophenotype but a heterogeneous multilineage differentiation potential. *Haematologica,* 88: 845-852.

Igura K, Zhang X, Takahashi K, Mitsuru A, Yamaguchi S, Takashi TA. (2004). Isolation and characterization of mesenchymal progenitor cells from chorionic villi of human placenta. *Cytotherapy,* 6: 543-553.

Fibbe WE, Noort WA. (2003). Mesenchymal stem cells and hematopoietic stem cells transplantation. *Ann NY Acad Sci,* 996: 235-244.

Uccelli A, Moretta L, Pistoia V. (2008). Mesenchymal stem cells in health and disease. Nature review immunology,9:726-736. doi: 10.1038/nri2395.

Ma S, Xie N, Li W, Yuan B, Shi Y, and Wang Y. (2014). Immunobiology of mesenchymal stem cells. *Cell Death and Differentiation*, 21:216–225

Sekiya I, Colter DC, Prockop DJ. (2001). BMP-6 enhances chondrogenesis in a subpopulation of human marrow stromal cells. *Biochem Biophys Res Commun*,284: 411-418

Friedenstein AJ, Gorskaja U, Kalugina NN. (1976). Fibroblast precursors in normal and irradiated mouse hematopoietic organs. *Exp Hematol*, 4: 267-274.

Tropel P, Noel D, Platet N, Legrand P, Benabid AL, Berger F. (2004). Isolation and characterization of mesenchymal stem cells from adult mouse bone marrow. *Exp Cell Res,* 295: 395-406.

Colter DJ, Sekiya I, Prockop DJ. (2001). Identification of a subpopulation of rapidly self-renewing and multipotential adult stem cells in colonies of human marrow stromal cells. *Proc Natl Acad Sci USA,* 98: 7841-7845.

Kassem M. (2004). Mesenchymal stem cells: biological characteristics and potential clinical applications. *Cloning Stem cells*,6:369-374.

Rosland V., Svendsen A., Torsvik A., Sobala E., McCormack E., Immervoll H., Mysliwi etz J., Tonn J.C., Goldbrunner R., Lonning P.E. (2009). Long-term cultures of bone marrow-derived human mesenchymal stem cells frequently undergo spontaneous malignant transformation. *Cancer Res*. 69:5331–5339, doi: 10.1158/0008-5472.CAN-08-4630

Chen G., Yue A., Ruan Z., Yin Y., Wang R., Ren Y., Zhu L. (2014). Monitoring the biology stability of human umbilical cord-derived mesenchymal stem cells during long-term culture in serum-free medium. *Cell Tissue Bank* ,15:513–521, doi:10.1007/s10561-014-9420-6.

Hang L., Jihee S., He S., Mark T.L., Rocky S.T. (2018). Bone marrow mesenchymal stem cells: Aging and tissue engineering applications to enhance bone healing. *Biomaterials*, https://doi.org/10.1016/j.biomaterials.2018.06.026.

Schwartz RE., Reyes M., Koodie L., et al. (2002). Multipotent adult progenitor cells from bone marrow differentiate into functional hepatocyte-like cells. *J Clin Invest*, 109:1291–1302.

Tropel P., Platet N., Plate JC., et al. (2006). Functional neuronal differentiation of bone marrow-derived mesenchymal stem cells. *Stem Cells*, 24:2868–2876.

Park JH., Hwang I., Hwang SH., Han H and Ha, H. (2012). Human umbilical cord blood-derived mesenchymal stem cells prevent diabetic renal injury through paracrine action. *Diabetes Res Clin Pract* 98: 465–473.

Daria SC., Kristina VK., Leysan GT., Victoria J., Albert AR., Valeriya VS. (2018). Application of Mesenchymal stem cells for therapeutic agent delivery in anti-tumor treatment. *Frontiers in Pharmocology.*

Schubert T., Xhema D., Vntriter S., Schubert M., Behets C., Delloye C., Gianello P. (2011). Bone Allografts using osteogenic-differentiated adipose-derived mesenchymal stem cells. *Biomaterials*, 34:8880.-8891.

Jang Yo, Kim MY., Cho MY., Baik SK., Cho YZ., Kwon SO. (2014). Effect of bone-marrow-derived mesenchymal stem cells on hepatic fibrosis in a thioacetamide-induced cirrhotic rat mode. *BMC Gastroenterol*,14:198, doi: 10.1186/s12876-014-0198-6.

Hynes RO. (2009).The extracellular matrix: not just pretty fibrils.Science,326:1216-1219, doi:10.1126/science.1176009.

Rolfe KJ and Grobbelaar AO.(2012). A review of fetal scarless healing. Dermatol, 2012:698034, doi: 10.5402/2012/698034.

Jarvelainen H., Sainio A., Koulu M., Wight T.N. and Penttinen R.(2009).Extracellular matrix molecules: potential targets in pharmacotherapy. *Pharmacol*,61:198-223.

Schaefer, L. and Schaefer, R. M. (2010). Proteoglycans: from structural compounds to signaling molecules. *Cell Tissue Res*,339: 237-246.

Iozzo R.V.,Zoeller J.J and Nystrom A.(2009). Basement membrane proteoglycans: modulators par excellence of cancer growth and angiogenesis. *Molecular Cells* ,27: 503-513.

Alberts B., Johnson A., Lewis J., Raff M., Roberts K. and Walter P.(2007). *Molecular Biology of the Cell*,3:401.

Kular J, Basu S, Sharma R.(2014). The extracellular matrix: Structure, composition, age-related differences, tools for analysis and applications for tissue engineering. *Journal of Tissue Engineering*,https://doi.org/10.1177/2041731414557112.

Rozario T. and DeSimone D.W. (2010). The extracellular matrix in development and morphogenesis: a dynamic view. *Dev. Biol*. 341:126-140.

Tsang K.V., Cheung M.C., Chan D and Cheah K.S.(2010).The development roles of the extracellular matrix: beyond structure of regulation. *Cell Tissue Res*. 339: 93-110.

Eckes B, Nischt R, Krieg T.(2010). Cell-matrix interactions in dermal repair and scarring. *Fibrogenesis Tissue Repair*.

Kuschel C,Steuer H,Maurer A.N.,Kanzok B.,Stoop R and Angres B.(2006). Cell adhesion profiling using extracellular matrix protein microarrays. *Biotechniques*, 40:523-531.

Badylak S.F.(2007).The extracellular matrix as a biologic scaffold material. *Biomaterials,* 28: 3587-3593.

Swinehart I and Badylak S.(2016).Extracellular matrix bioscaffolds in tissue remodeling and morphogenesis**.** *Dev Dyn*,3: 351–360.

Gundula Schulze-Tanzil , Onays Al-Sadi, Wolfgang Ertel and Anke Lohan.(2012).Decellularized Tendon Extracellular Matrix—A Valuable Approach for Tendon Reconstruction**.** *Cells* 4**:**1010-1028**.**

Ott HC., Matthiesen TS, Goh SK, Black LD, Kren SM, Netoff TI, Taylor DA.(2008).Perfusion-decellularized matrix: using nature's platform to engineer a bioartificial heart. *Nat Med* 2:213-21.

Bobis S., Jarocha D. and Majka M. (2006). Mesenchymal stem cells: characteristics and clinical applications. *Folia histochemical et cytobiologica*, 44:215-230.

Song, J and Ott, H.C. (2011). Organ engineering based on decellularized matrix scaffolds. *Trends Mol Med*,17: 424.

Mosser, G., Anglo, A., Helary, C., Bouligand, Y., and Giraud- Guille, M.M. (2006). Dense tissue-like collagen matrices formed in cell-free conditions. *Matrix Biol*, 25,:3.

Crapo, P.M., Gilbert, T.W., and Badylak, S.F. (2011). An overview of tissue and whole organ decellularization processes. *Biomaterials* 32:3233.

Brown B., Freund J., Han L., Rubin J., Reing J., Jeffries E, Wolf M., Tottey S., Barnes C., Ratner B., Badylak S. (2011). Comparison of Three Methods for the Derivation of a Biologic Scaffold Composed of Adipose Tissue Extracellular Matrix. *Tissue Engineering Part: C,* 411-423: 17, DOI: 10.1089/ten.tec.2010.0342.

Stone K.R., Ayala G., Goldstein, J., Hurst R., Walgenbach A., and Galili U. (1998). Porcine cartilage transplants in the cynomolgus monkey III. Transplantation of alpha-galactosidase treated porcine cartilage. *Transplantation* 1577: 65.

Choi, J.S., Kim, B.S., Kim, J.Y., Kim, J.D., Choi, Y.C., Yang, H.J., et al. (2011). Decellularized extracellular matrix derived from human adipose tissue as a potential scaffold for allograft tissue engineering. *Biomed Mater Res A,* 292:97.

Nelson, C.M., and Tien, J. (2006). Microstructured extracellular matrices in tissue engineering and development. C*urr Opin Biotechnology*, 518:17.

Heuther S and McCance K. 2008. Alterations of Hematologic Function. In: Understanding Pathophysiology. *Mosby/Elsevier Publishing*. 508-549.

Ha-Jing, Zheng Zhu, Long-ding ,Yun-zhang. (2007). Morphological properties of mesenchymal stem cells derived from bone-marrow of Rhesus monkeys. Zoology Research, 213-216.

Baydaa A., Alwachi S., Yaseen N., Shammari A. (2014). Isolation and Identification of mouse bone marrow derived mesenchymal stem cells. Iraqi Journal of Cancer and Medical Genetics, 49-55:7.

Mueller L. (2015). Decellularized Porcine bone-marrow derived Extracellular matrix supports in-vitro cultivation of Mouse Mesenchymal stem cells. Master's thesis, University of Houston-Clear Lake.